Masters Theses

Graduate School

6-1984

The Role of Molecular Weight in Controlling the Structure and Properties of High-Speed Melt Spun Nylon-6 Filaments

Jogendra Suryadevara
University of Tennessee - Knoxville

Follow this and additional works at: https://trace.tennessee.edu/utk_gradthes

Part of the Other Engineering Commons

To the Graduate Council:

I am submitting herewith a thesis written by Jogendra Suryadevara entitled "The Role of Molecular Weight in Controlling the Structure and Properties of High-Speed Melt Spun Nylon-6 Filaments." I have examined the final electronic copy of this thesis for form and content and recommend that it be accepted in partial fulfillment of the requirements for the degree of Master of Science, with a major in Polymer Engineering.

Joseph E. Spruiell, Major Professor

We have read this thesis and recommend its acceptance:

Edward S. Clark

Accepted for the Council:
Carolyn R. Hodges

Vice Provost and Dean of the Graduate School

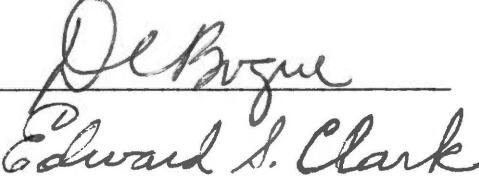(Original signatures are on file with official student records.)

To the Graduate Council:

I am submitting herewith a thesis written by Jogendra Suryadevara entitled "The Role of Molecular Weight in Controlling the Structure and Properties of High-Speed Melt Spun Nylon-6 Filaments." I have examined the final copy of this thesis for form and content and recommend that it be accepted in partial fulfillment of the requirements for the degree of Master of Science, with a major in Polymer Engineering.

Joseph E. Spruiell, Major Professor

We have read this thesis and recommend its acceptance:

Edward S. Clark

Accepted for the Council:

The Graduate School

THE ROLE OF MOLECULAR WEIGHT IN CONTROLLING THE STRUCTURE

AND PROPERTIES OF HIGH-SPEED MELT SPUN NYLON-6 FILAMENTS

A Thesis

Presented for the

Master of Science

Degree

The University of Tennessee, Knoxville

Jogendra Suryadevara

June 1984

Dedicated to My Grandfather

Sri Suryadevara Venkatappaiah Garu

ACKNOWLEDGMENTS

ABSTRACT

A comprehensive study of the structure development during high speed melt spinning of nylon-6 was performed. The major emphasis of the research was on the effect of molecular weight in the structure development of high speed melt spun nylon-6 filaments. The various measurements done on the filaments to determine their morphology included diameter, tensions in spinline, density as well as x-ray diffraction and birefringence measurements. The effects of mass throughputs were also studied. Tensile properties of conditioned fibers were measured and related to the spinning variables and molecular weight.

The spinline stresses measured increased rapidly with take-up velocity and molecular weight. The increase with molecular weight was more rapid at higher take-up velocities than at lower take-up velocities. The wide angle x-ray diffraction pattern indicated a significant level of crystallinity, and a high γ-phase content at high take-up velocities in low molecular weight samples. The total crystalline fraction and the γ-phase content decreased with increase in molecular weight. This is attributed to the slower crystallization rates for higher molecular weight samples.

The chain axis crystalline orientation function increased rapidly at the beginning with take-up velocity and then started to level off after reaching an attainable maximum at higher take-up velocities. Increase in spinline stresses increased crystalline

iv

orientation but not independent of molecular weight. Increased molecular weights resulted in increased crystalline orientation functions at low take-up speeds and they decreased at higher take-up speeds.

Birefringence measurements showed increases with take-up speeds and molecular weights and decreases with increased mass throughputs.

Densities increased with take-up velocity and molecular weight. The higher molecular weight samples had higher density, due to the high content of the more dense α-phase in them.

The tensile strength and modulus of the conditioned filaments increased, but the elongation at break decreased with increasing take-up velocity and spinline stress. Modulus and tensile strength increased with molecular weight. The increase in modulus with molecular weight was rapid at high take-up speeds, producing very high modulus fibers at high speeds and high molecular weight. The tensile properties correlated with spinline stress and birefringence, but not independent of mass throughput and molecular weight.

TABLE OF CONTENTS

LIST OF TABLES

LIST OF FIGURES

CHAPTER I

INTRODUCTION

The history of man-made fibers, although practically a story of the past 100 years, has come a long way during this period and has contributed greatly to our present-day society. The contributions include not only the kind of clothes we wear, but also to our wealth and comfort of living in the broadest sense of these words.

It was in an effort to synthesize polymers resembling natural materials like silk and wool, that "Nylon" was first made. "Nylon" is the generic name for any long chain synthetic polymeric amide which has recurring amide groups as an integral part of the main polymer chain and which is capable of being formed into a filament in which the structural elements are oriented in the direction of the axis (85).

The unique position of polyamides in the plastics field is, however, due largely to their strength and toughness, allied to which is their high melting point yet thermoplastic behavior, which allows their processing by conventional extrusion and molding.

Nylon-6 was the first important all synthetic fiber. Known for about fifty years now, nylon-6 is produced worldwide commercially and used mainly in apparel, carpet and tire industry. By far the most important use of nylon-6 is as a fiber.

Nylon-6 fibers are produced commercially by the melt spinning process of producing synthetic fibers. In this process, the fibers

are produced by first melting the polymer chips into a viscous medium, usually in a screw extruder, and then the molten polymer is pumped through a die or a spinneret forming continuous filaments. The filaments are solidified and taken-up by a winding device. Melt spun fibers generally have very high extensibility. Orientation and other physical properties vary to a great extent, depending upon the spinning conditions.

Extensive research was done and numerous papers were published in the technical literature concerning the relationship between spinning conditions and the fiber quality and properties. These relationships and the understanding of the structure development as a function of processing variables have enabled the fibers to be put to a great many uses. Nylon is a supreme example of a fiber whose properties have permitted exploitation in a vast range of products, which has increased steadily, ever since it was first made.

Experiments conducted by Bankar (8) revealed the morphological and rheological properties of nylon-6 fibers. Gianchandani (35) later studied the structural and morphological changes taking place in drawn and annealed nylon-6 fibers. Nylon-6 filaments studied so far in this Department were spun at speeds below 2,500 m/min.

Lately, a major commercial trend has been toward high winding speeds. Commercial winding speeds appear to have reached the 5,000 m/min range, while research on the effect of winding speed has reached the 9,000 m/min range (109). These studies showed that increasing spinning speeds has a profound effect on the fiber

characteristics. However, there is still very little information on certain aspects of high-speed melt spinning in the literature. In particular, there is little information about the interaction of the molecular weight and spinning speed on the structure and properties.

The objective of this present investigation is to provide a better understanding of the structure and properties of fibers melt spun from polymers over a range of molecular weights and at high take-up speeds. The major emphasis of the research was to establish correlations for fibers with different processing histories between spinline stresses and cyrstallinity, birefringence, density and mechanical property measurements. Of particular interest were the effect of molecular weight and mass throughout on the structure and properties of as-spun, conditioned nylon-6 filaments.

CHAPTER II

LITERATURE SURVEY

A. GENERAL BACKGROUND

Nylons belong to a general class of polyamides which are condensation products containing recurring amide groups NH-CO as integral parts of the main polymer chains. Wallace H. Carothers, who was appointed by E. I. DuPont de Nemours and Company in 1928 to carry out fundamental chemical research, and his colleague Julian W. Hill were the first to synthesize nylons. Nylon-6 seems to have first been made by Carothers and Brechet (19) in 1930. Nylon-6 polymers reported in 1932 by Carothers and Hill (20) had molecular weights of about 3,000 and were therefore unsuitable for making fibers.

Carothers applied his basic ideas on molecular chain growth in polymerization (21) to his research, and in May 1934, he demonstrated the production of polyamide fibers that were heat resistant and stood up to washing and dry cleaning. These were nylon-66 fibers. DuPont announced their development of a new group of synthetic polymers from which high-strength textiles could be produced. Nylon-66 was first produced commercially in 1939. In May 1940, nylon stockings were introduced to the public in the U.S. They were an instant success and plants to produce nylon polymer and yarn were erected in many parts of the U.S.

The dislosures by DuPont, in patents and other publications, of their success in the field of fiber-forming materials led to work

in that area in Germany. Success came in 1938, when Paul Schlack (100) of I. G. Farbenindustrie showed that by careful selection of catalysts, the ε-caprolactum ring could be opened and straight chain polymerization can be effected. The high polymers thus produced were similar to nylon-66 in properties and were designated "Perlon" (70).

An agreement between I. G. Farben and DuPont was arranged in 1939. With much of DuPont's know-how in fibers, the pace of development quickened and in the same year I. G. Farben's commercial production of nylon-6 filaments started at their Berlin-Lichtenberg plant, in small scale. Two years later in 1941, I. G. Farben's Landsberg plant went into large-scale production of nylon-6.

A number of countries quickly followed in setting up plants for polyamide polymer and fiber production. Different types of nylons were synthesized, which are distinguished from each other by a system of nomenclature which depends upon the number of carbon atoms in the starting materials used for making them (71).

Nylon-6 is polymerized from ε-caprolactum in the presence of water. A stabilizer such as acetic acid is added to control the molecular weight. The polycaprolactum is extruded into a water bath and then cut into small pellets. These pellets contain about 10 percent monomer and other oligomers. These are removed by leaching the pellets in boiling water, and are then dried to less than 0.10 percent moisture content by weight before spinning. The continuous process of polymerizing ε-caprolactum is described in the literature (15,62,101).

B. EFFECT OF MOISTURE

Dyeability of a fiber under normal pressure, as well as its comfort in wearing, is determined by its ability to absorb moisture. The static properties of nylons are also affected by the moisture content. All nylons absorb moisture readily from air, and will hold it firmly through hydrogen bonding with the amide groups. The higher the amide content, the greater is the affinity towards moisture.

The important factors in the establishment of an equilibrium between a polyamide and water-containing environment are: the relative humidity (RH), the amide content and the amount of crystallinity. In the case of nylon-6, which exhibits a high moisture absorption among the polyamides (79), the content of moisture reaches 9 to 10 percent at 100 percent RH (126). There is a significant decrease in moisture absorption with increase in crystallinity (32). The moisture absorbed serves as a plasticizer, reducing modulus and tensile strength, while increasing elongation as the moisture content increases (102).

Campbell's studies (18) on the effect of water on the x-ray diffractometer scans of nylon-6 films crystallized in the α form, showed that the changes were caused in both the amorphous and crystalline regions. He noted an increase in the intensity of (200) peak and a decrease in the intensity of combined (002) and (202) peaks on water absorption.

Nylon-6 is chemically unaffected by water at ordinary temperatures, but at high temperatures, in the presence of moisture,

hydrolysis and degradation take place. It is soluble in some acids and organic solvents. It is quite stable in alkaline solutions, but decomposes in acidic solutions. Nylon-6 melts at 215-220°C, depending upon its molecular weight.

C. STRUCTURAL FORMS OF NYLON-6

Nylon-6 is a linear molecule with a repeat unit

$$[-NH-\overset{\overset{O}{\|}}{C}-(CH_2)_5-]$$
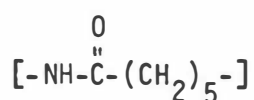
Hydrogen bonds are formed between the carbonyl groups of one chain and the amide groups of the other chain during crystallization from the melt. The hydrogen bonds were found to have a typical length of 11.8 Å from infrared studies (79).

The earliest investigations on the crystal structure of nylon-6 were carried out by Brill (16) in 1943, and later by Wallner (126). This was followed by the most complete crystal structure study by Holmes, Bunn and Smith (53). These authors proposed a monoclinic unit cell for nylon-6, containing eight monomeric units with the dimensions

a = 9.56 Å

b = 17.24 Å   angle β = 67.5°

c = 8.01 Å

The unit cell is shown in Figure II-1(a). The b-axis of the monoclinic unit cell is considered to be the axis of symmetry. For nylon-6, this b-axis is also the chain axis. This structure is

A. Unit Cell

B. Hydrogen Bonded Sheet
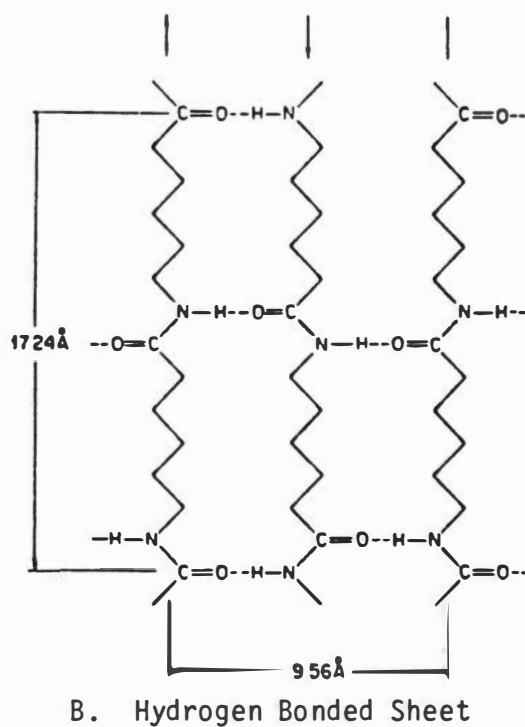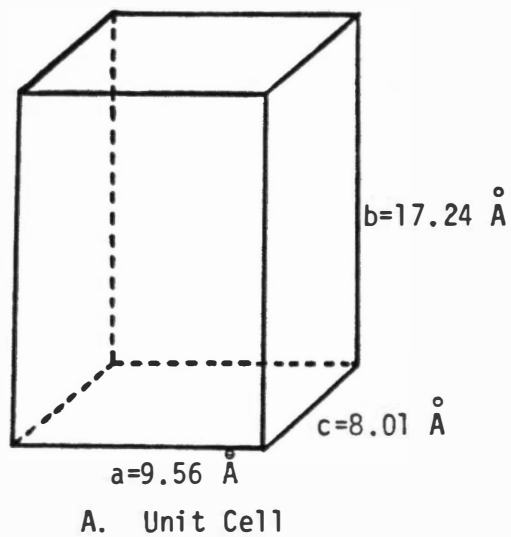
Figure II-1. Schematic of monoclinic crystal structure of nylon-6.

called the α form and has the extended chain structure shown in Figure II-1(b). Hydrogen bonding between the amide and carbonyl groups of adjacent nylon-6 chains results in the formation of hydrogen bonded sheets. A nylon-6 crystal is formed by sheets of planar zig-zag chains running antiparallel, stacked up. These sheets are staggered up and down.

All of the authors above recognized the existence of more than one crystalline form of nylon-6. A second crystalline form of nylon-6 referred to as the β or γ form was first detected by Holmes et al. (53). This form is now generally called the γ form. Holmes et al (53) suggested that it is due to a parallel relative shifting of alternate chains in the hydrogen-bonded sheets by about one atom. This leads to a modified unit cell with poorer hydrogen bonding.

This γ form, also known as the pseudohexagonal form, was also studied by Slichter (118) who proposed that it was due to parallel chains rather than antiparallel chains. Ziabicki (141) reported that a pseudohexagonal form can be obtained by melt spinning nylon-6. He also discussed the conversion of this phase to normal monoclinic phase (136). Tsuruta et al. (127) produced highly oriented γ form fibers using iodine-potassium iodide treatment, which made more detailed studies possible. Other papers were published (5,64,88,128) describing the transition between the α and γ crystals by iodine-potassium iodide treatment. Konoshita (68) and later Vogelsong (129) proposed a hexagonal or pseudohexagonal unit cell for the γ form,

composed of extended parallel chains with kinks. Vogelsong gave the
unit cell dimensions as

$$a = b = 4.79 \text{ Å}$$
$$b = 16.7 \text{ Å} \qquad \gamma = 60°$$

The unit cell would contain only two monomeric units. Later Arimoto
(6) proposed a monoclinic unit cell for the γ form with

$$a = 9.33 \text{ Å}$$
$$b = 16.88 \text{ Å} \qquad \beta = 121°$$
$$c = 4.78 \text{ Å}$$

This cell nearly exhibits pseudohexagonal symmetry and contains four
monomeric units.

There is a marked difference between the diffraction patterns
from the two crystalline forms of nylon-6, α (monoclinic) and γ
(pseudohexagonal) (13,53,78,92). Two equatorial peaks are present
in the α pattern against only a single peak in the γ pattern. Also
a strong meridional peak is present in the γ form as opposed to a
very weak one which is sometimes in the α form. A major difference
is the reduced repeat distance of the γ form compared to the α form,
which results in a change in layer line spacing.

Besides these, the major crystal structures of nylon-6,
Roldan and Kaufman (92) summarized a series of studies by proposing
that nylon-6 can exist as an "α" crystal (Holmes et al.), an "α
paracyrstal" (Brill) with variable unit cell parameters, a stable
"β" structure (in drawn fibers) and an unstable pseudohexagonal
structure similar to a nematic liquid crystal which they called the

"γ" crystal (Ziabicki-Kedzierska). Several other authors (7,13,14, 56,88) have proposed different crystal structures. Parker and Lindenmeyer (89) have summarized the unit cell data (converted to monoclinic form) for nylon-6.

Although numerous investigators have studied the structure and properties of nylon-6, only a few have described methods of obtaining the relative amounts of phases present. All such methods are approximate and depend on the nature of the various approximations made in the analysis. Recently, an extensive literature review has been done by Gianchandani et al. (35,36) regarding the different structural forms of nylon-6 and the different approaches made by researchers in trying to separate the relative amounts of α, γ and amorphous phases. They have also determined quantitatively the relative amounts of phases by their own method which uses a combination of x-ray and density data. Their technique utilizes two standard samples. One, the γ standard, which is high in γ-phase content and the other, the α standard, high in α-phase content. They use the integrated intensities of the equatorial scan in the range 14-28° 2θ and that of the 020 meridional reflection at about 11° 2θ. A more detailed description of their method of analysis is given in Chapter III. The α-phase which Gianchandani et al. (36) obtained in as-spun fibers was very poorly developed paracrystalline and pseudohexagonal. Their α form corresponds to the γ^* form of Illers et al. (56) and to the pleated α form of Stepaniak et al. (124,125). Their results show that the α-phase which predominates at low spin draw ratio is a very imperfect

paracrystalline form. They conclude that the γ-type phase is given by the strain induced crystallization occurring from the oriented melt under dry conditions. The fact that an increase in spin draw ratio tends to increase the amount of γ-type phase leads them to this conclusion. Both the α and γ fractions in spun filaments exhibit a poorly developed pseudohexagonal structure.

The other authors who attempted to separate the relative amounts of phases include Roldan et al. (93), who assumed the existence of a β phase in their method of determination. Although there are many good features of their approach, the assumption of separate β- and γ-phases makes their method obsolete in the context of the present view of the literature. Dismore and Statton (29) employed the crystallization perfection index for nylon-66 which can be applied for nylon-6 and would involve a calculation of the separation of the (200) and (002, 202) maxima. This method is therefore limited to samples where the maxima can be easily resolved, e.g., in a fairly well-developed α structure. Kyotani and Mitsuhashi (73) use peak heights instead of the areas under the curves to determine the relative amounts of phases. Their method is hence influenced by the crystallite size and perfection, and will be subject to errors if the peak widths differ in different samples. Stepaniak et al. (124,125) used a method which involves the separation of intensity distribution from a randomized sample in the range of 15-30° 2θ into α, γ and amorphous contributions. They obtained an amorphous "template" by scanning the azimuthal intensity distribution

of a highly oriented sample. Hence, a total crystalline contribution
of the sample was obtained by then subtracting the amorphous intensity
from the overall intensity. They assume that the (200) and (202, 002)
reflections of the α form occur at $2\theta = 20°$ and $24°$, respectively.
Hence all the crystalline scatter in the range of $2\theta = 18-20°$ and
above $24°$ results from the α form. The rest of the scattering is
part α and part γ.

A mathematical model was used by Heuvel et al. (50) for the
separation of the two crystal structures. Three curves, assumed to
represent α and γ equatorial diffraction, are fitted by the computer
to the equatorial diffraction scans. However, an apparent limitation
of this method is that the γ and amorphous contributions are treated
as one of the three curves. Later Heuvel et al. (48) developed a
five line model that allowed the separation of the diffraction pro-
file into amorphous peak, two γ and two α peaks. This allows the com-
putation of α, γ and amorphous fractions, but is rather complicated.
The results of Gianchandani et al. (36) were found to be consistent
qualitatively with those of Heuvel et al. (50). By far, the simplest
method seems to be that of Gianchandani et al. (36) for separating
the relative amounts of phases using the 020 reflection. The method
does not involve complicated analytical procedures to separate over-
lapping reflections. Stepaniak et al. (125) cautioned against using
the 020 reflection due to the possible effect of slippage of the
hydrogen-bonded sheets in the γ structure. Gianchandani et al. (36)
argue that this effect is less troublesome compared to the problems
associated with separating the equatorial scan into its components.

D. CRYSTALLINITY

Polymer fibers possess a complex structure and are frequently found to be crystalline. There are different physical methods for determining the degree of crystallinity interpreted in terms of a two-phase model. However, there is no "absolute" measurement or a universally acceptable definition of the degree of crystallinity. The reason is, if we consider the x-ray scattering method for instance, the amorphous scattering will include a contribution from the crystalline defects. This affects the calculation of the amounts of amorphous and crystalline phases. On the other hand, if we use the density or specific volume method, it may be affected by the fact that the molecular orientation may cause a change in the density of the amorphous fraction. Microvoids also affect the density.

Density or Specific Volume

Measurement of crystallinity is usually done by the density method (2,103). In this method, we use the following expression, assuming that the crystalline and amorphous regions have fixed but different densities:

$$\bar{x}_c = \frac{\rho_c(\rho - \rho_a)}{\rho(\rho_c - \rho_a)} \tag{II-1}$$

where

$\bar{x}_c$ = weight fraction of crystalline material;

ρ = density of the fiber sample;

ρ_a = density of the amorphous component;

ρ_c = density of crystalline component.

Equation (II-1) represents the crystallinity of the fiber sample in the as-spun state, if there are no appreciable voids present in the fiber, and there is only a single crystalline phase.

X-Ray Diffraction

In this method, the scattering from crystalline and amorphous regions has to be separated and a suitable integration of each performed. The crystallinity can then be estimated approximately by:

$$x_c = \frac{\text{total intensity of crystalline scattering}}{\text{total coherent intensity scattered (crystalline + amorphous)}}$$

Nylon-6

On-line studies by Bankar et al. (10) and Gianchandani et al. (36) show that nylon-6 is amorphous in the spinline and crystallizes only on the bobbin. They point out that crystals are formed during conditioning by the cold crystallization process and therefore conditioning increases crystallinity. Gianchandani et al. (36) note that the crystals formed are very small and/or paracrystalline. These rather imperfect crystals exhibit pseudohexagonal symmetry. Parker and Lindenmeyer (89) have observed an increase in the tendency for γ-phase formation with increased spin draw ratio. Similar trends were obtained by Gianchandani et al. (35,36) from the examination of the increase in relative intensity of the 020 meridional reflection. They have used the γ index method to characterize the trend more quantitatively. Results showed that low spin draw ratios produced filaments low in γ-phase content ($x_\gamma < 0.1$) and high paracrystalline α-phase content ($x_\alpha = 0.35$). As the

spin draw ratio increases, the γ-phase content increases along with the total crystalline content. At high spin draw ratios the γ-phase content levels out at about $x_\gamma = 0.25$, while the α-phase content levels at $x_\alpha = 0.2$. They point out that the observation of pseudo-hexagonal symmetry does not necessarily imply the presence of γ-phase nor the absence of paracyrstalline α-phase.

There have been some papers published on the quantitative determination of crystalline orientation functions of nylon-6. Sakoku, Morosoff and Peterlin (96) reported chain axis orientation functions of nylon-6 bristles. They make use of the Wilchinsky (132) analysis for (200), (002) and (202) reflections of the monoclinic nylon-6 crystals. They reported an increase in the chain axis orientation factor when nylon-6 samples are drawn. Bankar et al. (8,10) calculated the crystalline orientation factors of spun filaments using a hexagonal symmetry. Their results show that the crystalline orientation factor, f_c, increases with take-up velocity and spinline stress, but f_b decreases. As the take-up velocity increases, the c-axes tend to become more aligned to the fiber axis while the b-axes tend to become more perpendicular to the fiber axis. Gianchandani et al. (35,36) also reported an increase in the orientation factors of nylon-6 with draw down. The increase was from 0.07 to 0.71 for an increase in spin draw ratio from 15 to 240, but it is little affected by annealing. Gianchandani et al. (35,36) also followed the change in chain axis crystalline orientation of nylon-6 when the spun filaments were drawn at 90°C. Several other

authors (31,58,91,121,125) have calculated the orientation factors of nylon-6. The general trend in these studies was that the chain axis orientation factor increased with take-up velocity and also when the samples were drawn.

E. DYNAMICS AND FORCE BALANCE

Although the studies of melt spun fibers began in 1932 by Carothers and Hill (21), the first detailed series of studies of both theoretical and experimental aspects of the melt spinning process was studied by Ziabicki and Kedzierska (138,141,141,142,143,144,145) in 1959. They used the framework of continuum mechanics to formulate the governing equations of mass, momentum and energy balance in the spinline. The continuity equation was expressed as (142):

$$A \cdot V \cdot \rho = W = \text{constant} \tag{II-2}$$

where A is the cross-sectional area, V the velocity and ρ the density of the fiber, while W is the mass flow rate.

The force balance on the spinline between any position "X" on the spinline and position "L" at the take-up device was expressed as (135):

$$F_{ext}(L) = F_{rheo}(X) + F_{drag}(X) - F_{gravity}(X) + F_{inertia}(X) \tag{II-3}$$

where

F_{ext} = external force applied at the take-up device;

F_{rheo} = rheological force;

F_{drag} = aerodynamic drag on the filament;

$F_{gravity}$ = gravity force;

$F_{inertia}$ = inertial force.

From the studies of Bankar et al. (9) and Chen (23), the gravity force F_{grav} is important only at low take-up velocities and large filament diameters. At intermediate take-up velocities, F_{grav} and $F_{inertia}$ tend to cancel out, while at high take-up velocities, F_{drag} and $F_{inertia}$ become important. They also report that the spinline take-up force F_{ext} and the spinline stress (σ) increase with increasing take-up velocities. At low take-up velocities, F_{rheo} decreases along the spinline, while it increases at higher take-up velocities (9).

F_{grav} and F_{iner} can be evaluated easily, using the available experimental data. But the estimation of F_{drag} is not simple. Since

$$F_{drag} = \int_x^L \sigma_f \pi d(x) dx \qquad (II-4)$$

we have to find out the value of σ_f, the shearing stress on the surface of the fiber. The general expression for σ_f is (21,75,95,99, 139):

$$\sigma_f = C_f \frac{\rho V^2}{2} \qquad (II-5)$$

where C_f is the friction factor whose value is to be determined as a function of the related variables.

Andrews (3) studied experimentally the air-drag on a stationary filament in a wind tunnel. His results in terms of friction factor and the Reynolds number Re can be expressed as

$$C_f = 1.30 \ (Re_d)^{-0.61} \qquad\qquad\qquad (II-6)$$

where Re_d is the Reynolds number based on the diameter of filament. Similar experiments by Aoki, Suzuki and Ishimoto (4) gave

$$C_f = 0.18 \ (Re_d)^{-0.44} \qquad\qquad\qquad (II-7)$$

Sakiadis (95) used laminar and turbulent boundary layer analysis to calculate the drag on a cylinder of a constant diameter running through a stationary medium at constant velocity. Sano and Oni (99) and Hamana et al. (39) measured tension at various points of a solidified running filament and obtained

$$C_f = 0.68 \ Re_d^{-0.8} \qquad \text{Sano and Oni} \quad 10 < Re_d < 50 \quad (II-8)$$

$$C_f = 0.37 \ Re_d^{-0.61} \qquad \text{Hamana et al.} \quad 10 < Re_d < 260 \quad (II-9)$$
$$\text{and Matsui}$$

Matsui did the experiments at spinning speeds of 6000 m/min (74). Gould and Smith (38) suggested that

$$C_f = 0.43 \ Re_d^{-0.61} \qquad 40 < Re_d < 400 \qquad\qquad (II-10)$$

Kwon and Prevorsek (72) reported that their experimentally determined values of the drag forces were much higher than those

predicted theoretically by Glauert and Lighthill (37) and Sakiadis (95).

Extensive literature review on the various methods and corrections between C_f and Re_d evaluated by many investigators is done by Bankar (8) and Chen (23). Chen's own experiments with an aspirator to evaluate the air drag resulted in

$$C_f = 0.91 \ Re_d^{-0.61} \qquad\qquad (II-11)$$

Though the constant 0.91 is larger than the values of earlier researchers (4,38,39,72,75,99), the exponential value -0.61 is the same.

F. STRUCTURE DEVELOPMENT DURING MELT SPINNING

Low and Moderate Speeds

General. Mechanical and optical properties of melt spun fibers depend largely upon their structure-formation which in turn depends upon the spinning conditions. Carothers and Hill (21) were the first to realize the importance of the effects of spinning variables like fiber tension on the x-ray diffraction patterns of polyamides and polyesters. They correctly attributed these effects to the molecular orientation. Keller (66) presented x-ray data from nylons, polyethylene and polyethylene terephthalate to support his qualitative discussions on orientation and crystallinity in melt spun fibers. Ziabicki and Kedzierska (141,144,145) were the first to publish x-ray patterns and birefringence data of melt spun fibers,

and showed that orientation of molecules increased with take-up
stresses. Abbot and White (1) examined the variation of orientation
and crystallinity with spinning speed, melt flow rate and melt tem-
perature in melt spun, high density polyethylene fibers. The modulus
and tensile strength were found to increase with increasing
crystalline orientation.

Spinline stresses were studied by Henson and Spruiell (44),
and Nadella et al. (82) for polypropylene fibers. They concluded that
the morphology developed during melt spinning is determined primarily
by the spinline stresses. Relationship between spinline stresses and
crystallization were studied by Nakamura et al. (83), Dumbleton (30),
Ziabicki and Kedzierska (144) and Benaim (11) for polyethylene
terephthalate. It was found that polyethylene terephthalate
crystallizes due to enhanced crystallization kinetics at large spin-
line stresses.

SAXS studies (24,44,81,85,99,119) from polypropylene showed a
continuous ring at low take-up velocities, interpreted by Samuels (98)
as being due to unoriented lamellar superstructure which could be
due to a spherulitic structure. Keller et al. (51,65,67) and later
Fung and Carr (33), from the electron micrographs concluded the
presence of row nucleated structure caused by orientation of melt
during draw-down in polyethylene.

Simpson et al. (115), Chappel et al. (22), Slichter (116,117),
Starkweather (120,121) and Danford et al. (25) have studied the
crystallinity and orientation of nylon-66 samples using WAXS. On-line

x-ray diffraction measurements were made by Chappel et al. (22), Katayama et al. (61) and Spruiell and White (119) to study the development of crystallinity along the spinline. On-line birefringence was measured by Oda et al. (86), Bankar et al. (10), Chappel et al. (22) and Danford et al. (25).

Nylon-6. Ziabicki and Kedzierska (141,144) were among the earliest to make basic studies of structure development during melt spinning. They studied the WAXS patterns and birefringence of spun fibers and correlated the birefringence with an increasing function of spinline stress. Hamana, Matsui and Kato (39,40) and Ishibashi, Aoki and Ishii (59) made on-line birefringence measurements and determined Δn as a function of spinline position. Ishibashi and Ishii (61) and Ishibashi and Furukawa (60) studied the effect of heating chambers placed around the spinline on birefringence of the running filament. They suggest that the increase in birefringence is due to crystallization of the filament.

Studies of melt spun nylon-6 have also been published by Pasika, West and Thurston (90), Sakoaku, Morosoff and Peterlin (96), Wasiak and Ziabicki (131), Slichter (118) and Ruland (94). Bankar et al. (10) and Hirami and Tanimura (52) made on-line WAXS and birefringence measurements. Bankar et al. concluded that as-spun fiber is amorphous and that the crystallization of nylon-6 takes place on the bobbin. The authors report a gradual increase in birefringence with increasing take-up velocity.

Structure development in the wet spinning of nylon-6 has been studied by Kiyotosukuri, Hasegawa and Imamura (69) and by Hancock, Spruiell and White (42). The authors report that in most cases, wet spun fibers exhibited the α-monoclinic crystal structure.

Recently Gianchandani et al. (36), from the WAXS and birefringence measurements, concluded that nylon-6 filaments undergo both primary and secondary crystallization. They predict strain-induced crystallization on the running threadline. The authors have made a quantitative analysis of the α and γ fractions present in nylon-6, using a method developed by them, which involves the combination of x-ray and density data. They conclude that the relative amounts of phases in nylon-6 filaments depend upon the molecular orientation developed during spinning. Higher amorphous and α-phase fractions and lower γ fractions were obtained for low orientation samples than for higher spin orientation samples.

High Speed Melt Spinning

General. High speed spinning was originally aimed at eliminating the drawing step. Higher molecular orientation and better mechanical properties were obtained for high speed spun fibers when compared to fibers spun at lower speeds. Early studies of Ziabicki and Kedzierska (144) and Nakamura et al. (83) on the structure of fibers spun at 3,000-4,000 m/min showed this and also that the mechanical properties of high speed spun fibers are inferior to those of drawn fibers spun at lower speeds. Studies by Shimizu et al. (112) and Heuvel and Huisman (47) revealed that high speed

spun fibers exhibited a high degree of crystallinity, comparable to that in drawn material, but they required considerable improvement in their mechanical properties.

High speed spinning also gives higher per spindle productivity, but this would be only of secondary importance, if the properties can match those of the drawn fibers, which would be of great importance. Research on high speed spinning is, therefore, of interest to many researchers. There has been, however, very little information in literature to date on high speed melt spinning. This could be attributed to the complications that arise in devising the take-up equipment to wind fibers at high speeds and also the proprietary nature of such research. Hasegawa (43) discusses the mechanics of high speed take-up machines and the problems associated with them. A great difficulty with high speed spinning is the filament breakage during winding. In spite of the difficulties, fibers have been spun at speeds up to 10,000 m/min (108,114).

Shimizu et al. (114) were the earliest to publish a paper on high speed melt spinning of polypropylene. Remarkable increases in crystallinity and crystalline and amorphous orientations were achieved as noted by Shimizu et al. (105,108,112), and Heuvel and Huisman (47). These authors report a distinct crystalline structure found in poly-ethylene terephthalate spun at speeds greater than 4,000 m/min, from the WAXS patterns, while below 4,000 m/min, WAXS shows an amorphous halo (113). Birefringence studies (76,105,110,144) show an increase with take-up speeds.

Molecular orientation was found to vary along the radius of the fiber (108). Orientation is higher at the surface than at the center of the fiber. Shimizu et al. (107) studied the effects of melt-draw ratio and mass flow rates on the high speed melt spun PET fibers. Their x-ray patterns indicate that an increase in the melt-draw ratio with a decrease in mass flow rate result in increased crystallinity and orientation. Birefringence increases with increase in melt-draw ratio. In another study, Shimizu et al. (111) report a decrease in crystalline orientation and birefringence as the molecular weight increases. Hamidi et al. (41) studied the structure transition in PET at high speeds.

Crystallite sizes were found to increase with spinning speeds (47,104). The degree of perfection was found to be greater in high speed spun PET fibers than drawn fibers (135). Yasuda (135) showed that the mass flow rate increase decreases the crystallite size. He also reports an increase in orientation and decrease in density and birefringence with the decrease in the mass flow rate.

The elastic and tensile properties are strongly affected by the fiber orientation and its structure resulting from high speed spinning. An increase in modulus and tensile strength and a decrease in the elongation were observed for polypropylene fibers spun at high speeds (106). Similar results were obtained for high speed spun PET samples (49,76,113). Ziabicki in a recent paper (140) discusses the theoretical aspects of high speed spinning.

Nylon-6. Studies on high speed melt spun nylon-6 fibers were carried out by Heuvel and Huisman (48) and Shimizu et al. (109). These studies were done on nylon-6 fibers spun at speeds higher than those studied earlier by Ziabicki and Kedzierska (144) and Nakamura et al. (83). High crystallinity and orientations were observed with increased take-up speeds by Heuvel and Huisman (48) and Shimizu et al. (109) which were similar to the results from high speed spinning of PET (47,113).

Heuvel and Huisman's results (47) show that nylon-6 yarns spun at speeds below 3,000 m/min are not completely crystallized and that crystallization also takes place after moisture pick up during conditioning. Yarns spun at speeds higher than 3,000 m/min, however, produce a stable crystal structure and there is little crystallization occurring. Birefringence data collected by Shimizu et al. (109) as a function of time after spinning support Heuvel and Huisman's results. All these authors report an increase in γ-phase with an increase in the take-up speed, and the increase becomes lesser at higher speeds. Drawing the filaments resulted in the transition from γ to α-form. Heuvel and Huisman (48), who emphasized the characterization of the crystalline phase, used a five-line model to computer fit the equatorial profile, to separate the x-ray scattering from the γ-phase from that from the amorphous phase (49). They propose that at take-up speeds greater than 2,500 m/min, γ-crystals are mainly generated from orientation induced nuclei and α-crystals grow slowly after moisture pick-up. They obtained better oriented γ-crystals and larger

in dimensions compared to the α-crystals. Mechanical properties study of nylon-6 filaments spun at high speeds by Shimizu et al. (109) indicate that high speed spinning increases the tensile strength and reduces elongation of the fibers.

CHAPTER III

EXPERIMENTAL DETAILS

A. MATERIAL

The nylon-6 polymers used in this study were of five different
molecular weights. The two nylon-6 polymers with lower viscosity
average molecular weight ($\overline{M}_V$) were supplied by the American Enka
Company and the remaining three polymers of higher viscosity average
molecular weight were supplied by Allied Fibers and Plastics. The
polymers received from American Enka Company (the two low $\overline{M}_V$ polymers)
were undried and had to be dried before using them for any experi-
ments. The polymers sent by Allied Fibers and Plastics (the three
higher $\overline{M}_V$ polymers), however, were dried and therefore could be used
directly for the experiments.

Dilute solution viscosity measurements were carried out with
all the polymers to determine the relative viscosity (η_r), intrinsic
viscosity ($[\eta]$) and the viscosity average molecular weight ($\overline{M}_V$). A
solution of 1.0 percent nylon-6 in 85 percent formic acid at 20°C
was used to obtain the relative viscosity of the samples. The dilute
solution viscosity data are listed in Table 1.

B. DRYING OF NYLON-6

Drying was carried out in a laboratory type vacuum oven
model 5831, manufactured by National Appliance Company, Portland,

Table 1. Dilute solution viscosity data

Material	Relative Viscosity η_r, at 1.0 gm/dl	Intrinsic Viscosity $[\eta]$	Viscosity Average Molecular Weight $(\overline{M}_v)$
Enka CN9984 undried	2.028	0.862	23,550
CN9984 dried	2.090	0.905	25,250
CN0002 undried	2.103	0.883	24,370
CN0002 dried	2.124	1.007	29,400
Allied LSB	2.490	1.170	36,440
BHS 72918	2.692	1.525	53,210
HMW	3.104	1.901	72,900

Oregon. The drying was carried out in batches of about 1200 gm of the polymer under an absolute pressure of 0.5 inches mercury and 110°C. The polymers from American Enka were dried under these conditions for sixteen hours, after which they were placed in desiccators to allow the polymer to cool down to room temperature. The samples were then stored in glass jars until ready to use. This procedure of drying nylon-6 has been used earlier by Gianchandani (35) and Bankar (8) and was found to be satisfactory in bringing the moisture content down to 0.03-0.04 percent from an initial content of about 0.34 percent.

C. DILUTE SOLUTION VISCOSITY MEASUREMENTS

Solutions of nylon-6 in 85 percent formic acid were made at concentrations ranging from 0.0625 gm/dl to 1.00 gm/dl. Viscosities of these solutions were measured using an Ubbelhode capillary viscometer. The viscometer with the solution was kept in a cold water bath at 20°C for 30 minutes before measurement. Efflux times for the solutions, as well as the solvent, were measured. Relative viscosity of the solution (η_r) is given by

$$\eta_r = \frac{\text{efflux time of solution}}{\text{efflux time of solvent}} \qquad \text{(III-1)}$$

and specific viscosity η_{sp} by

$$\eta_{sp} = (\eta_r - 1) \qquad \text{(III-2)}$$

The inherent viscosity η_{inh} is given by

$$\eta_{inh} = \frac{\ln \eta_r}{c} \qquad \text{(III-3)}$$

where c is the concentration in g/dl. Plots of η_{sp}/c and η_{inh} versus concentration are made and extrapolated to zero concentration to obtain the intrinsic viscosity $[\eta]$. A plot of η_{sp}/c and η_{inh} versus concentration is shown in Figure III-1. Intrinsic viscosity is related to the viscosity average molecular weight $\overline{M}_v$ by the Mark-Houwink equation

$$[\eta] = k(\overline{M}_v)^a \qquad \text{(III-4)}$$

where k and a are constants for a particular solvent-solute system at a given temperature.

For a solution of nylon-6 in 85 percent formic acid at 20°C, Bennewitz (12) obtained

$$k = 75 \times 10^{-5} \ dl/gm$$

and

$$a = 0.70$$

Therefore for nylon-6 we have

$$[\eta] = 75 \times 10^{-5}(\overline{M}_v)^{0.7} \qquad \text{(III-5)}$$

or

$$\overline{M}_v = \left(\frac{[\eta] \times 10^5}{75}\right)^{1/0.7} \qquad \text{(III-6)}$$
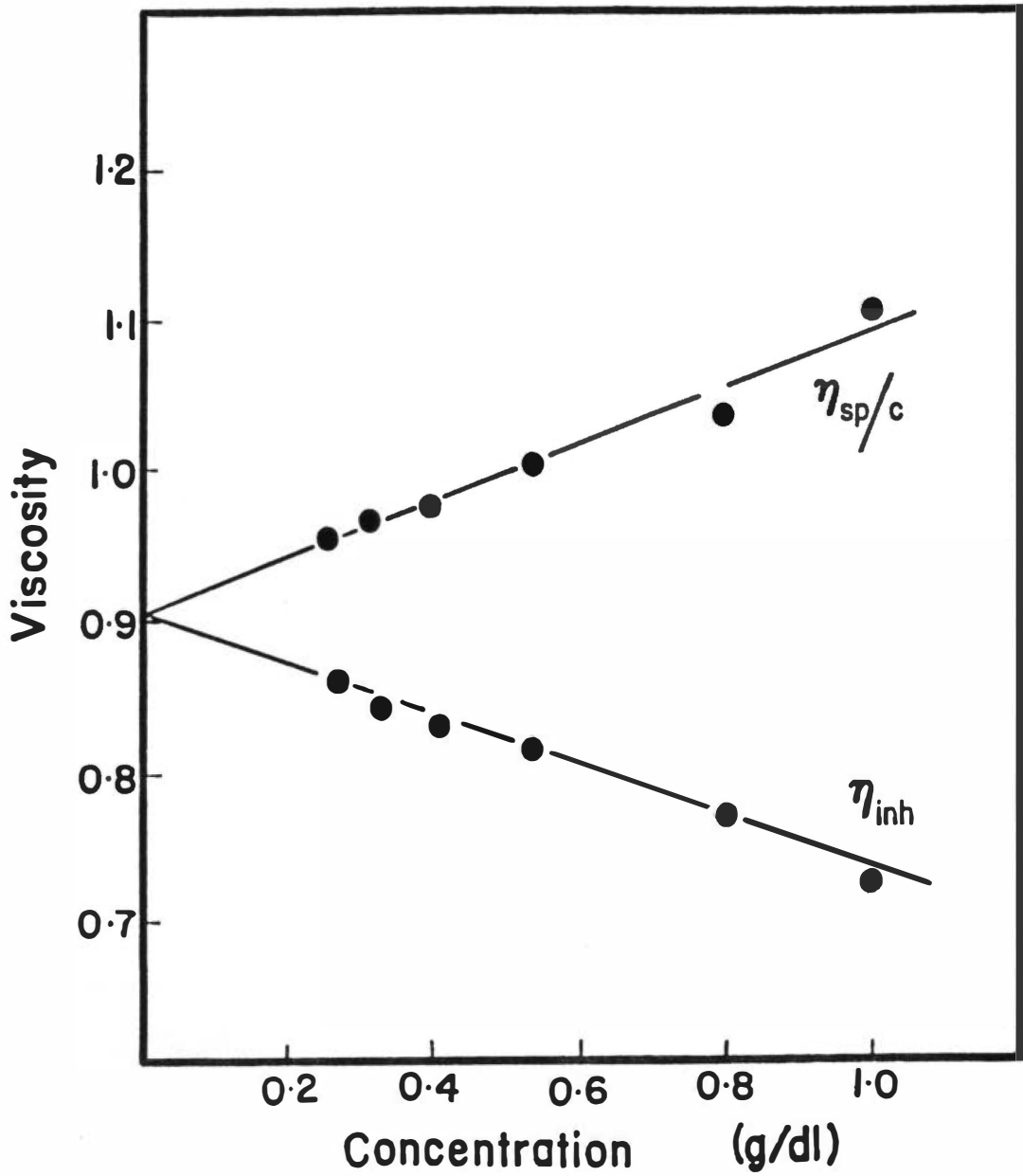
Figure III-1.   Dilute solution viscosity data for the low molecular
weight material.

Thus, the viscosity average molecular weights were calculated for each nylon-6 polymer from their corresponding intrinsic viscosities. The values are given in Table 1.

D. DEGRADATION CHARACTERISTICS

Degradation of each polymer was studied after they were melt spun. Nylon-6 polymer was melted in the extruder barrel and was extruded out, allowing the fiber to fall due to gravity without using a take-up device. Dilute solution viscosity measurements were made on the fibers thus collected. The procedures for determining the intrinsic viscosity and the viscosity average molecular weight were the same as described earlier. Table 2 shows the intrinsic viscosities and viscosity average molecular weights before and after extrusion and the percent drop in the viscosity average molecular weight. The undried extrudates were used here and the molecular weight drop would have been lower, had the extrudates been dried before measurement.

E. MELT SPINNING EXPERIMENTS

The Fourne extruder-spinning machine made by Fourne Associates of West Germany was used to spin the nylon-6 filaments. A schematic of a conventional melt spinning process is shown in Figure III-2. Fibers were melt spun at different take-up velocities and different mass throughputs.

Table 2. Degradation characteristics

Material	Intrinsic Viscosity $[\eta]$		Viscosity Average Molecular Weight, $\overline{M}_v$		Percent Drop in $\overline{M}_v$
	Before Extrusion	After Extrusion	Before Extrusion	After Extrusion	
Allied					
LBS	1.170	1.1375	36,440	35,000	3.95
BHS72918	1.525	1.402	53,210	47,190	11.32
HMW	1.901	1.66	72,900	60,070	17.61
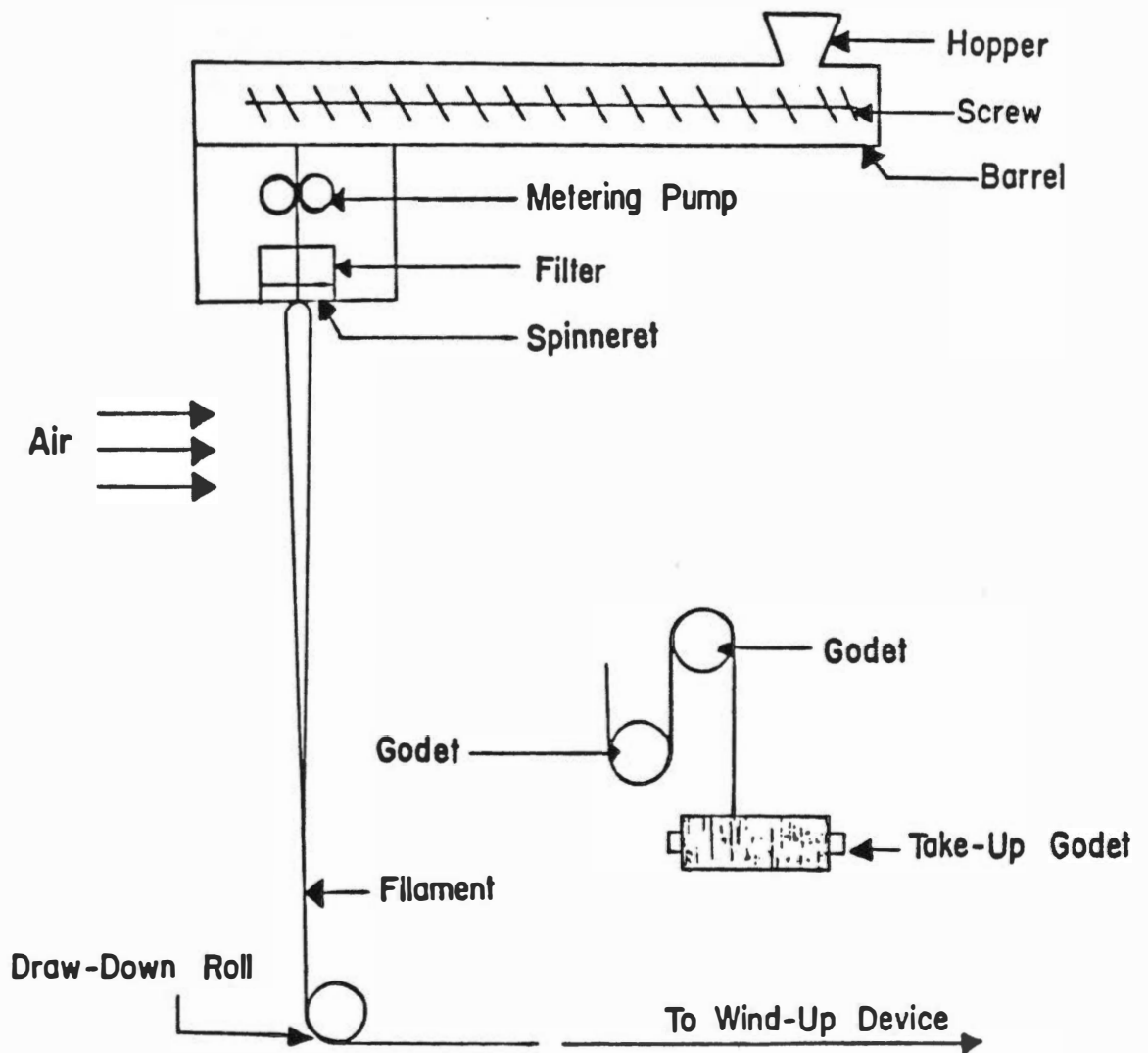
Figure III-2. Schematic of melt spinning process.

Fourne Screw Extruder

The Fourne screw extruder consists of a 13 millimeter diameter screw which receives polymer pellets by gravity feed from a 7 liter, nitrogen purged hopper. The extruder supplies molten polymer at constant pressure to a gear pump which provides a constant polymer flow rate to the spinneret. The discharge stream from the meter pump passes through a 325 mesh filter screen and through a single capillary spinneret. The dimensions of the capillary were 0.762 mm diameter and 3.81 mm long, with an L/D ratio of five. The extruder and spinning head assembly was wrapped with electric band heaters arranged to provide four separate heating zones. Four controllers were used to maintain the desired temperatures in each of these four zones.

Two platinum-resistance thermometers are inserted into the polymer stream to measure the polymer temperature at the two points. They are positioned in the extruder discharge stream and the meter pump discharge stream, and the temperatures are indicated by a meter on the control panel. The melt pressure is indicated by a Dyanisco pressure gauge. Feedback to the extruder speed controller also causes slight changes in the screw speed to assist in maintaining constant extruder discharge pressure. Gear pump speed can be manually adjusted by means of a variable speed box to obtain a desired flow rate of the polymer melt. Once set, the flow rate remains constant.

The entire assembly of the extruder and spinning block is mounted on a vertical steel column. It can be moved up and down the

column with the help of a motor. Further details of the various parts of the extruder and its operating and maintenance instructions are given in (26).

All except the highest molecular weight (HMW) polymer were melt spun at 260°C. For the HMW, due to filament breakage at 260°C, the experiments were conducted at 265°C. The filaments were spun at different air intake pressures of the aspirator, ranging from 2 psig to 85 psig. Two different mass flow rates, 3.55 gm/min and 5.55 gm/min, were used in the study. The spin path was about 13 feet and the ambient air at 21°C. The take-up velocity in meters/minute were calculated from the diameter and density of the filament, and the mass flow rate

$$m(\frac{gm}{min}) = \rho(\frac{gm}{cm^3}) \times A(cm^2) \ V(\frac{cm}{min}) \qquad (III-7)$$

where m is the mass flow rate, ρ the density, A the cross-sectional area ($\pi d^2/4$, d is the diameter in (cm)). Equation III-7 can be expressed as

$$V = m \times \frac{1}{\rho} \times \frac{4}{\pi d^2} \qquad (III-8)$$

V the take-up velocity in m/min is thus calculated.

Take-Up Machine

A schematic of the air jet aspirator is shown in Figure III-3. This device, supplied by Rhone Poulene of France, was used to draw
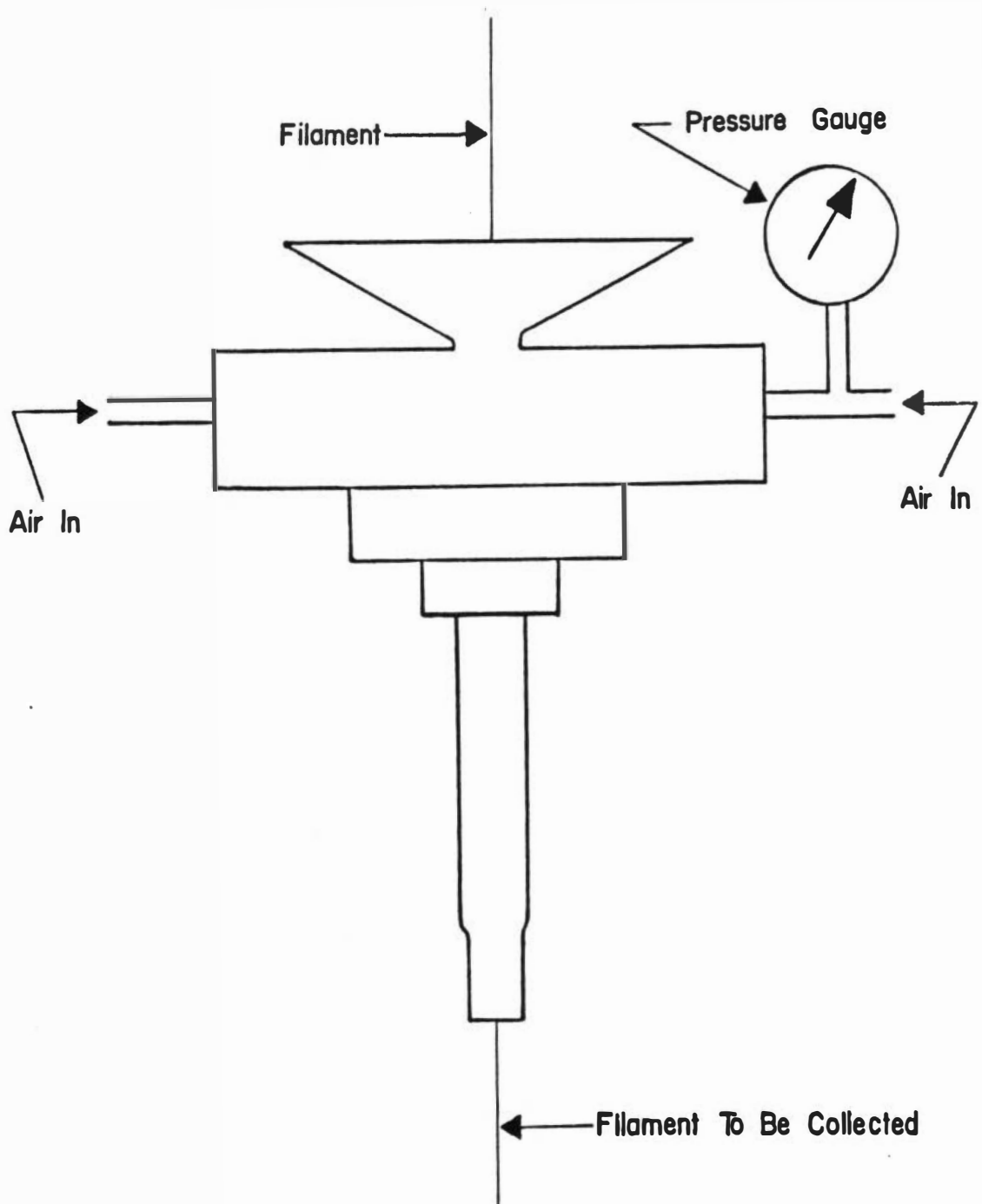
Figure III-3.   Schematic of air-jet aspirator.

down the spun nylon-6 filaments. Pressurized air was used to produce a suction force at the filament entrance of the aspirator. The device also has a pressure indicator of the air applied. The filaments are sucked down and emerge from the bottom of the tube. They are often collected in a cardboard box or on a clear sheet of cardboard. The aspirator was positioned at a distance of 13 feet (or 400 cm) from the spinneret (Figure III-4). Distances between the aspirator and spinneret significantly less than 400 cm resulted in filament breakage. Filaments are usually drawn at pressures of 2, 20, 40, 60, 70 and 85 psig. The linear fiber velocities were evaluated based on the fiber diameter and density and the mass flow rate.

Fiber Diameter Measurements

The diameters of spun, conditioned nylon-6 filaments were measured using an Olympus microscope, model POS, with a 10X lens and a 0.10 cm microscale. Twenty filaments were picked from different parts of the fiber bundle and their diameters measured. The average was calculated and the diameters expressed in microns. These are also expressed in denier by using the expression from the definition of a denier:

1 denier = weight of 9000 m of fiber

i.e.,

$$1 \text{ den} = \frac{\pi d^2}{4} \times 9 \times 10^5 \times \rho \qquad \text{(III-9)}$$
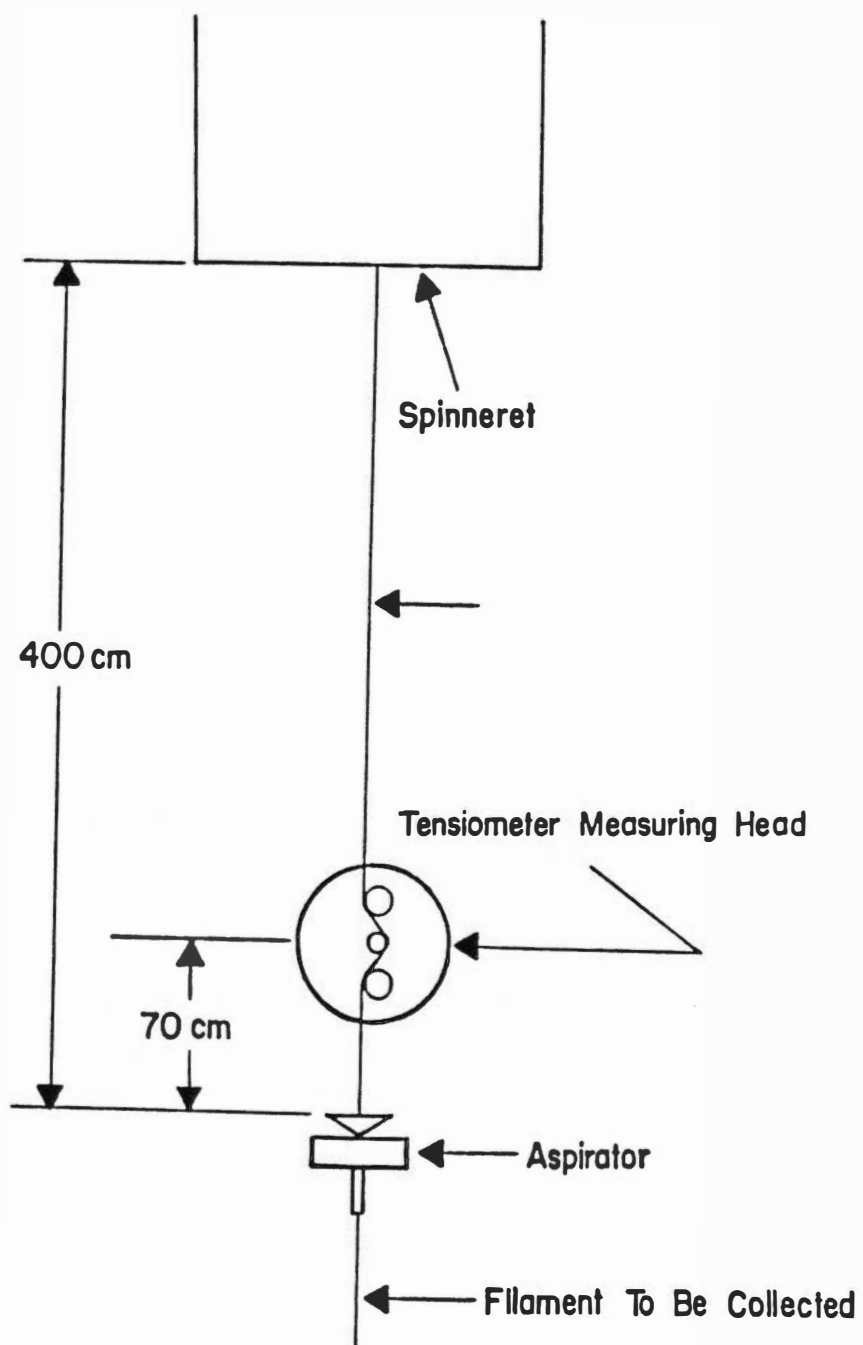
Figure III-4. Schematic of draw down and tension measurement.

where

    d is the diameter of fiber in cm,

    ρ is the density of fiber in g/cm^3.

Fiber Tension Measurements

Spinline tensions were measured using a Rothschild tensiometer equipped with a four gram measuring head. The schematic of the experimental setup for spinline tension measurement is shown in Figure III-4. The measuring head was positioned at a distance of about 70 cm above the inlet of the aspirator. All measurements were made on the zero to ten scale in this study. The calibration of the instrument was done according to the manufacturer's instructions. The instrument was calibrated everytime the fiber diameter changed.

Conditioning of Fibers

All spun filaments were conditioned at 65 percent relative humidity and 68°F in a conditioned room. The filaments were allowed to equilibrate for 24 hours before any characterization was done.

F. CHARACTERIZATION OF SPUN FILAMENTS

Structural characterization of spun, conditioned nylon-6 filaments was done by density measurements, wide angle x-ray diffraction (WAXS) and birefringence studies. The relative amounts of crystalline and amorphous phases were estimated using the procedure of Gianchandani et al. (36), which involves the combination

of density and WAXS data. WAXS and birefringence measurements were used to study the orientation of the filaments. Mechanical properties were obtained for the samples, using an instron tensile testing machine.

Density

Densities of the samples were determined by a density gradient column which was built according to the specifications of the American Society of Testing Materials under the designation D1505-68 (28).

A mixture of carbon tetrachloride and toluene was used to make solution A (heavy) and solution B (light). Two concentric cylinders connected by a glass tube were used to facilitate the mixing of solution A and solution B. The density gradient column was maintained at 23°C by means of circulating water. Six floats varying in densities from 1.10 to 1.15 gm/cm^3 were used to standardize and calibrate the column. The details of the calculations involved in the building of this column are given in Appendix A. Density readings for the different samples were obtained after the samples had stabilized in the column for at least 12 hours.

Wide Angle X-Ray Scattering (WAXS)

Flat plate film, wide angle x-ray diffraction patterns for the spun samples were obtained using a Philips Norelco x-ray generator. The radiation used was nickel filtered CuK_α of wavelength 1.542 Å. The x-ray unit was operated at 40 kv and 15 mA. The sample to film

distance was 2.91 cm, and the sample was fixed on a sample holder which was attached to the beam collimator. An exposure time of about 6 hours was allowed before developing the film.

X-Ray Diffractometer Scans

A Rigaku x-ray diffractometer was used to obtain 2θ scans of the spun sample. Fibers wound on H-frames in a parallel alignment were used. The diffractometer was used to obtain both the 2θ scans to evaluate the different phases and the azimuthal scans to evaluate the orientation factors. To obtain the orientation factors, the 2θ value for an hkl plane was determined and the diffractometer was set at this 2θ value. The sample was then rotated through the angle from equator to meridian in steps of 2 degrees and the intensity of the diffracted beam at each angle was measured in counts using a counter. The intensities were used to calculate the average of $\cos^2\phi$ using the equation

$$\overline{\cos^2\phi} = \frac{\int_0^{\pi/2} I_{hkl}(\phi) \cdot \cos^2\phi \cdot \sin\phi \, d\phi}{\int_0^{\pi/2} I_{hkl}(\phi) \cdot \sin\phi \, d\phi} \qquad \text{(III-10)}$$

where $I_{hkl}(\phi)$ is the intensity of the diffracted beam from the (hkl) planes making an angle ϕ with the fiber axis. Before integrating, the background intensity was subtracted from the measured intensity. The background intensity was obtained by measuring the scattered intensity with 2θ value set at positions on either side of $2\theta_{hkl}$ position.

For spun nylon-6 samples, (020) reflections with $2\theta = 11$ degrees were used. The b-axis orientation factors were obtained from

$$f_b = \frac{3 \overline{\cos^2 \phi} - 1}{2} \qquad \text{(III-11)}$$

These orientation factors were obtained for fibers spun at different take-up velocities.

Birefringence Measurements

Birefringence of the spun filaments were measured using an Olympus polarizing microscope, model POS, with a Lietz (10λ) Berek compensator. The birefringence was calculated by dividing the measured retardation by the fiber diameter. The diameters of the fibers were measured with a Bausch and Lomb filar micrometer eye-piece. The compensator constant required for calculating the retardation was obtained by using two test plates of known retardation and then using the average of the two constants. The two plates used were a one-fourth wavelength plate and a one-half wavelength plate. The compensator constant for the Lietz (10λ) Berek compensator was found to be c/10,000 equal to 2.065.

The amorphous orientation factors can be determined by the equation

$$\Delta n = \overline{x} \, \Delta_c^o \, f_c + (1 - \overline{x}) \, \Delta_a^o \, f_a + \Delta n_{form} \qquad \text{(III-12)}$$

where

n is the total measured birefringence;

$\bar{x}$ is the total crystalline fraction;

Δ_c^o is the intrinsic birefringence in the crystalline phase;

f_c is the crystalline orientation function;

Δ_a^o is the intrinsic birefringence of the amorphous phase;

f_a is the amorphous orientation function;

Δn_{form} is the form birefringence.

For nylon-6, Δ_c^o and Δ_a^o have values of 0.0963 and 0.0825, respectively (77). The total crystalline fraction and the crystalline orientation function used were those obtained from WAXS.

Quantitative Analysis of X-Ray Patterns

The relative amounts of α, γ and amorphous phases were evaluated by the method of Gianchandani, Spruiell and Clark (36). The amount of γ-phase in a given sample was obtained by

$$X_\gamma = \frac{R - R_\alpha^S}{R_\gamma^S - R_\alpha^S} \cdot X_\gamma^S \qquad (III-13)$$

where

X_γ is the mass fraction of the sample which is γ-phase;

R is the intensity ratio of the sample;

R_α^S is the intensity ratio of the standard α sample;

R_γ^S is the intensity ratio of the standard γ sample;

X_γ^S is the mass fraction of γ-phase in the standard γ sample.

Standard α and γ samples were made by Gianchandani et al. (36) and the values obtained for R_α^S, R_γ^S and X_γ^S were 1.11×10^{-2}, 128×10^{-2} and 0.75, respectively. The standard α and γ samples were assumed to contain negligible amounts of γ and α-phases, respectively. R was obtained by

$$R = \frac{\int I_{020} \, d(2\theta)}{\int_{14°}^{28°} I_{eq} \, d(2\theta)} \qquad (III\text{-}14)$$

where I_{020} is the intensity obtained from the meridional scan containing the 020 peak at about 11° 2θ. A 2θ scan from 7-15° was made. I_{eq} is the intensity obtained from the equatorial scan in the range 14-28° 2θ. The γ-phase fraction was calculated using these relationships. The α-phase fraction is given by

$$x_\alpha = \frac{(\bar{V} - \bar{V}_{am}) - x_\gamma(\bar{V}_\gamma - \bar{V}_{am})}{\bar{V}_\alpha - \bar{V}_{am}} \qquad (III\text{-}15)$$

which resulted from

$$x_\gamma + x_\alpha + x_{am} = 1.0 \qquad (III\text{-}16)$$

and

$$\bar{V} = x_\gamma \bar{V}_\gamma + x_\alpha \bar{V}_\alpha + x_{am} \bar{V}_{am} \qquad (III\text{-}17)$$

In Equations (III-14), (III-15) and (III-16),

x_α is the mass fraction of α-phase in the sample;

x_γ is the mass fraction of γ-phase in the sample;

x_{am} is the mass fraction of amorphous phase in the sample;

$\bar{V}$ is the specific volume of the sample;

$\bar{V}_\gamma$ is the specific volume of the γ-phase;

$\bar{V}_\alpha$ is the specific volume of the α-phase;

$\bar{V}_{am}$ is the specific volume of the amorphous phase.

The specific volumes were obtained from the densities of the samples. The values ρ_γ = 1.17 gm/cm^3, ρ_α = 1.23 gm/cm^3 and ρ_{am} = 1.08 gm/cm^3, which were obtained by Gianchandani et al. (36) were used in our calculations. Equations (III-12), (III-14) and (III-15) allow computation of x_γ, x_α and x_{am} for any sample from the measurement of R and the density (specific volume) of that sample.

Mechanical Properties

A table model Instron Tensile Tester maintained by the U.S. Department of Agriculture was used to obtain the force-elongation data for fibers spun at different take-up velocities and different mass throughputs. All tests were made after conditioning the samples in 65 percent relative humidity and 68°F for 24 hours. The tests were also made at the same conditions in a conditioning room also maintained by the U.S.D.A.

A gauge length of one inch and a cross-head speed of one inch per minute were used. Tensile strength, initial modulus and elongation at break were evaluated from the force-elongation data.

CHAPTER IV

STRUCTURE DEVELOPMENT OF MELT SPUN FIBERS

A. GENERAL

Previous studies by Bankar et al. (8,10) have shown that nylon-6 is amorphous in a running spinline at speeds up to 1000 m/min, and the development of crystallinity takes place on the bobbin. Gianchandani et al. (35,36) have studied the development of crystallization and analyzed the primary and secondary stages of crystallization. They have also evaluated the relative amounts of crystalline and amorphous phases present in nylon-6 filaments, using their newly developed γ-index method. Since all these studies were done at low speeds, it was decided in the present work to undertake studies at higher spinning speeds and also to investigate the effect of molecular weight on the structure and properties of these fibers. An air jet aspirator described in Chapter III was used to obtain nylon-6 samples at high speeds. The maximum attainable take-up velocity using the air jet device was reduced as the molecular weight of the polymer increased. Figure IV-1 shows the take-up velocities achieved for different air pressures in the air jet aspirator for a polymer mass throughput of 3.55 g/min. It shows clearly the decrease in take-up velocity at any given air pressure as the molecular weight of the polymer increases. For the lower
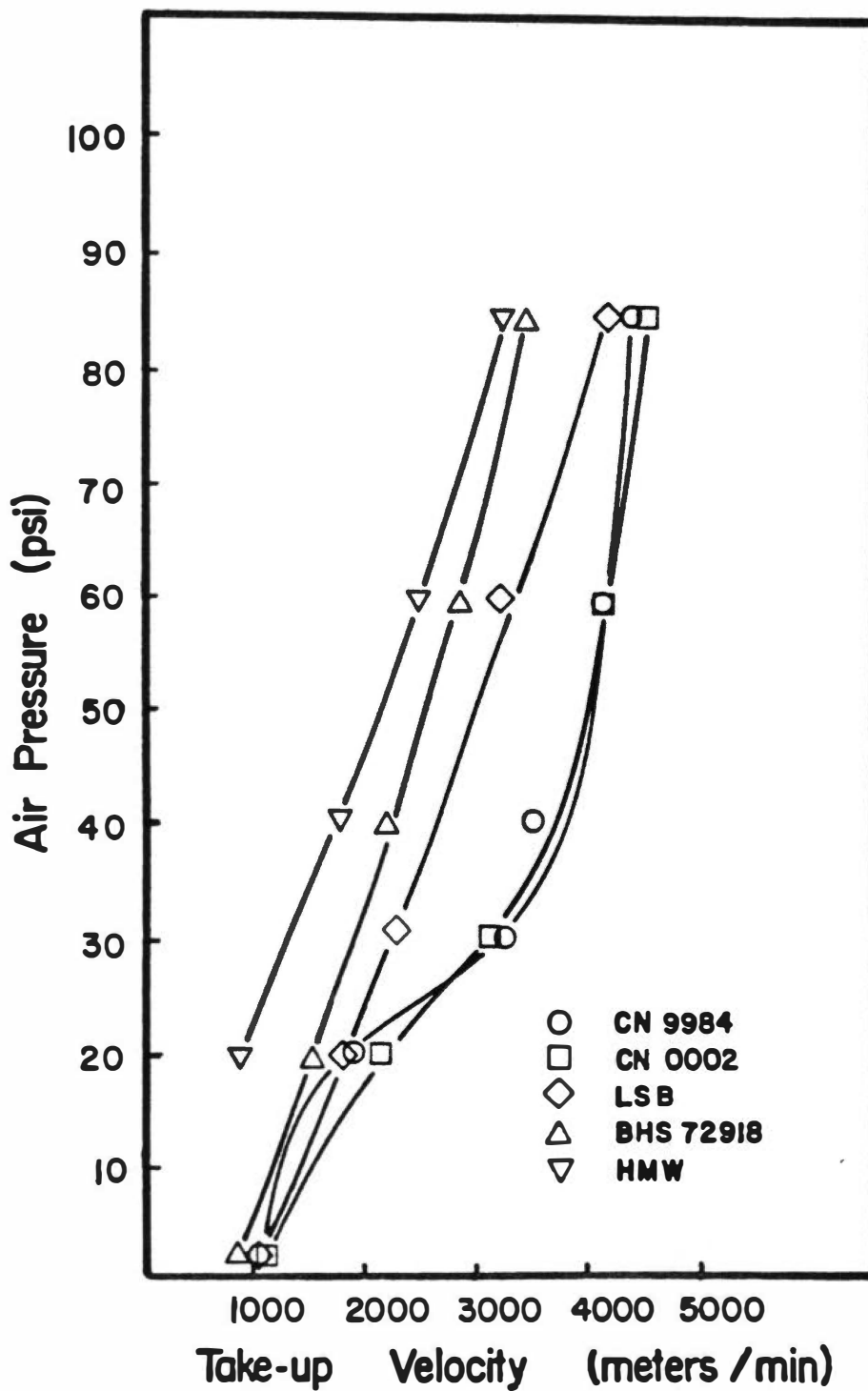
Figure IV-1. Take-up velocity as a function of air pressure in the aspirator (mass throughput - 3.55 g/min).

molecular weight polymers, formation of a neck is observed at speeds above 2000 m/min and the reason for this is not understood.

It is to be noted that the fiber diameter or fiber denier decreases as the take-up velocity increases, since the mass through-put remains constant. For example, in the case of the high molecular weight (HMW) samples, the diameter of the fiber spun at about 870 m/min and 3.55 g/min throughput is 67.5 microns (or 36.3 denier) while that spun at a speed of about 3200 m/min has a diameter of 35.4 microns (or 10.0 denier). The diameters of fibers spun at roughly the same two speeds but at a higher throughput of 5.55 g/min are 86.3 microns (or 59.4 denier) and 43.8 microns (or 15.4 denier), respectively. The diameter data in microns and denier for all the fibers are given in Appendix B.

B. THE DEVELOPMENT OF STRESSES IN THE SPINLINE

Figures IV-2 and IV-3 show the variation of spinline stresses with take-up velocity and mass flow rate for polymers of different molecular weights. The spinline stress was found to increase with take-up velocity for all the polymers at a specified mass flow rate. An increase in the mass flow rate resulted in a decrease in the spinline stress at a given take-up velocity. Such an increase in throughput also results in an increase in denier at a given take-up velocity, as noted earlier. The effect of increasing the mass throughput at constant denier (and hence much higher take-up velocities) is to produce higher spinline stresses.
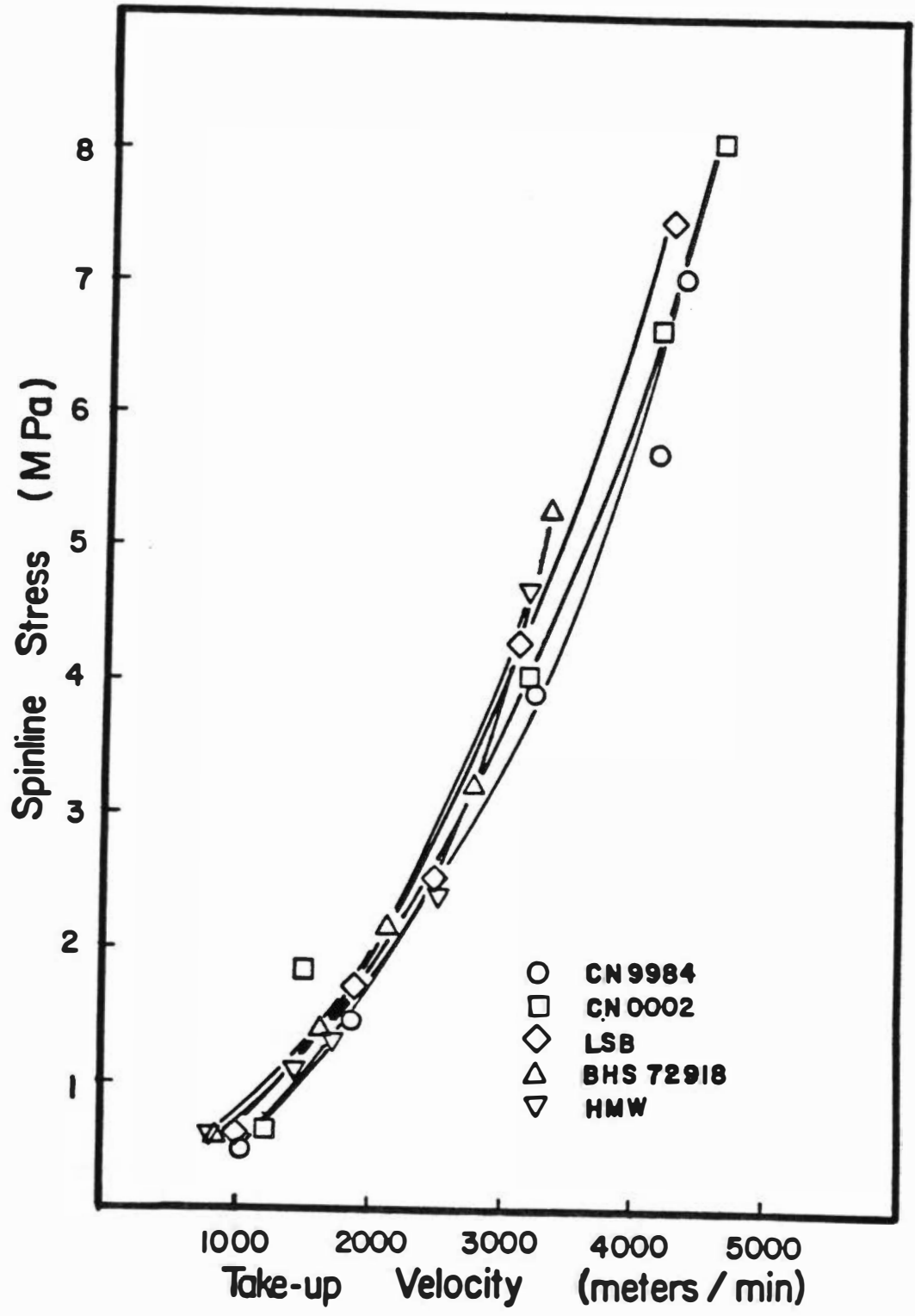
Figure IV-2. Spinline stress of nylon-6 fibers as a function of take-up velocity (mass throughput - 3.55 g/min).
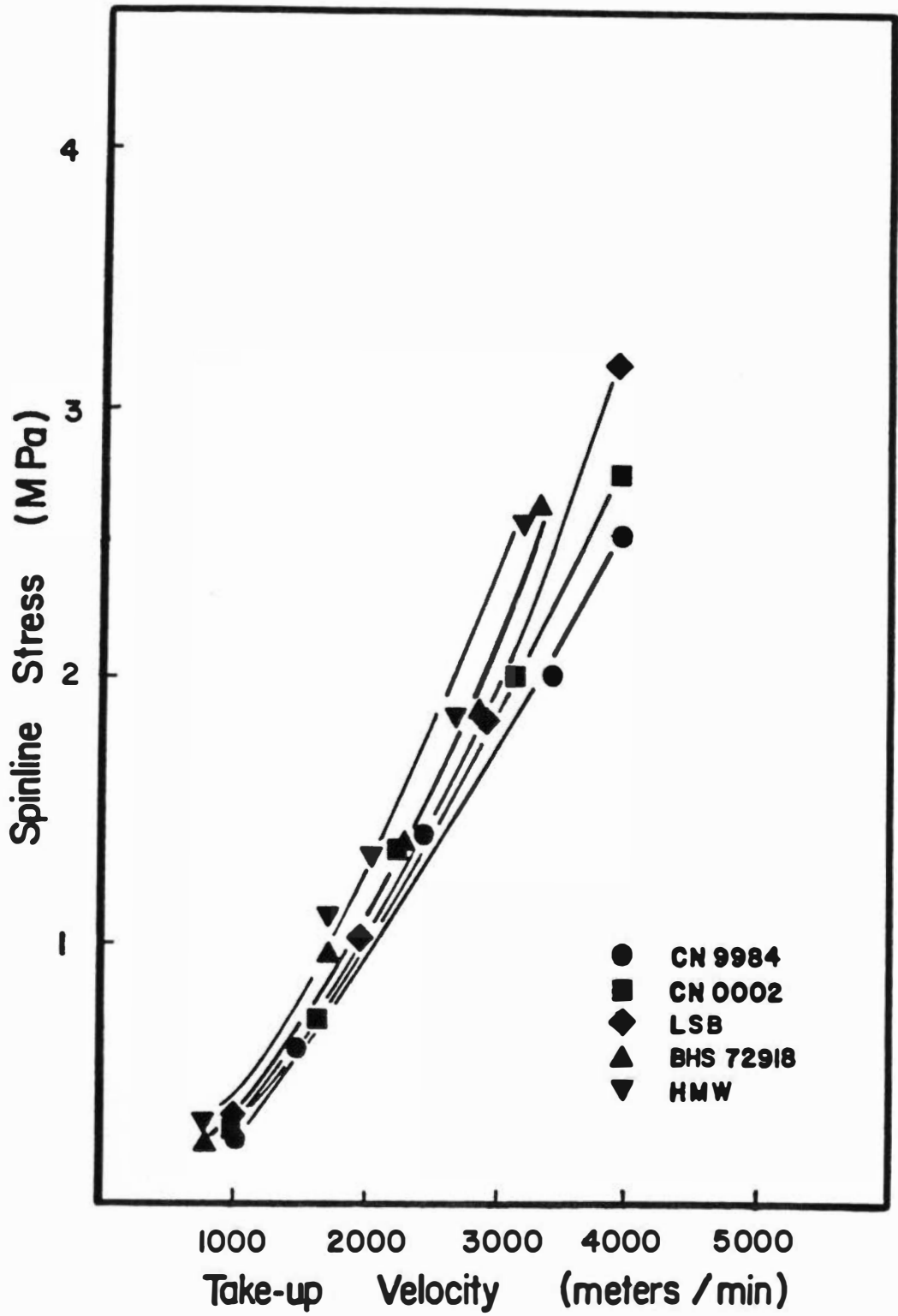
Figure IV-3. Spinline stress of nylon-6 fibers as a function of take-up velocity (mass throughput - 5.55 g/min).

The effect of molecular weight on the spinline stresses is shown more clearly in Figure IV-4. There is a good correlation between molecular weight and spinline stress. Though the general trend is toward an increased spinline stress with increasing molecular weight, the increase is higher at higher take-up velocity. This is evident from Figure IV-4 and would be expected based on the higher melt-elongation rates accompanying the higher take-up velocities. The stress levels in the melt ranged from 0.50 MPa to 8.0 MP for lower mass flow rates and from 0.25 MPa to 3.25 MPa for higher mass flow rates.

The effect of spinline stresses on morphology and mechanical properties are dealt with in a later part of this chapter and next chapter, respectively.

C.   QUALITATIVE STRUCTURAL CHARACTERISTICS

Figure IV-5 shows the WAXS patterns for conditioned filaments of low molecular weight material (CN9984) spun at different take-up velocities and a mass throughput of 3.55 g/min. The patterns indicate that a significant level of crystallinity is present. At lower spinning speeds, the patterns exhibit a broad equatorial peak and relatively weak meridional peaks are observed. As the take-up velocity increases, the equatorial peaks become much sharper. The meridional peaks become sharper, more intense and have lower azimuthal spread. At 4500 m/min, the 020 peaks become very intense and sharp. These reflections indicate a high γ-phase content in these fibers at high take-up velocities.
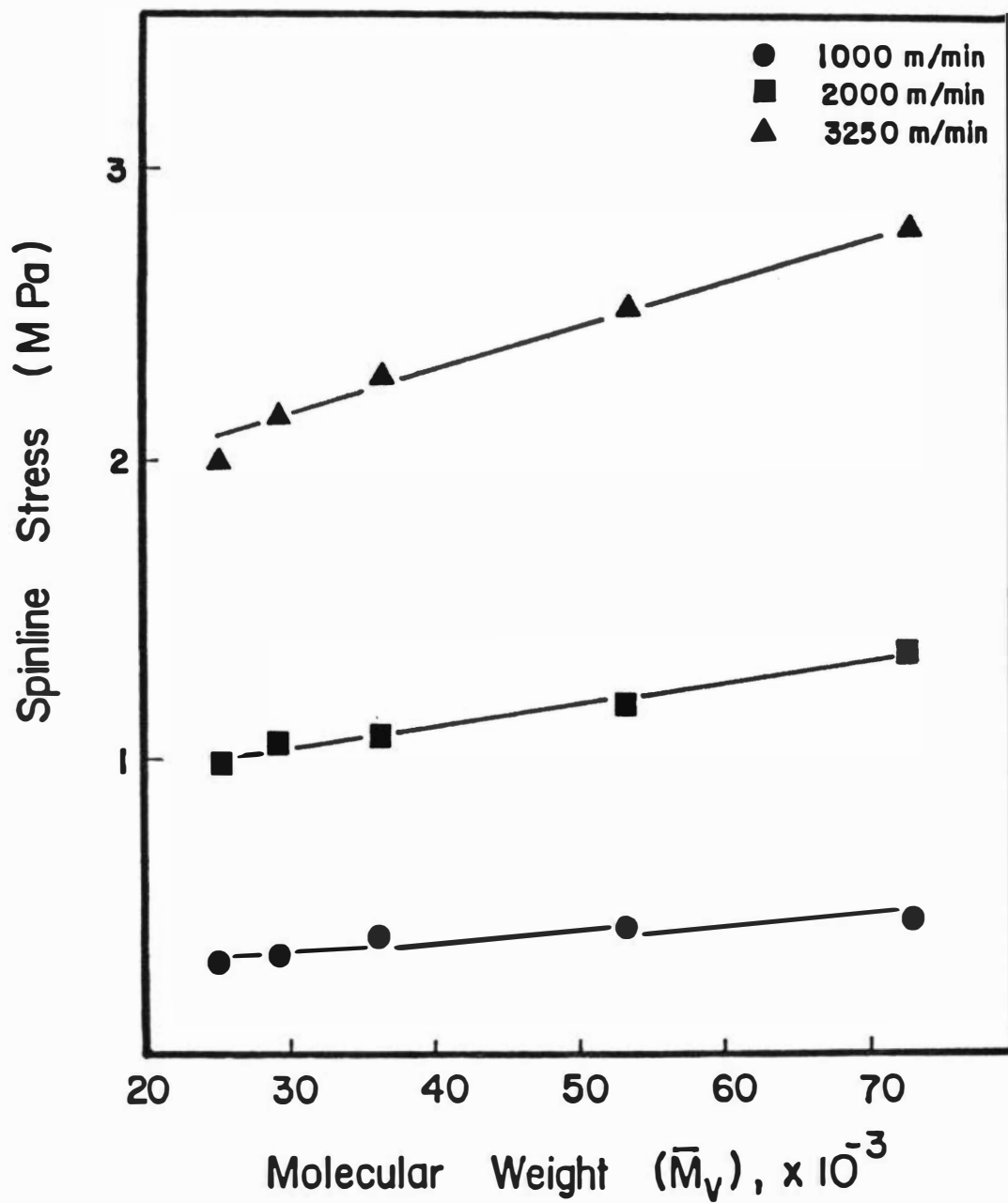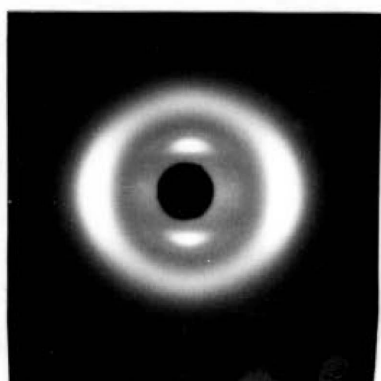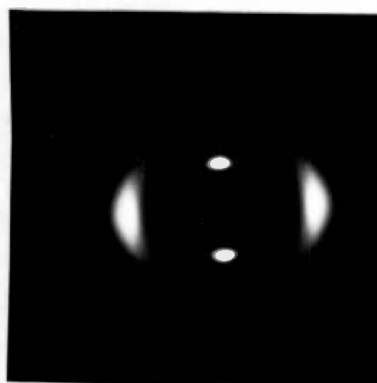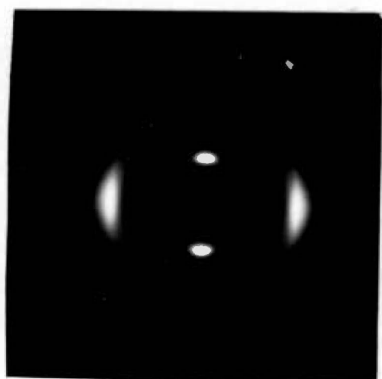
Figure IV-4. Spinline stress of nylon-6 fibers as a function of molecular weight (mass throughput - 5.55 g/min).
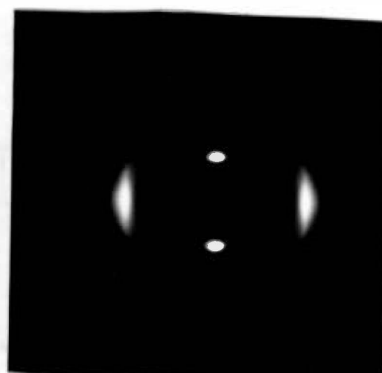
1000 m/min

2000 m/min

3200 m/min

4400 m/min

Figure IV-5. WAXS patterns of low molecular weight spun and con-
ditioned nylon-6 fibers (mass throughput - 3.55 g/min).

D. CRYSTALLINITY AND RELATIVE AMOUNTS
OF α AND γ-PHASES

The densities of the conditioned filaments were found to increase with the increase in take-up velocity, as shown in Figure IV-6 for lower throughputs and in Figure IV-7 for higher throughputs. The raw density data for each sample is tabulated in Appendix B. Figures IV-6 and IV-7 indicate that higher molecular weight samples generally show a higher density at a given take-up velocity. This could be due to a high α-phase content present in the higher molecular weight samples. The general trend seems to be an initial sharp increase and then a leveling off at high take-up velocities, though this is not the case with all the polymers.

The crystallinity and the relative amounts of α and γ-phases were calculated by the method of Gianchandani et al. (36) described in Chapter III. Variations in crystallinity with increase in take-up velocity for all the different molecular weight polymers are shown in Figure IV-8 for lower mass throughput and in Figure IV-9 for a higher mass throughput. It can be seen from these figures that crystallinity increases rapidly at lower take-up velocities and indicates a leveling-off trend as the take-up velocities increase. Comparison of these two figures shows that for a given polymer, the general trends at each mass flow rate are similar. The effects of molecular weight are best seen by cross plotting the data as in Figure IV-10. Increase in molecular weight increases the crystallinity slightly at lower take-up velocity, but this trend changes at higher take-up velocities.

Figure IV-6. Density of spun and conditioned nylon-6 fibers as a
function of take-up velocity (mass throughput -
3.55 g/min).

Figure IV-7. Density of spun and conditioned nylon-6 fibers as a function of take-up velocity (mass throughput - 5.55 g/min).

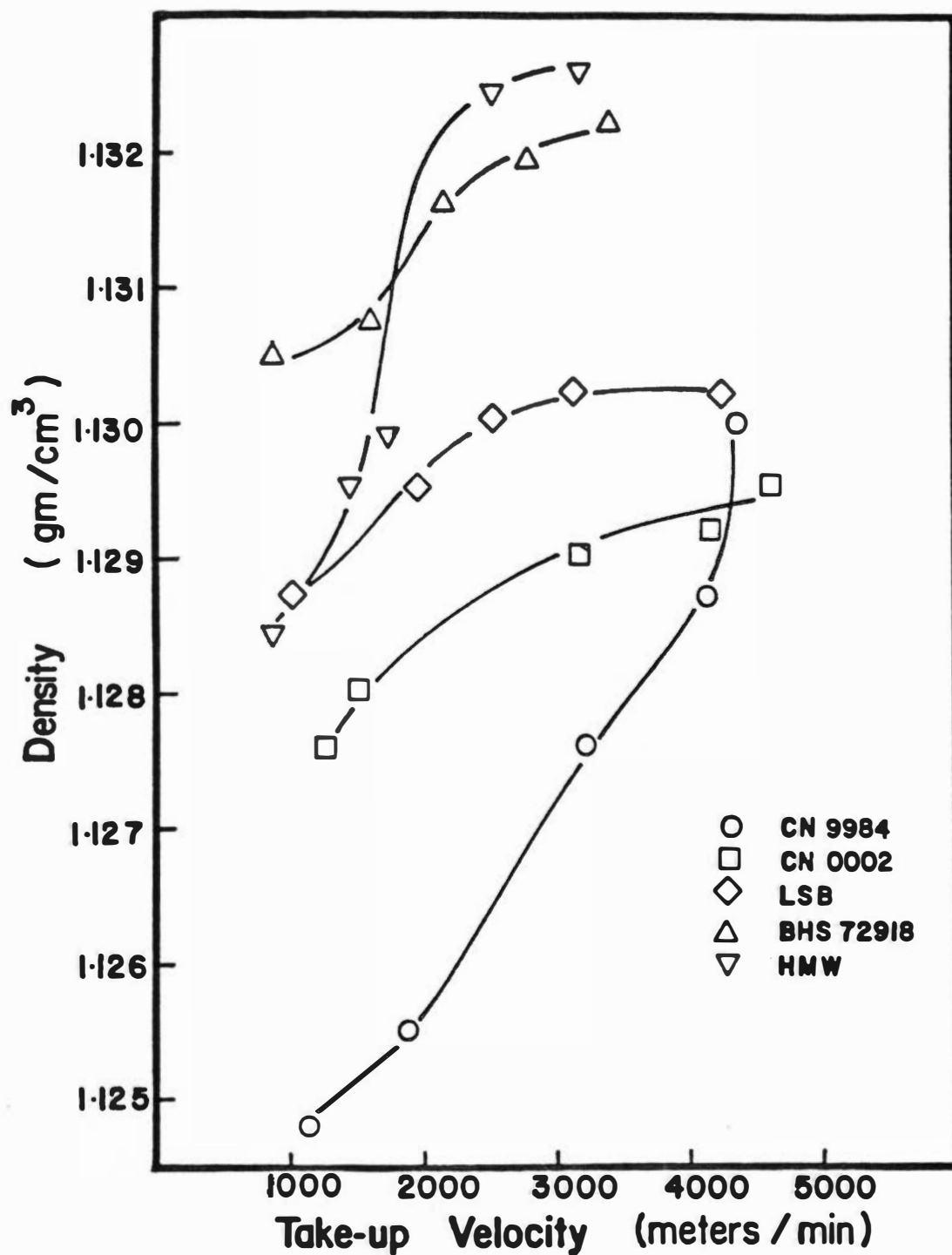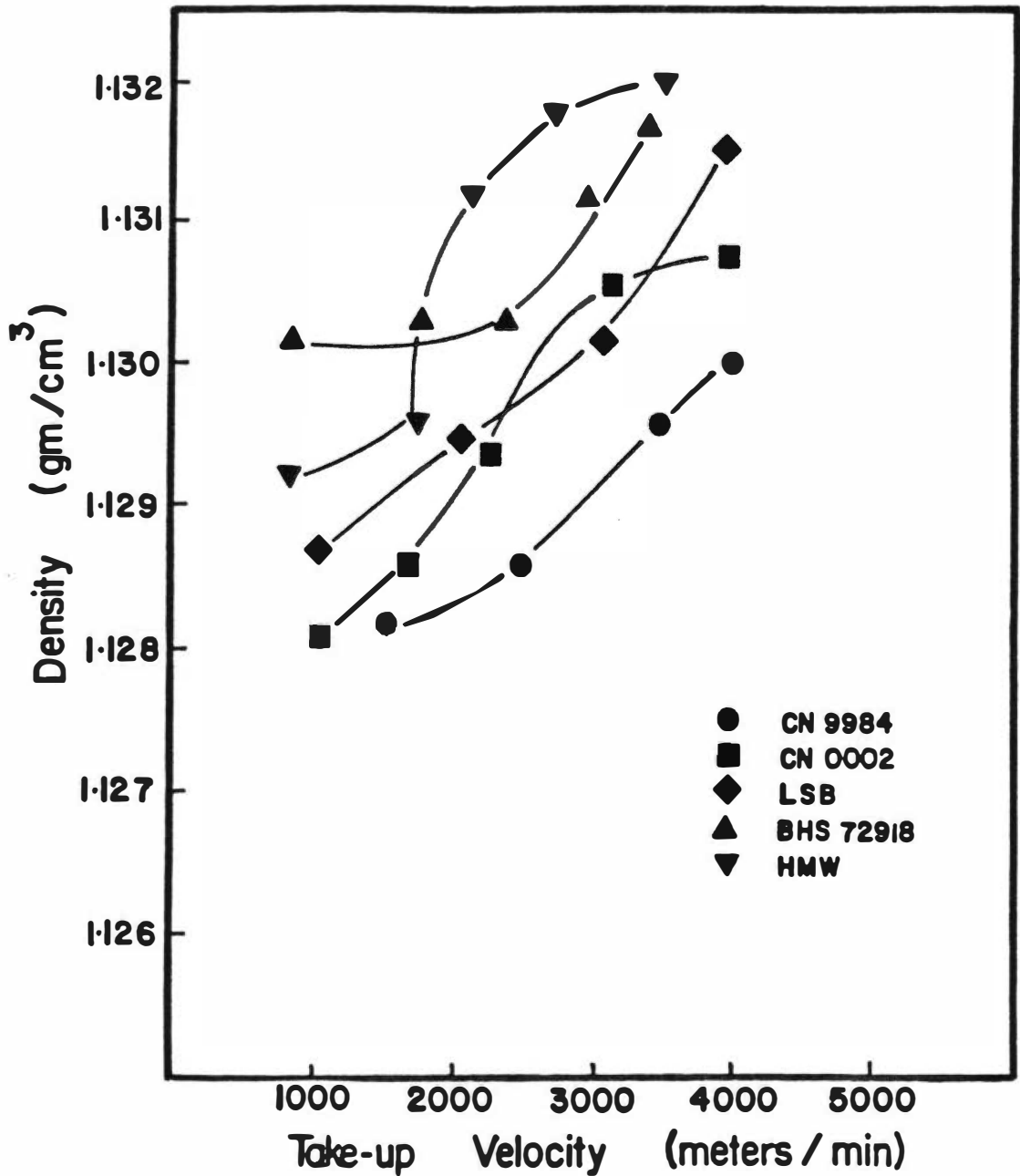Figure IV-8. Total crystalline fraction of spun and conditioned nylon-6 fibers as a function of take-up velocity (mass throughput - 3.55 g/min).
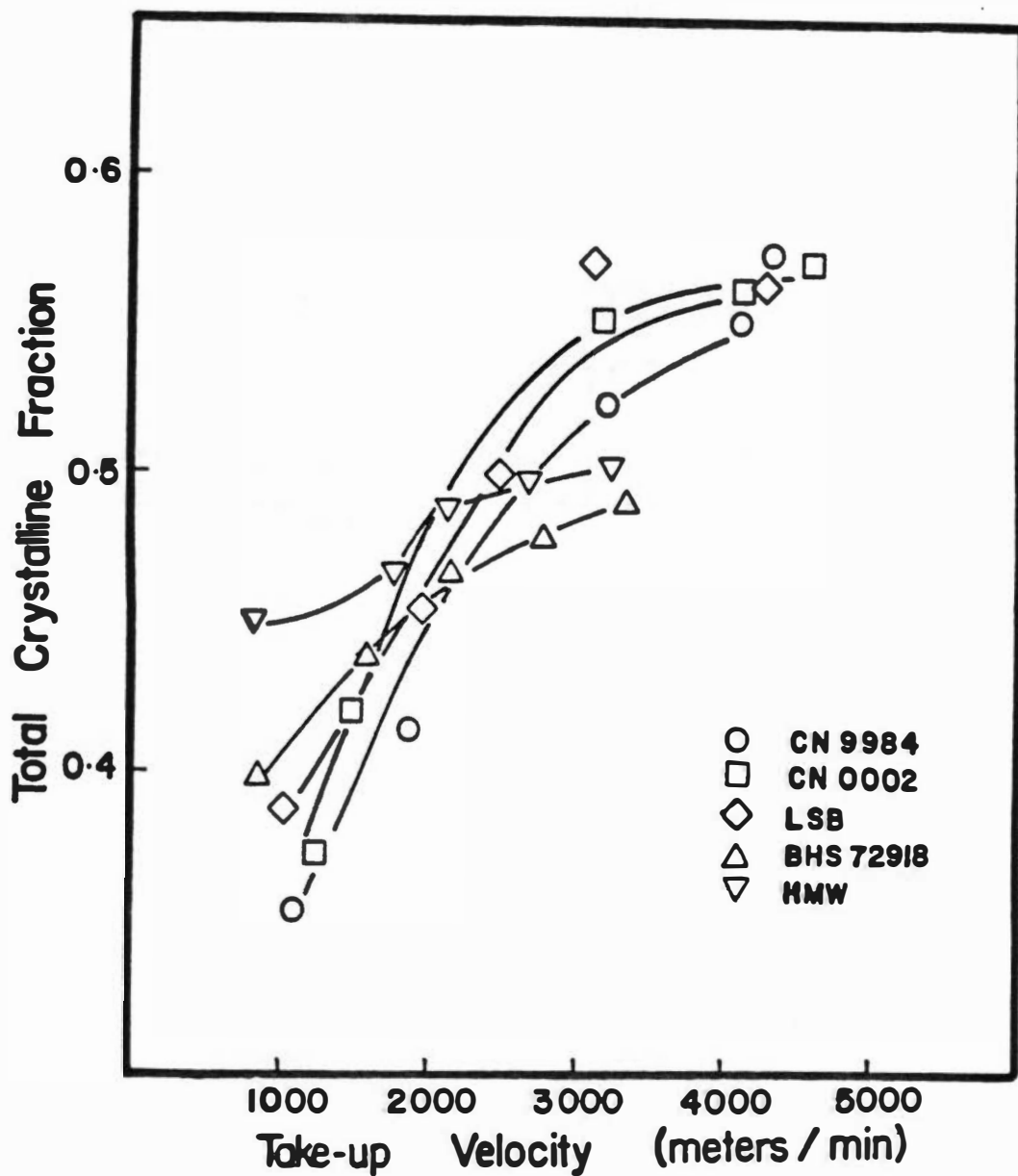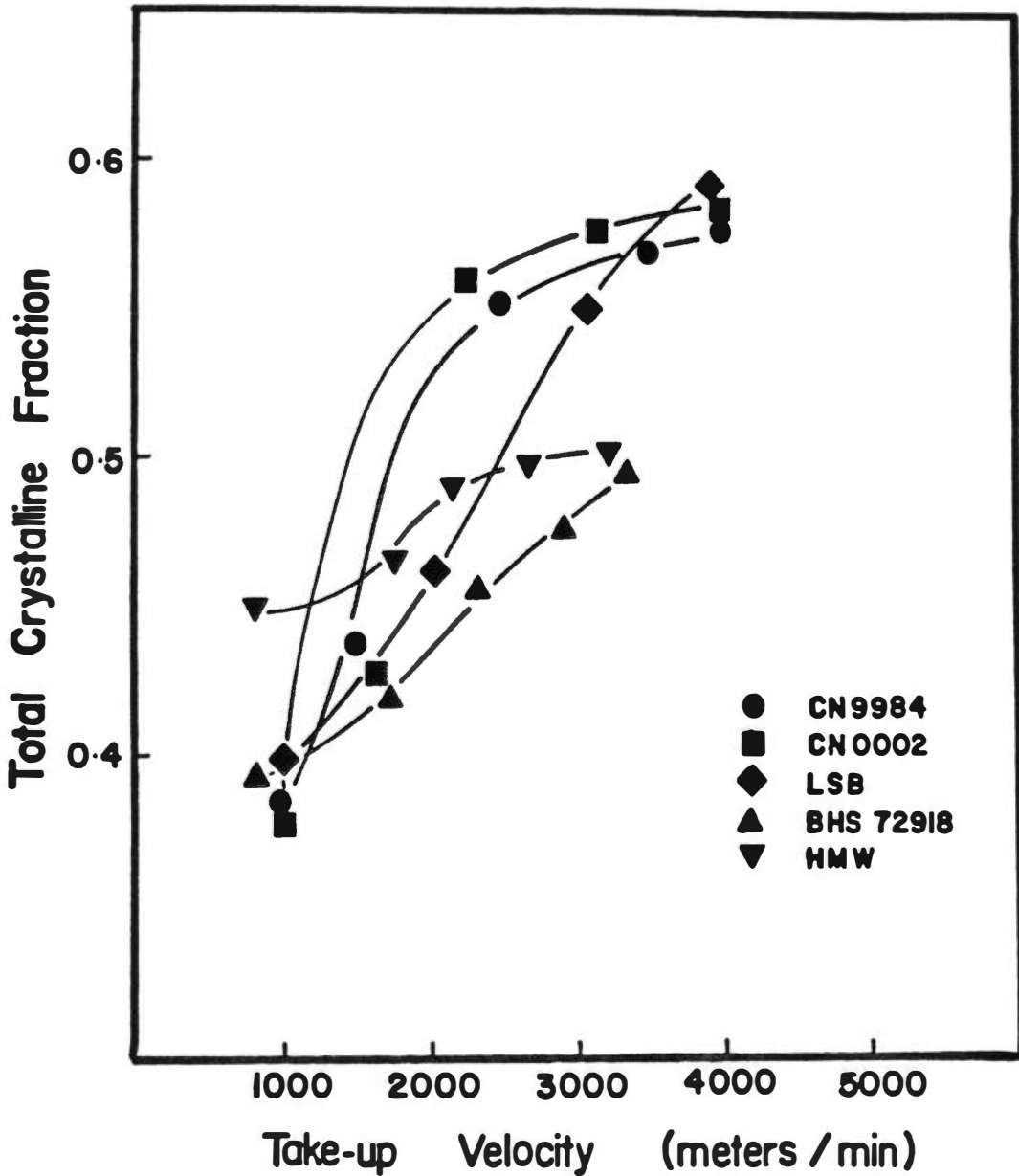
Figure IV-9. Total crystalline fraction of spun and conditioned nylon-6 fibers as a function of take-up velocity (mass throughput - 5.55 g/min).
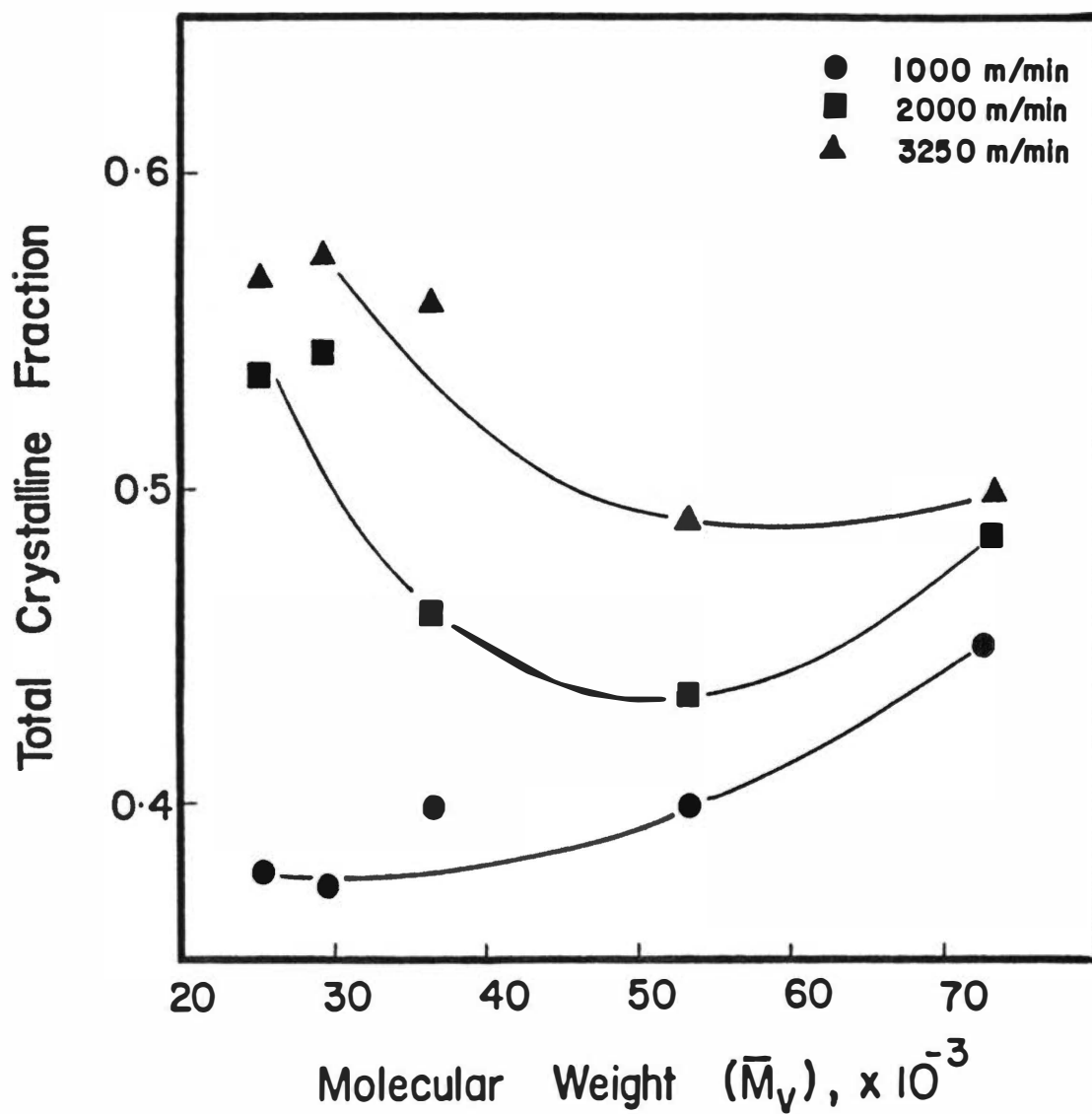
Figure IV-10. Total crystalline fraction of spun and conditioned nylon-6 fibers as a function of molecular weight (mass throughput - 5.55 g/min).

The effect of spinline stresses on the crystallinity is shown in Figures IV-11 and IV-12. The crystalline fraction increases up to stresses of about 2.0 MPa and then starts leveling off with further increase in the spinline stresses. The crystalline fraction starts from about 0.375 at stresses less than 0.5 MPa and reaches a value of almost 0.60. The crystallinity varies significantly from one molecular weight sample to another. The higher molecular weight samples seem less sensitive to stress level than do the three lower molecular weight samples. Since it is not known just what proportion of the crystallinity is developed on the threadline, and which developed during conditioning for each sample and take-up velocity, it is not possible to further interpret these results. It seems likely that differences in the relative amounts of crystallization in the threadline might produce such differences. Higher crystalline fractions are obtained for the higher mass throughput at a given stress. This probably results from the different cooling rates in the spinline caused by different mass flow rates.

Figures IV-13 and IV-14 show the effect of take-up velocity on γ-phase fraction and Figures IV-15 and IV-16 show the effect of take-up velocity on α-phase fraction for different mass throughputs. The γ-phase increases with take-up velocity until a certain value and starts to level off, while the α-phase decreases correspondingly before starting to level off with further increase in take-up velocities. A cross plot of the data showing the dependence of the relative amounts of phases upon the molecular weight is shown in
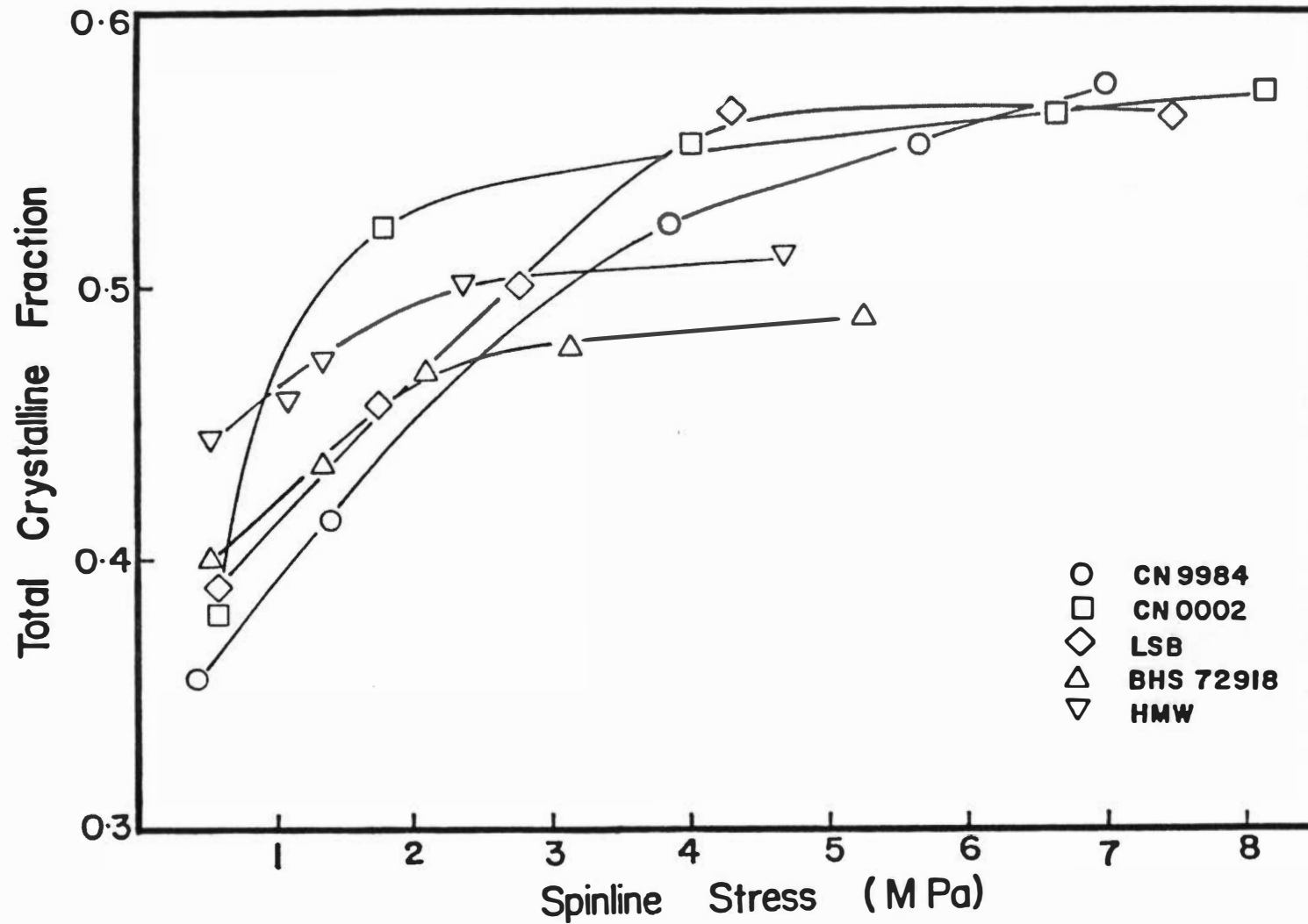
Figure IV-11. Total crystalline fraction of spun and conditioned nylon-6 fibers as a function
of spinline stress (mass throughput - 3.55 g/min).

Figure IV-12. Total crystalline fraction of spun and conditioned nylon-6 fibers as a function of spinline stress (mass throughput - 5.55 g/min).

Figure IV-13.   γ-Phase fraction of spun and conditioned nylon-6
fibers as a function of take-up velocity (mass
throughput - 3.55 g/min).

Figure IV-14. γ-Phase fraction of spun and conditioned nylon-6 fibers as a function of take-up velocity (mass throughput - 5.55 g/min).

Figure IV-15. α-Phase fraction of spun and conditioned nylon-6 fibers as a function of take-up velocity (mass throughput - 3.55 g/min).
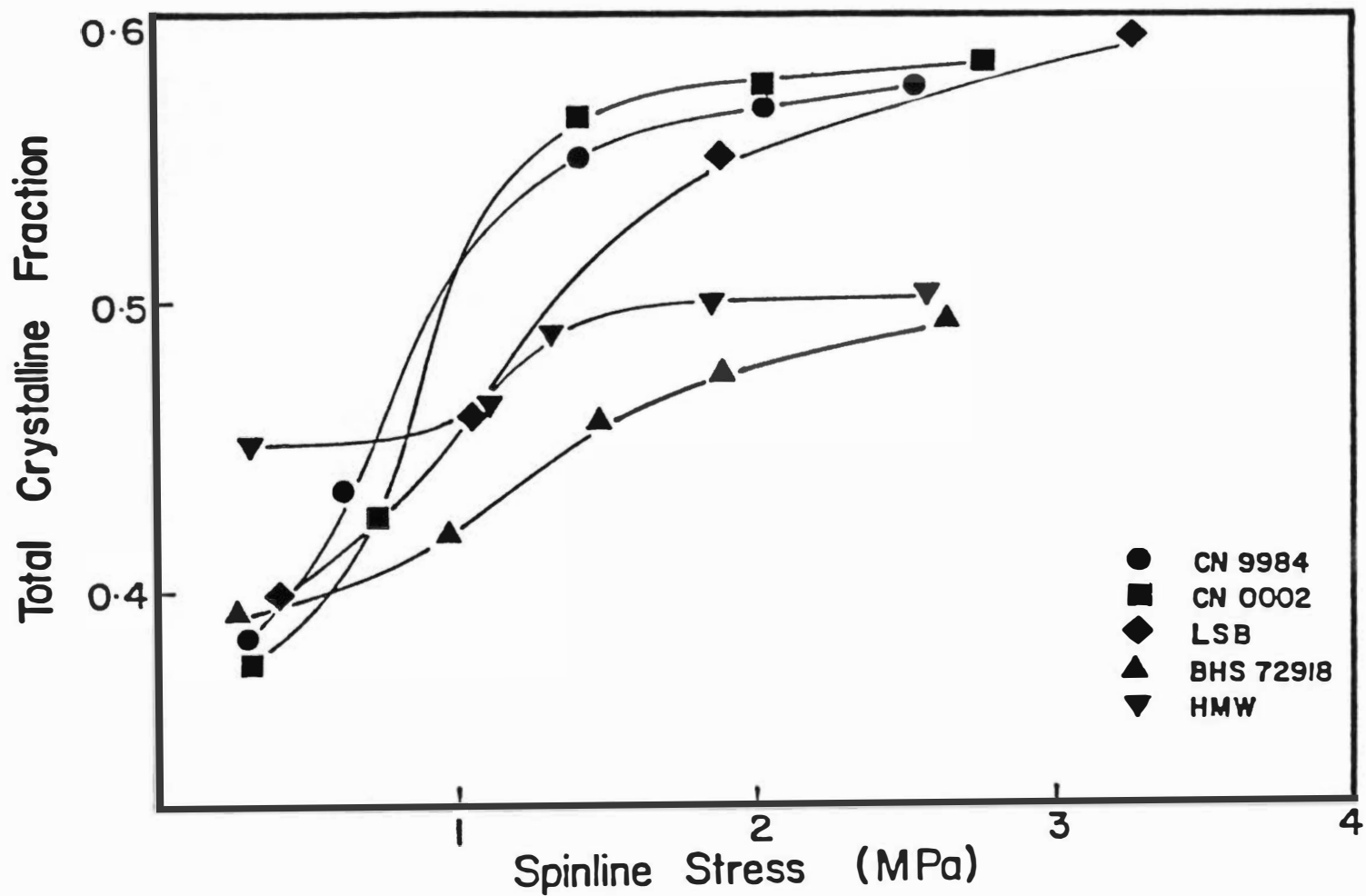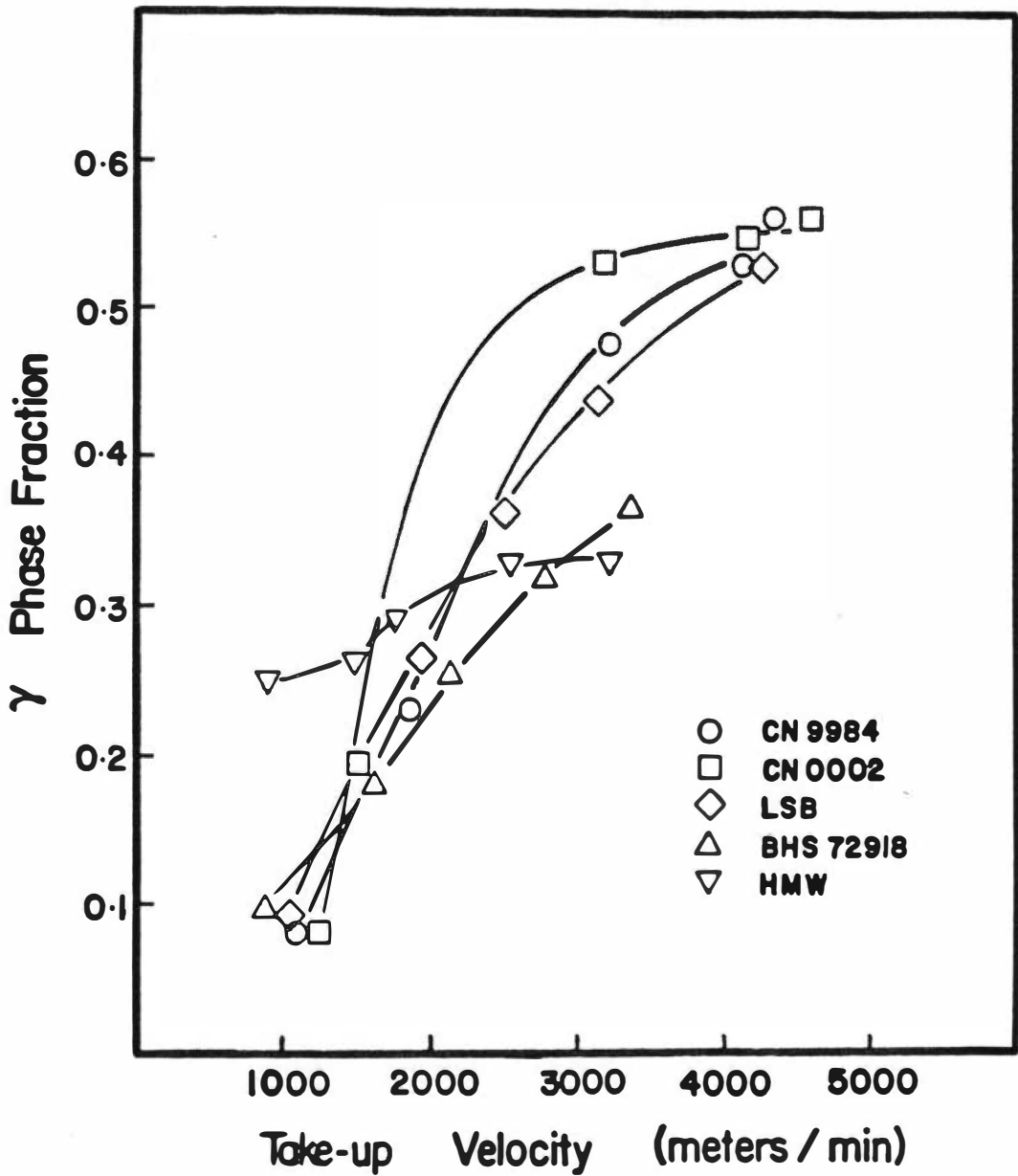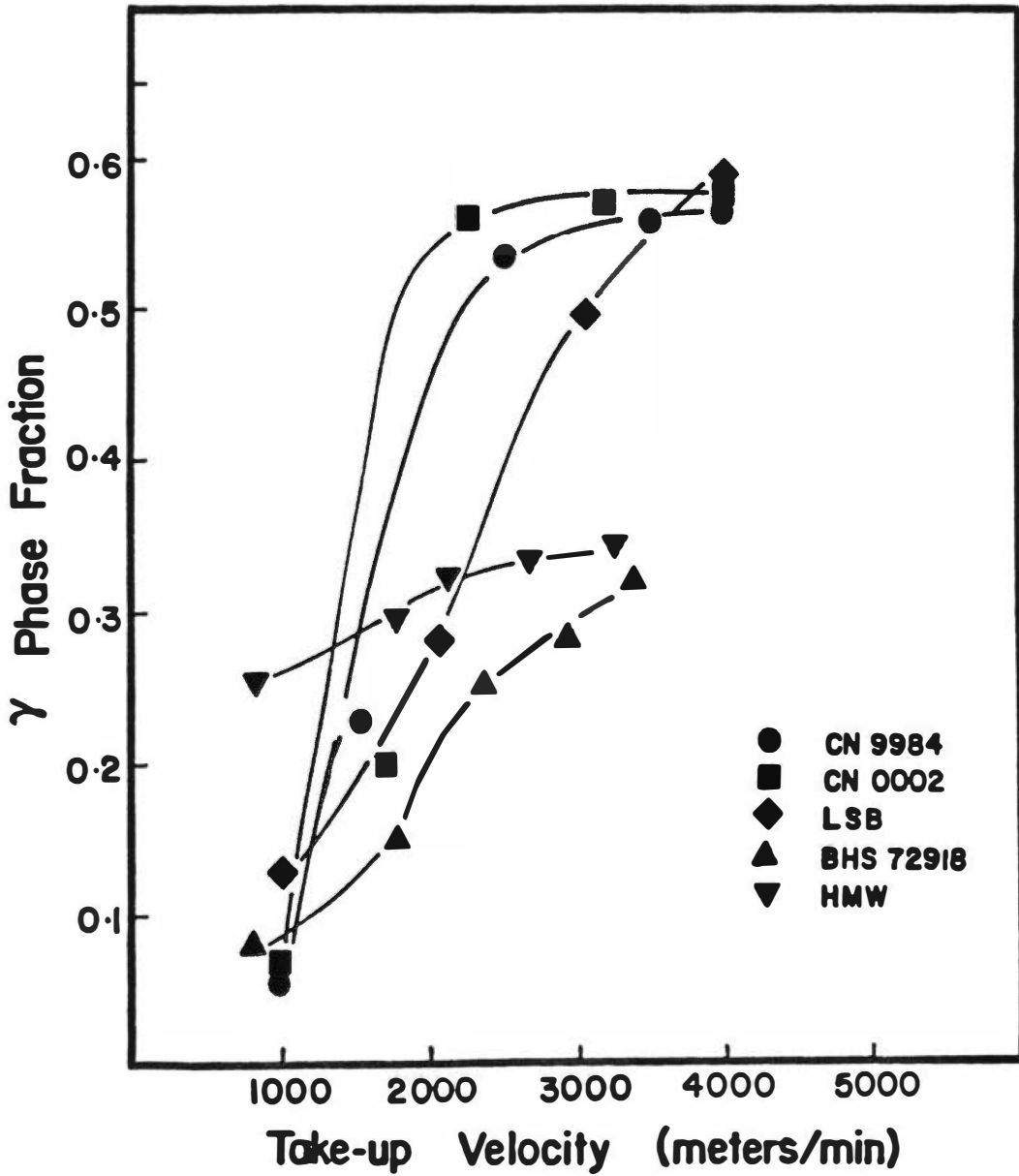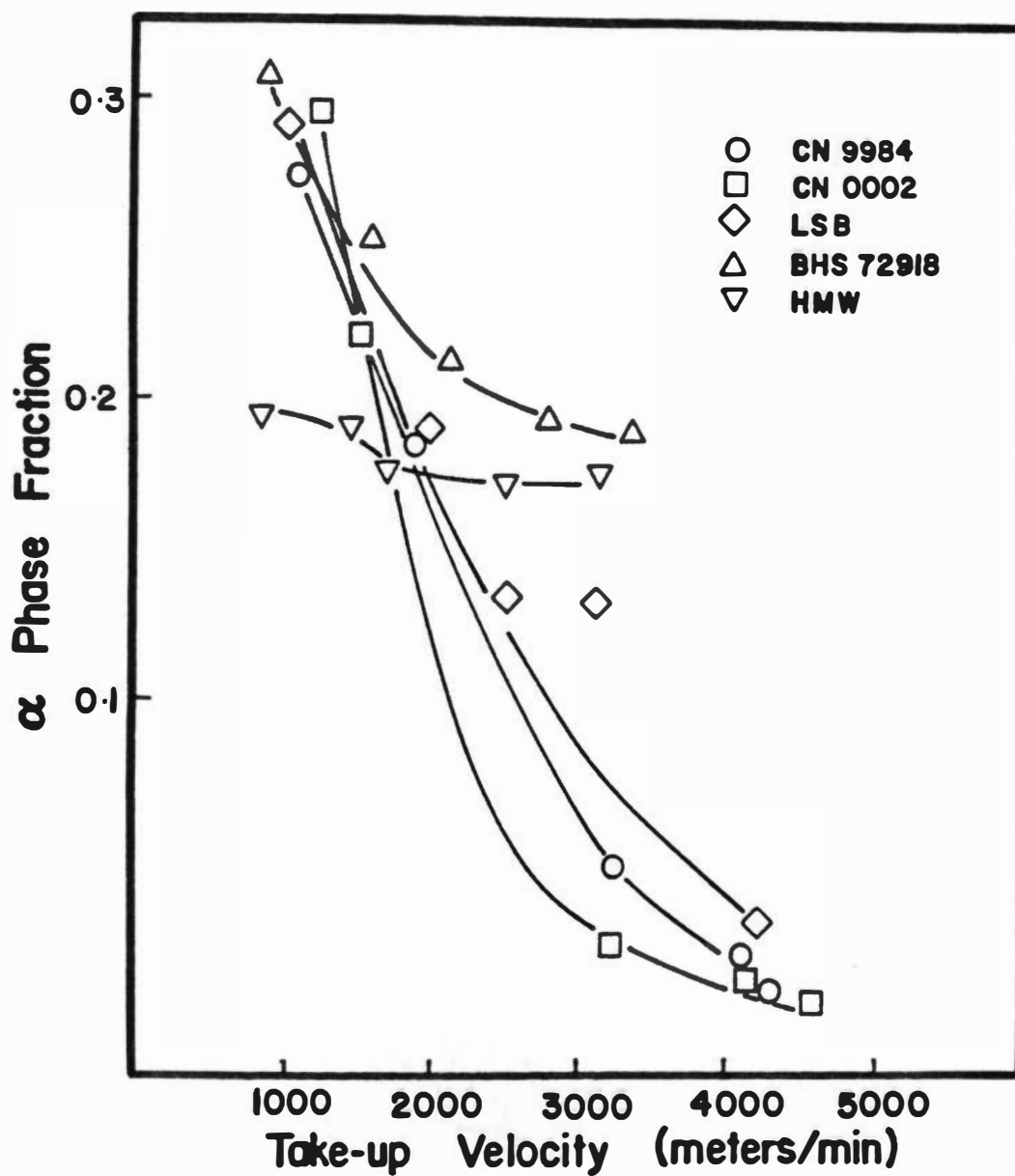
Figure IV-16. α-Phase fraction of spun and conditioned nylon-6 fibers as a function of take-up velocity (mass throughput - 5.55 g/min).

Figures IV-17 and IV-18. The amount of γ-phase increases gradually
and the α-phase decreases correspondingly with increase in molecular
weight at low take-up velocity. At higher take-up velocities, how-
ever, the γ-phase content is high at low molecular weights and lower
at intermediate and high molecular weights. The α-phase content at
higher take-up velocities increases with increasing molecular weight
until intermediate molecular weights and then starts decreasing.

E. CRYSTALLINE ORIENTATION FACTORS

The chain axis (b-axis) crystalline orientation functions for
nylon-6 are plotted against take-up velocity in Figures IV-19 and
IV-20 for different mass throughputs. The crystalline orientation
function increases steadily with take-up velocity for all samples.
The values range from less than 0.25 at lower take-up speeds to
about 0.75 at high take-up speeds for low molecular weight samples.
The effect of molecular weight on the chain axis orientation is
shown in Figure IV-21 for the 5.55 g/min flow rate data. At lower
take-up velocity, the chain axis orientation increases steadily
with increase in molecular weight, while it decreases gradually at
higher take-up velocities. The magnitude of the effect of molecular
weight seems to be greater at low take-up velocities than at the
higher take-up velocities. This is probably a result of the fact
that the orientation has approached a limiting value for all
samples in the high take-up velocity range, whereas the lower
molecular weight samples are not approaching this saturation point
at a take-up velocity of 1000 m/min.

Figure IV-17.   γ-Phase fraction of spun and conditioned nylon-6
fibers as a function of molecular weight (mass
throughput - 5.55 g/min).
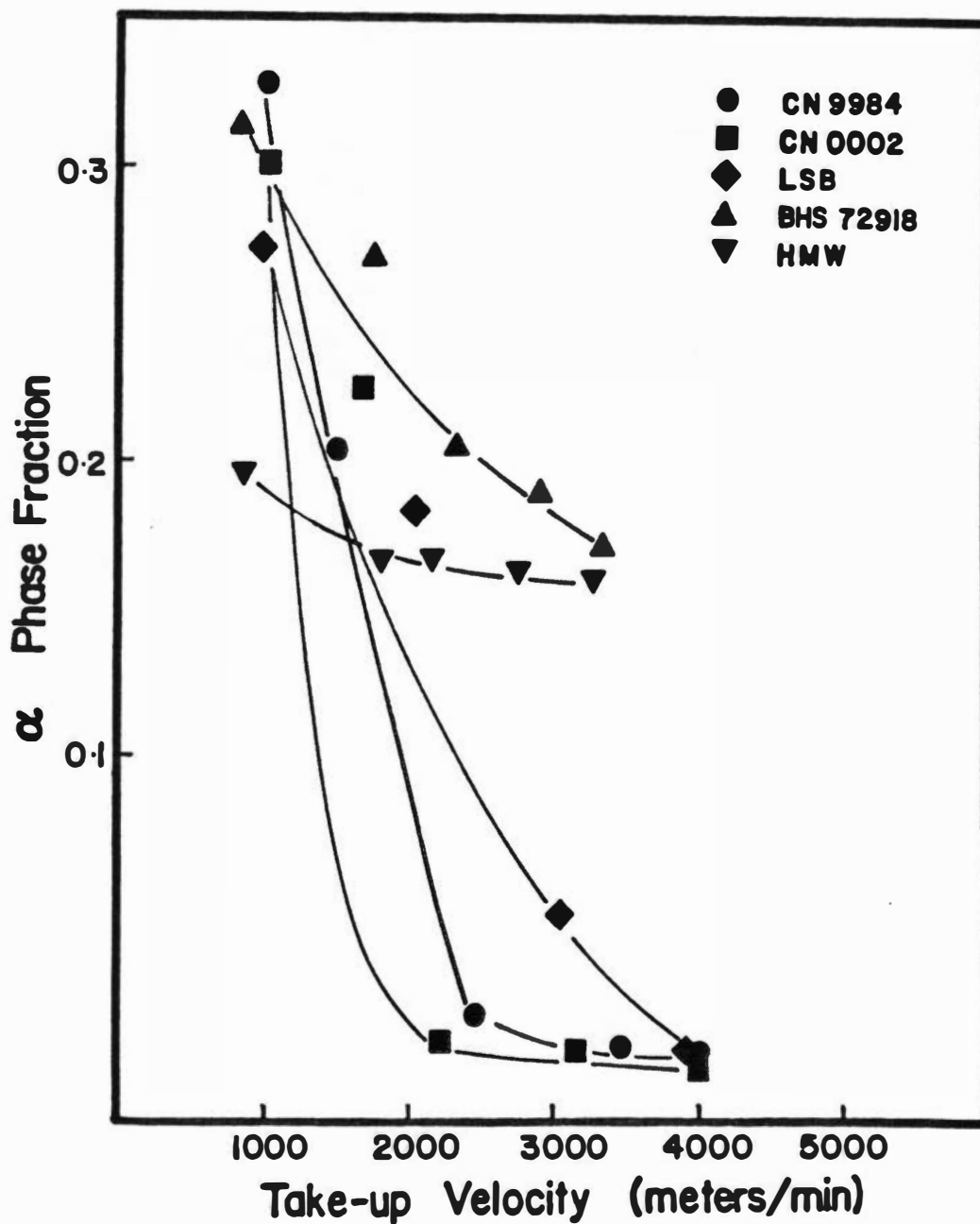
Figure IV-18. α-Phase fraction of spun and conditioned nylon-6 fibers as a function of molecular weight (mass throughput - 5.55 g/min).

Figure IV-19. Chain axis orientation of spun and conditioned
nylon-6 fibers as a function of take-up velocity
(mass throughput - 3.55 g/min).

Figure IV-20. Chain axis orientation of spun and conditioned nylon-6 fibers as a function of take-up velocity (mass throughput - 5.55 g/min).
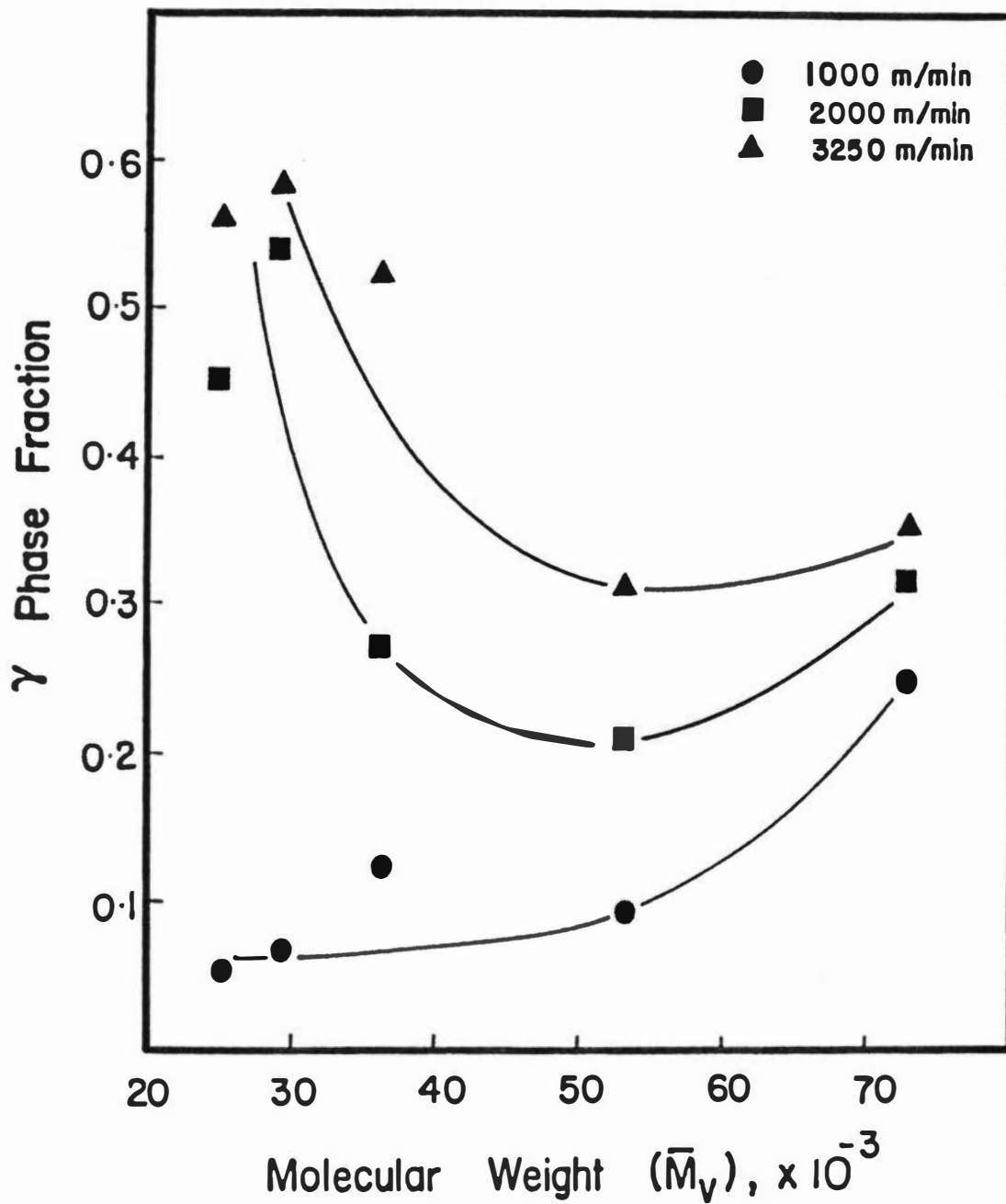
Figure IV-21. Chain axis orientation of spun and conditioned
nylon-6 fibers as a function of molecular weight (mass
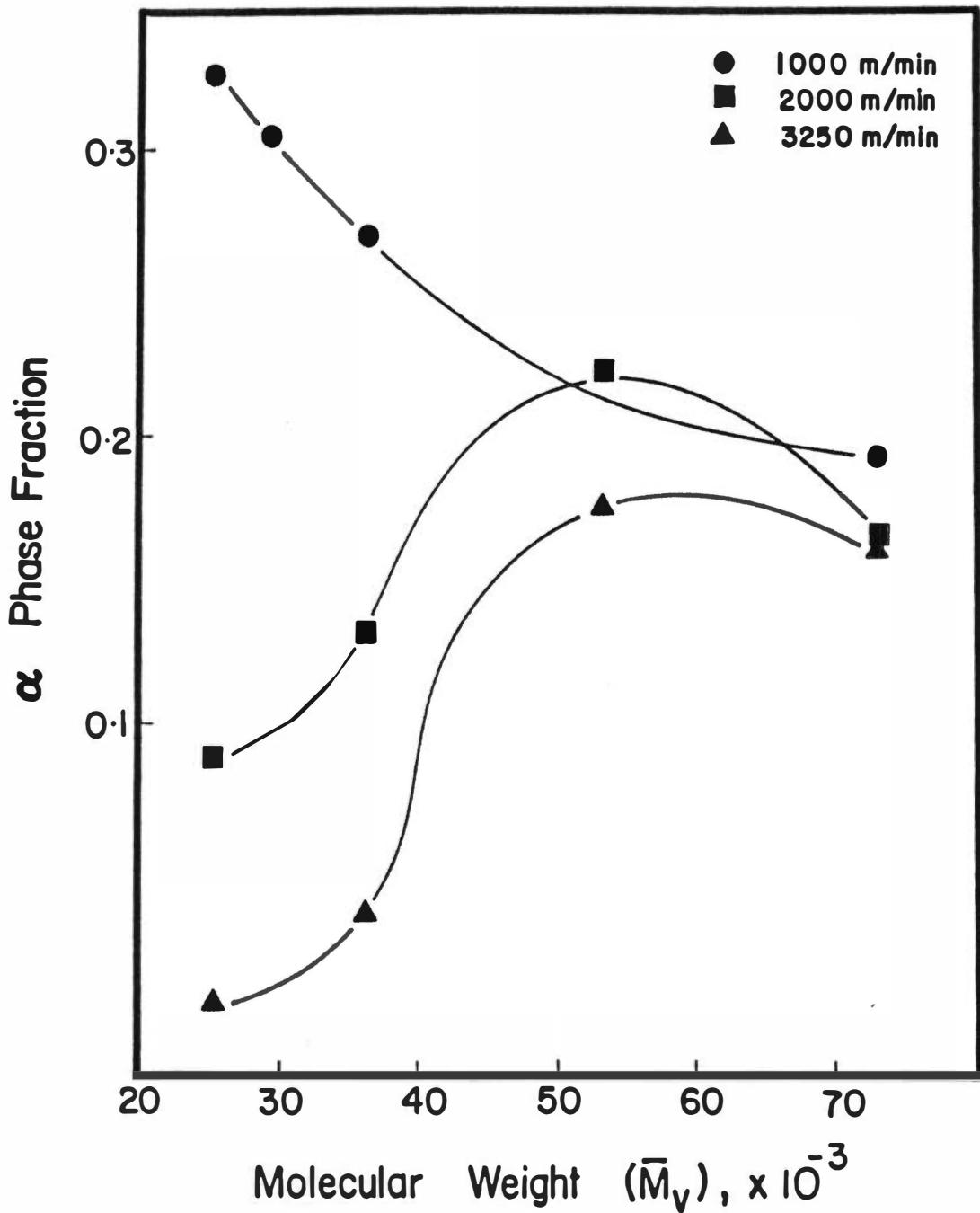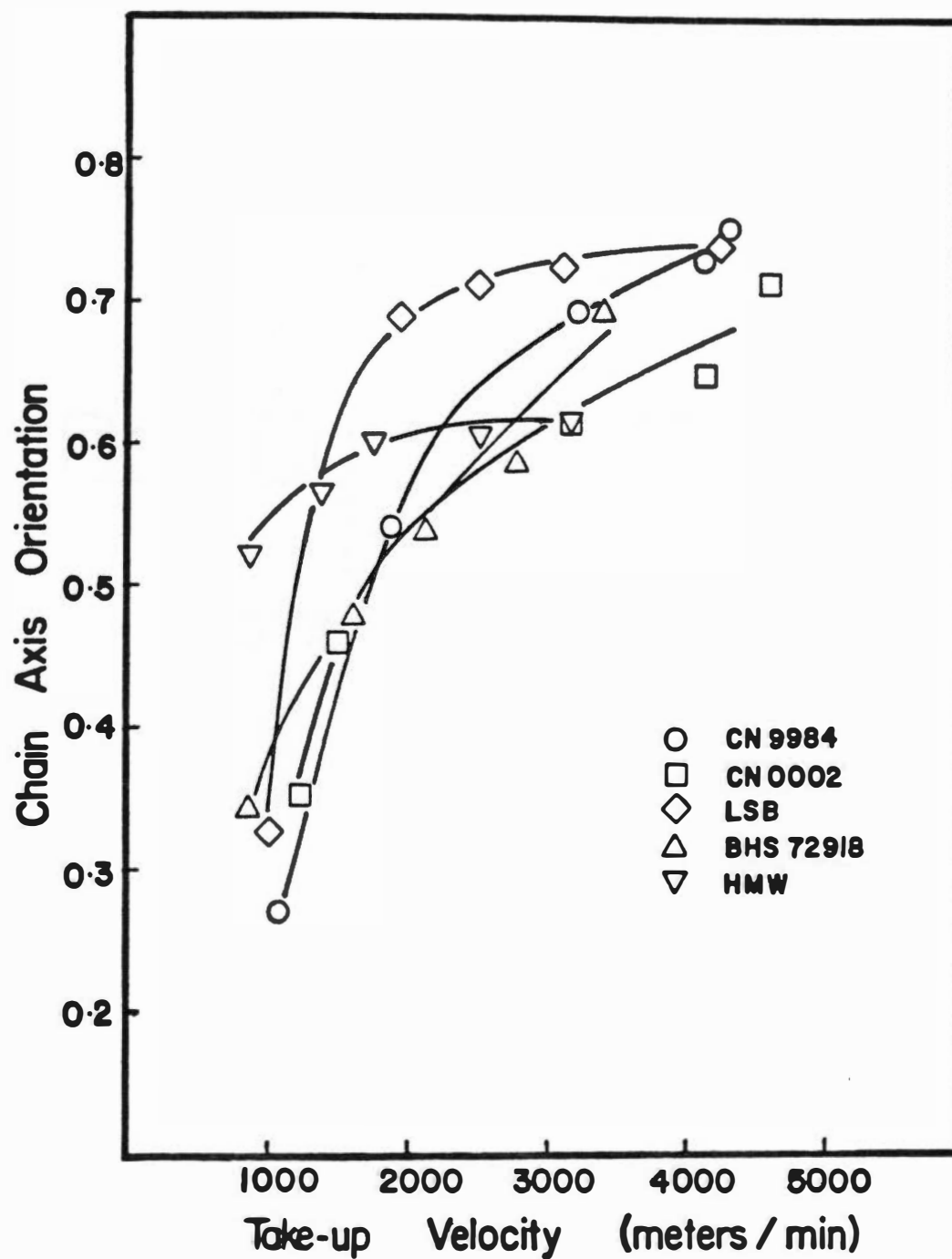throughput - 5.55 g/min).

An increase in spinline stress results in a better alignment of the chain axis with the fiber axis as shown in Figures IV-22 and IV-23, but there is no single correlation of the crystalline orientation developed with the spinline stress independent of molecular weight in nylon-6, as was observed for polypropylene by Nadella et al. (81). This is probably due to the complications associated with the development of crystallinity in nylon-6. Some samples may crystallize on the threadline while others crystallize during conditioning. It is likely that the relative amounts of crystallization on the threadline increase with take-up velocity but may decrease with increasing molecular weight.

F. BIREFRINGENCE AND AMORPHOUS ORIENTATION

The orientation factors discussed earlier were for the crystalline phase of the samples. Since nylon-6 fibers are less than 100 percent crystalline, they also have an amorphous phase where chain orientations may exist. The measured birefringence is a measure of the average molecular orientation in the samples.

The measured birefringence is plotted against take-up velocity in Figures IV-24 and IV-25. The birefringence increases with take-up velocity and molecular weight. It does, however, decrease slightly with increase in mass throughputs.

The variation of birefringence with spinline stresses is shown in Figures IV-26 ane IV-27. As in the case of crystalline orientation, the birefringence does not correlate with spinline stress independent of molecular weight.

Figure IV-22. Crystalline orientation function of spun and conditioned nylon-6 fibers as a function of spinline stress (mass throughput - 3.55 g/min).

Figure IV-23. Crystalline orientation function of spun and conditioned nylon-6 fibers as a function of spinline stress (mass throughput - 5.55 g/min).
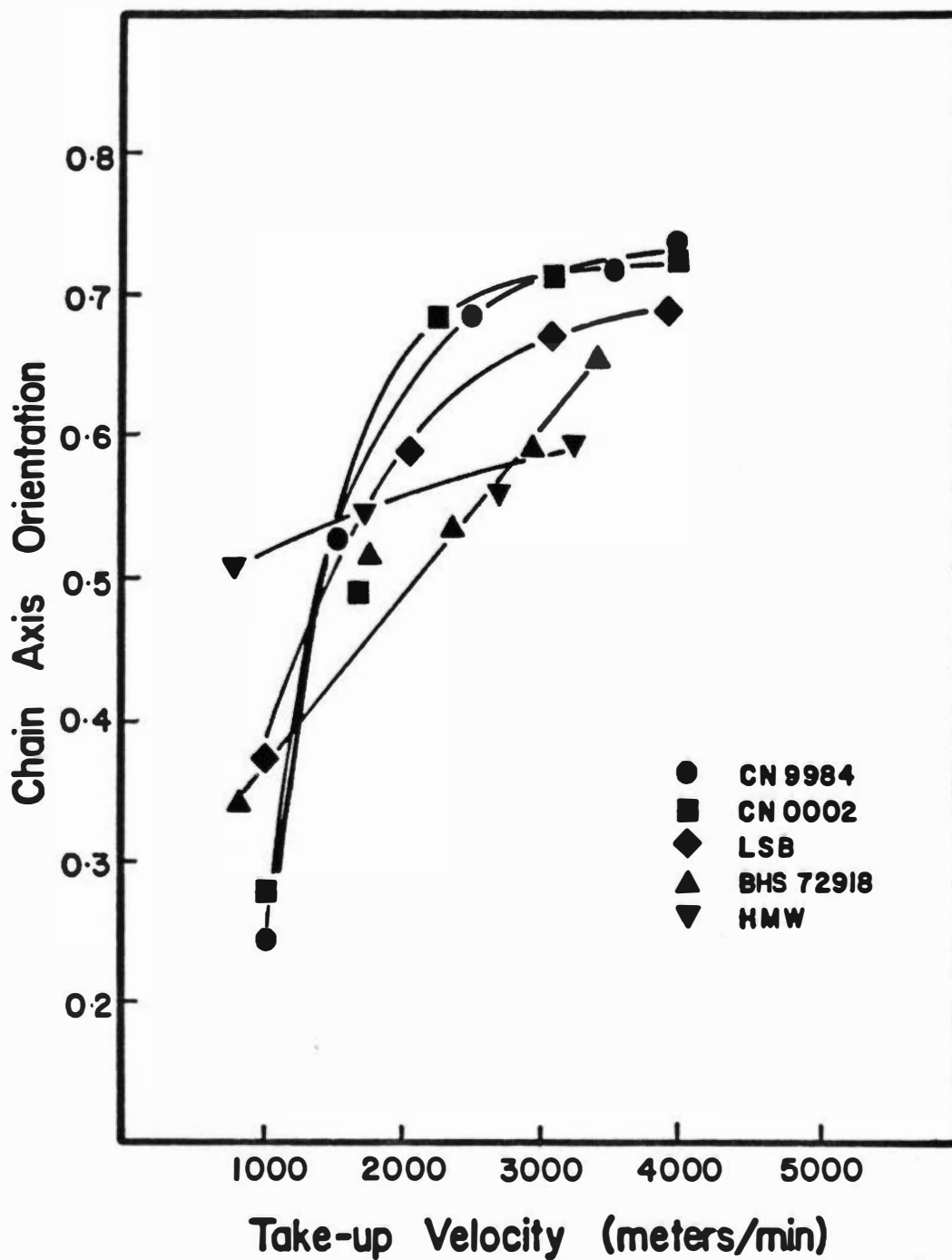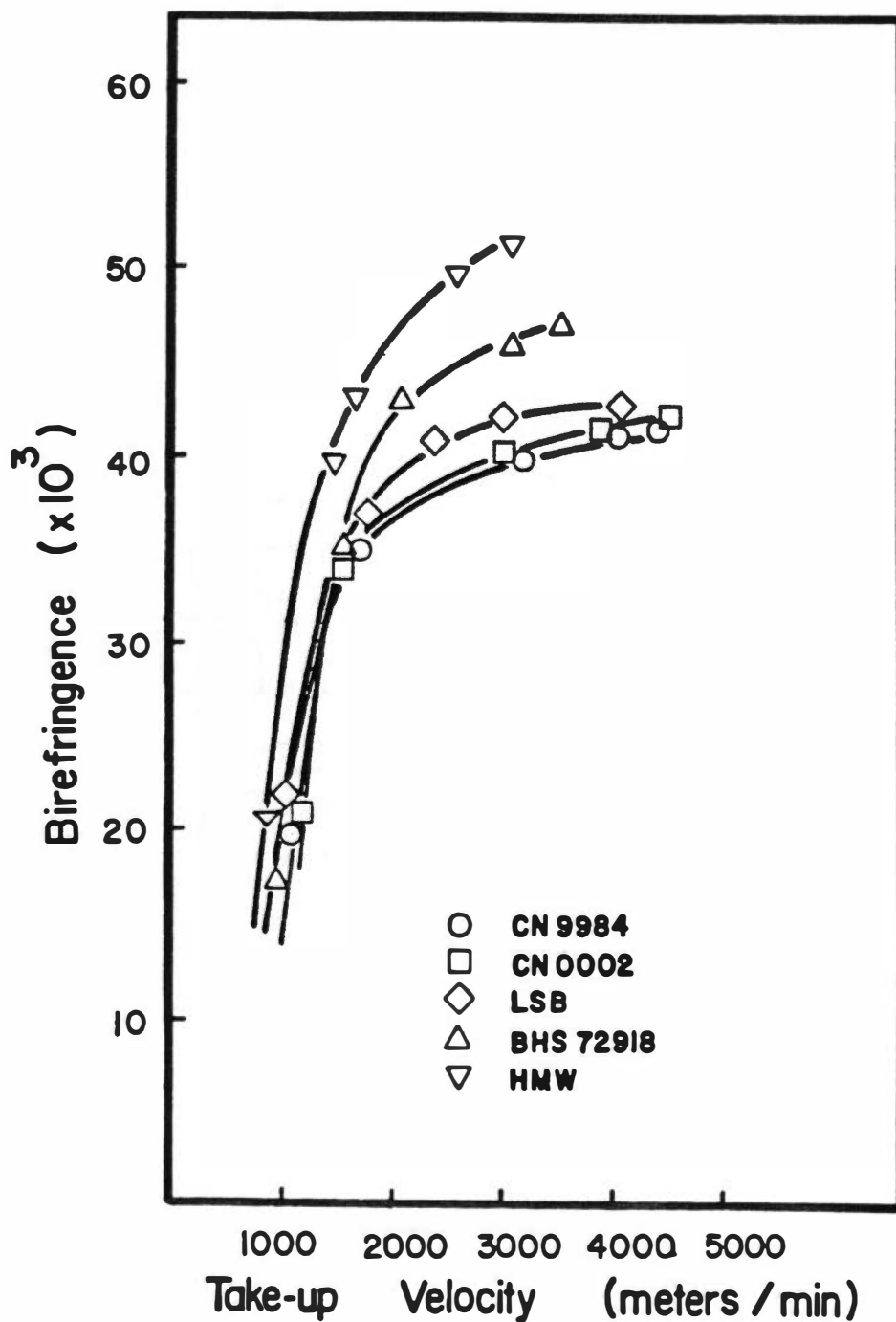
Figure IV-24. Birefringence of spun and conditioned nylon-6 fibers as a function of take-up velocity (mass throughput - 3.55 g/min).
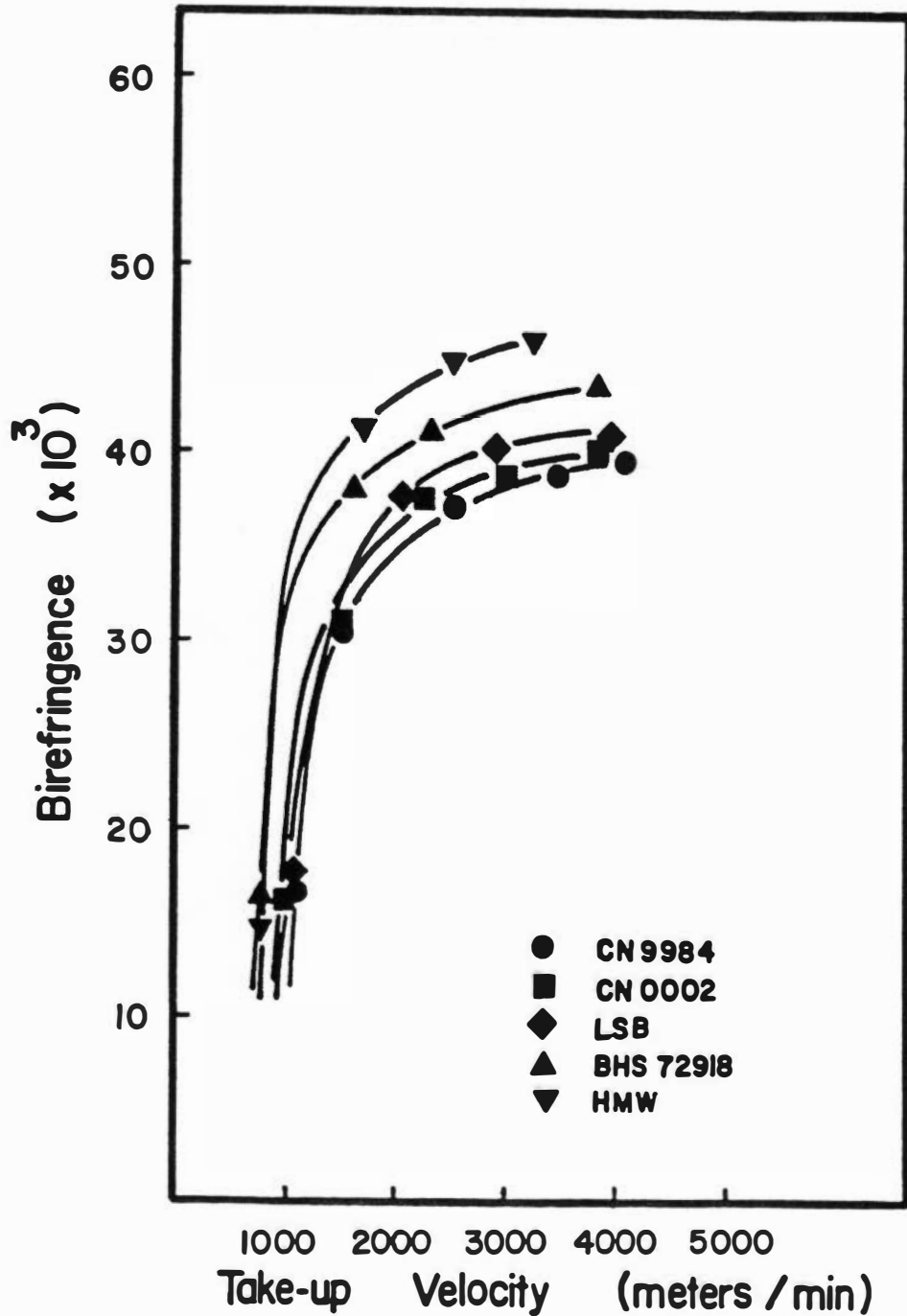
Figure IV-25.   Birefringence of spun and conditioned nylon-6
fibers as a function of take-up velocity (mass
throughput - 5.55 g/min).
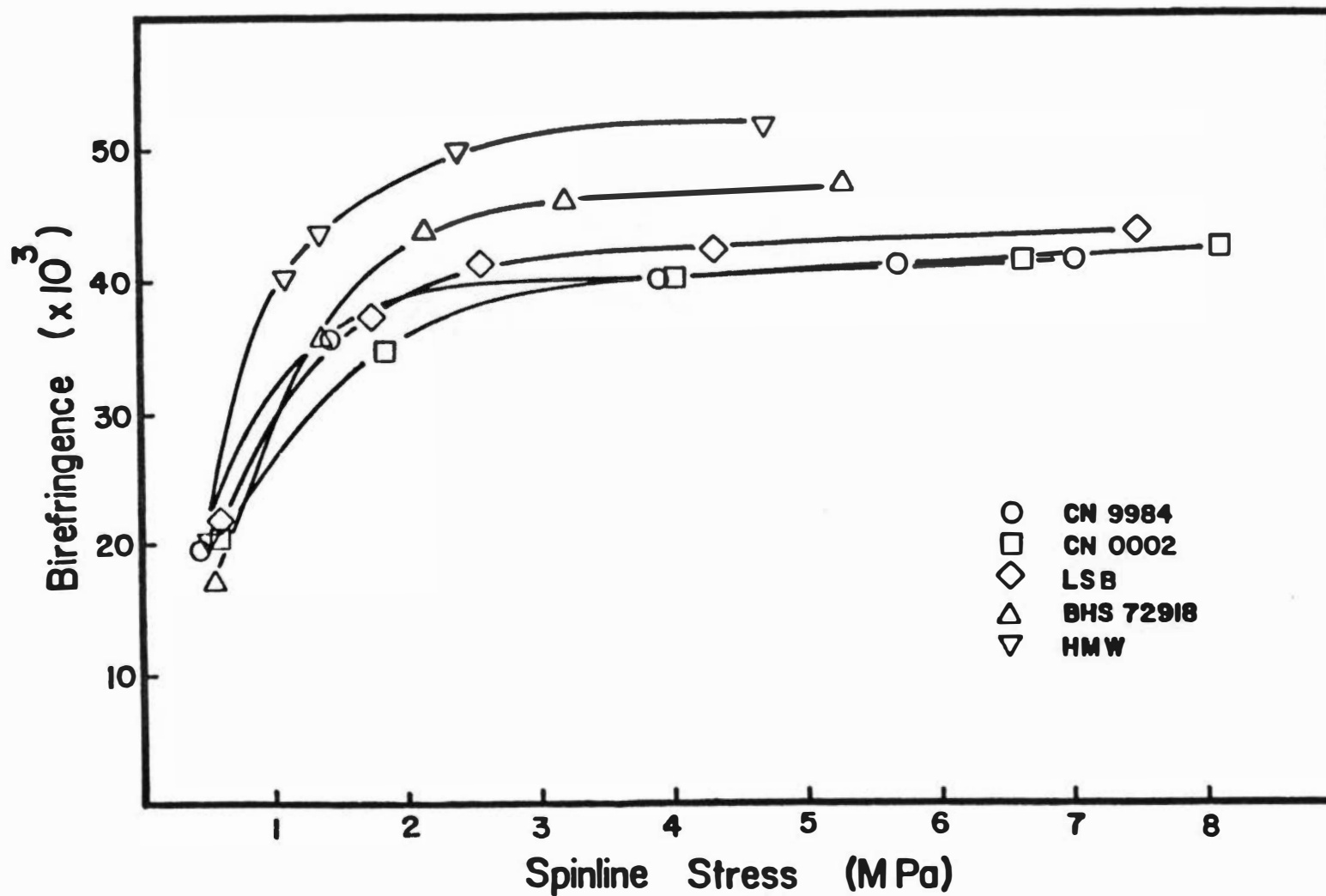
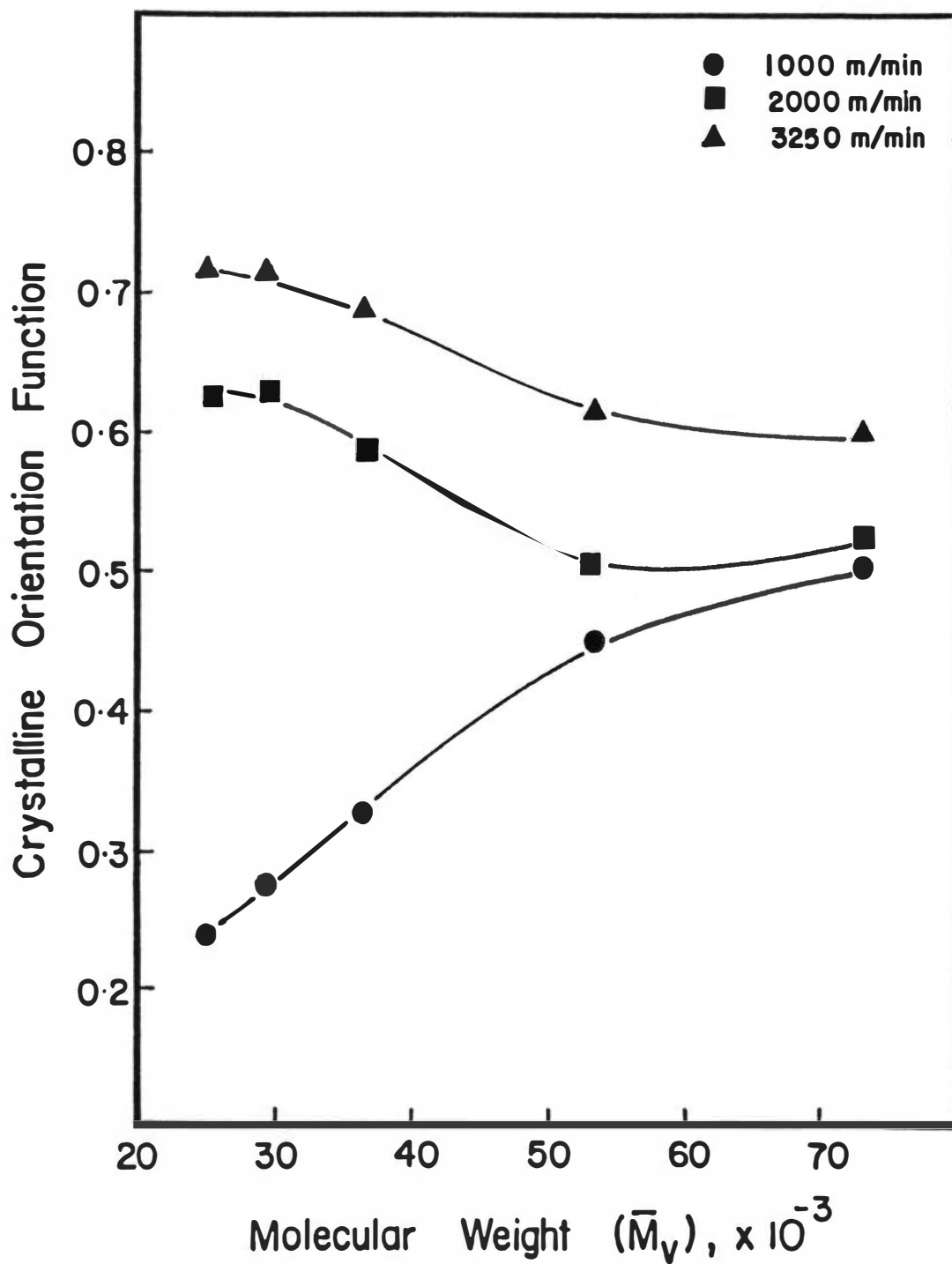Figure IV-26. Birefringence of spun and conditioned nylon-6 fibers as a function of spinline stress (mass throughput - 3.55 g/min).
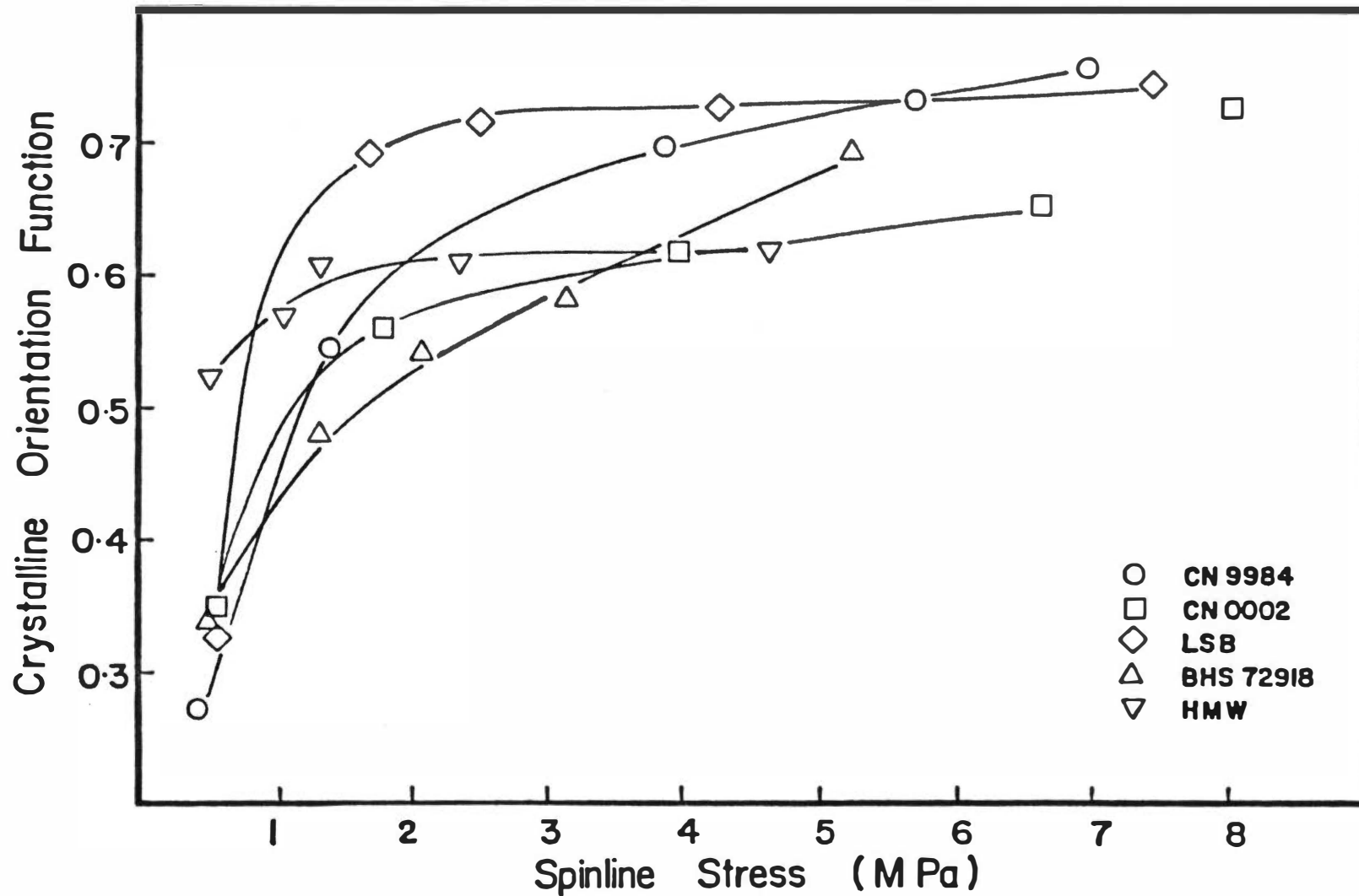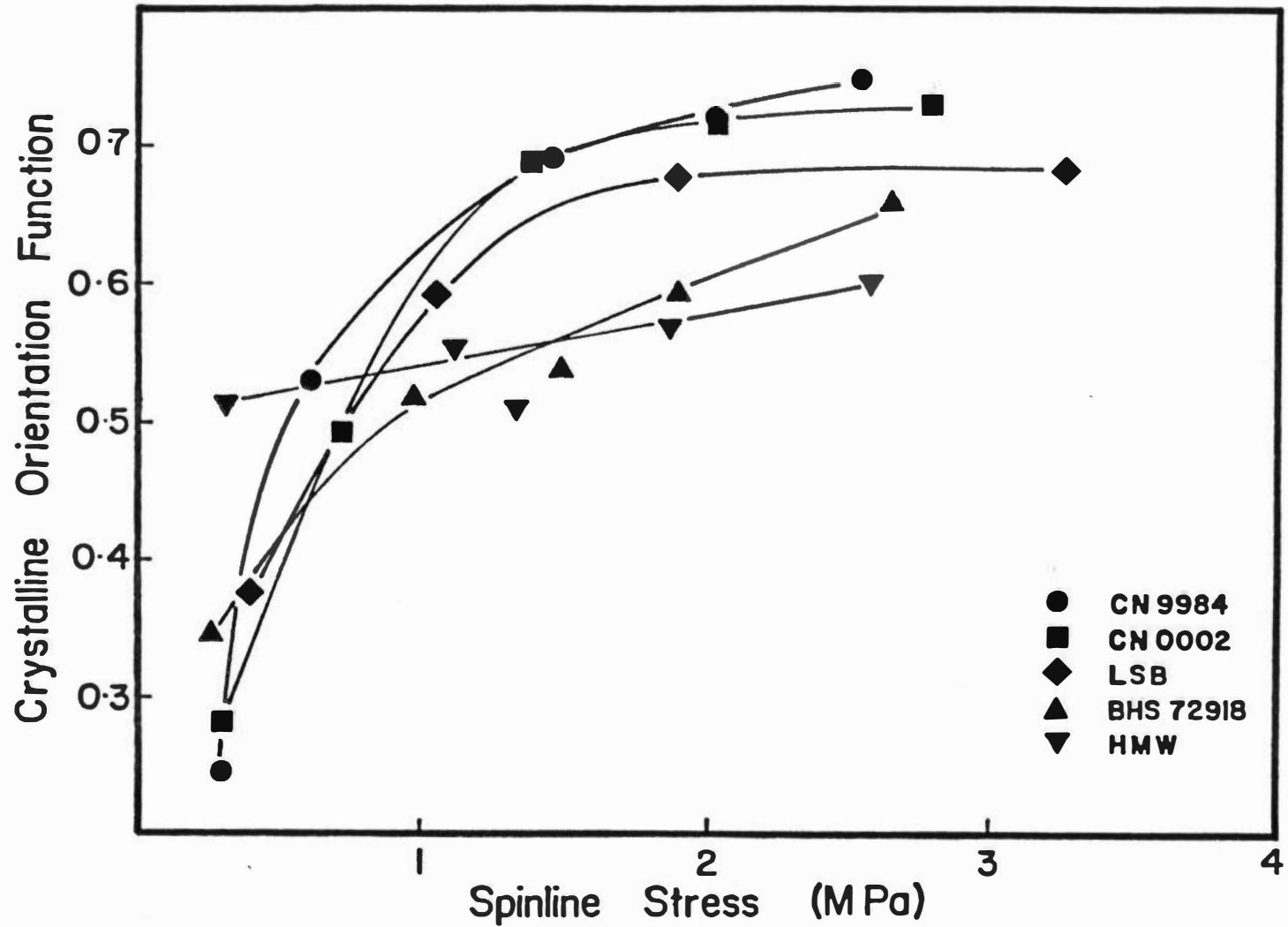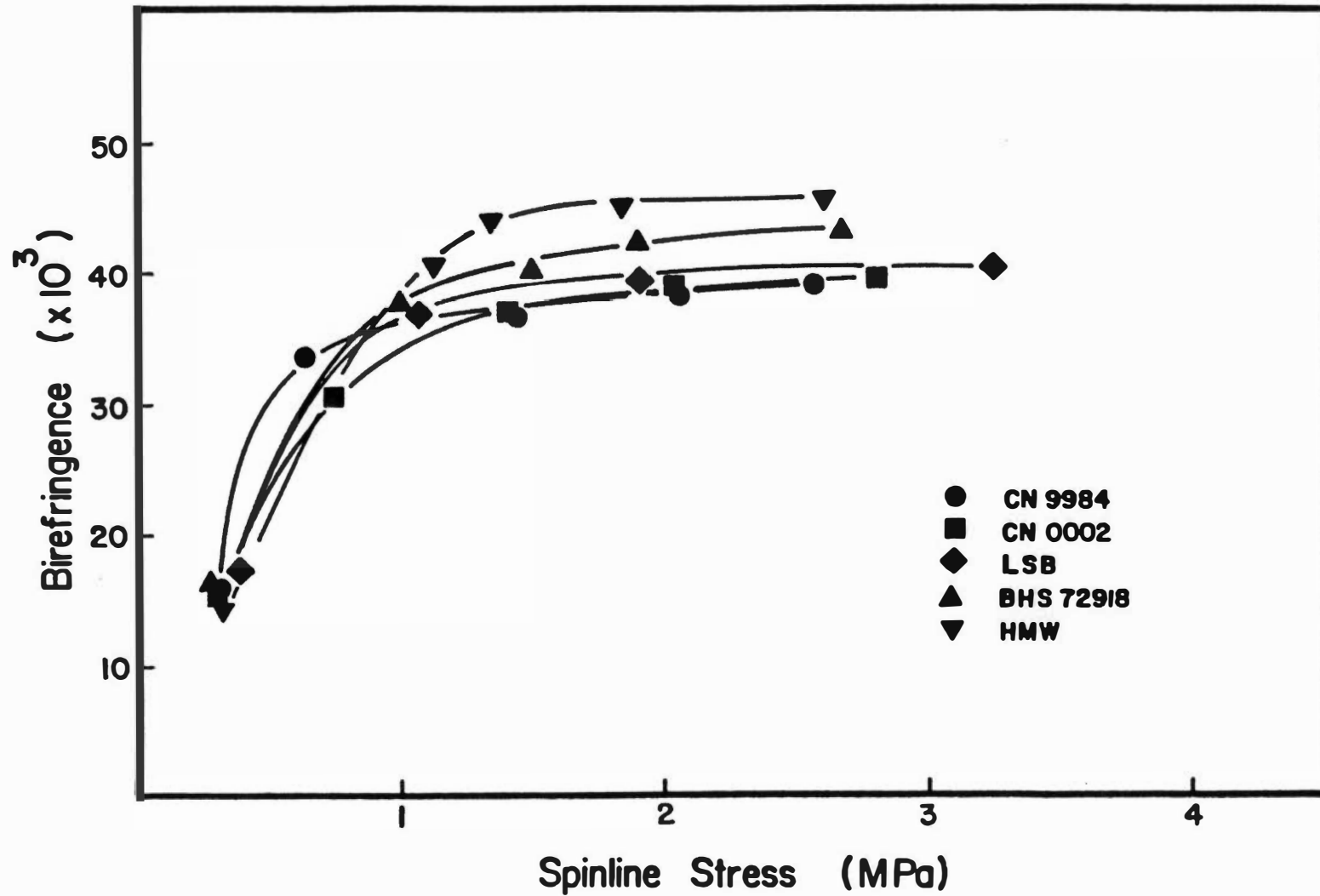
Figure IV-27. Birefringence of spun and conditioned nylon-6 fibers as a function of spinline stress (mass throughput - 5.55 g/min).

G. DISCUSSION OF STRUCTURE OF MELT SPUN FIBERS

Nylon-6 fibers were found to be amorphous on the threadline from the online studies of Bankar et al. (10) even at 1000 m/min. The filaments were found to crystallize on the bobbin and the process is enhanced by conditioning the filaments. The molecular weight studied by Bankar et al. (10) falls in the lower part of our molecular weight range. The WAXS patterns of the present samples show well-defined peaks to indicate the existence of crystallinity in the samples. The crystalline fraction increases as the take-up velocities are increased. Lower molecular weight of fiber results in crystallinities of up to 60 percent with increase in spinline stresses.

Previous investigators (36,109) studying low molecular weight nylon-6 found that the crystallization rate increased with increase in take-up velocity. At sufficiently high take-up velocity, Shimizu et al. (109) found that nylon-6 crystallizes on the threadline rather than the bobbin. These changes would seem to be involved in the increase in crystallinity with increased take-up velocity. The present data imply that these changes are also sensitive to molecular weight effects. The situation is further complicated by the α and γ crystalline forms. The present data and previous data indicate that a greater fraction of γ forms with increasing take-up velocity. These results suggest that γ may nucleate and grow under conditions that favor rapid crystallization, while slower crystallization may favor the formation of less γ-phase

and lower overall crystallinities. If, in addition, we argue that the crystallization rates decrease with increase of molecular weight, we can explain qualitatively the observed differences in total crystallinity and γ-phase fractions with molecular weight. In general, then, the data obtained in this study seem to be consistent with a hypothesis that factors that lead to higher crystallization rates such as increased melt state molecular orientation caused by increased spinline stresses (increased take-up velocity) and lower molecular weight tend to enhance the formation of the γ-phase and increase the total crystallinity present after conditioning. Also, the high γ-phase content in the lower molecular weight samples is probably due to online crystallization, while the lower crystallinity and γ-phase content of the high molecular weight samples may mean that they do not crystallize on the threadline as rapidly.

Higher speeds of spinning result in filaments which are similar to drawn filaments in many aspects. The α and γ-phase fractions, however, take an opposite trend at higher speeds when compared to drawing which increases the α-phase fraction and decreases the γ-phase fractions while the total crystallinity increases, as shown by Gianchandani et al. (36) and Stepaniak et al. (124).

The average molecular orientation increases with increased take-up velocity and increased molecular weights as shown by the birefringence data in Figures IV-24 and IV-25. Similar results were obtained for polypropylene filaments by Nadella et al. (82). The

higher molecular orientation is generated as a result of higher spinline stresses. The striking difference the increase in spinline stress causes in the birefringence is seen in Figures IV-26 and IV-27. The birefringence at lower take-up velocity increases rapidly with increasing molecular weight compared to that at higher take-up velocities where the increase is gradual. Higher mass throughputs which result in lower spinline stresses decrease the birefringence. The chain axis crystalline orientation function shows a rapidly increasing trend with increase in birefringence in Figure IV-28. The amorphous orientation function calculated by the procedure described in Chapter III decreases with increasing take-up velocity, after a slight initial increase. This is the case for the lower molecular weight samples, while for the higher molecular weight samples the trend is toward an increase and then leveling off or a slight decrease. This effect is shown in Figure IV-29. This could probably be due to the crystallization of the crystallites in the amorphous region after the amorphous chains in the region reach a certain orientation. Thus the more oriented amorphous chains are incorporated into the crystalline region, leaving the amorphous region with low oriented chains. This effect is especially noticeable for the three lower molecular weight samples. As the molecular weight increases, this decrease in the amorphous orientation becomes less and shows a leveling-off trend for the high molecular weight samples.

Increased take-up velocity results in fibers with better alignment of the chain axes with the fiber axis. The higher stresses
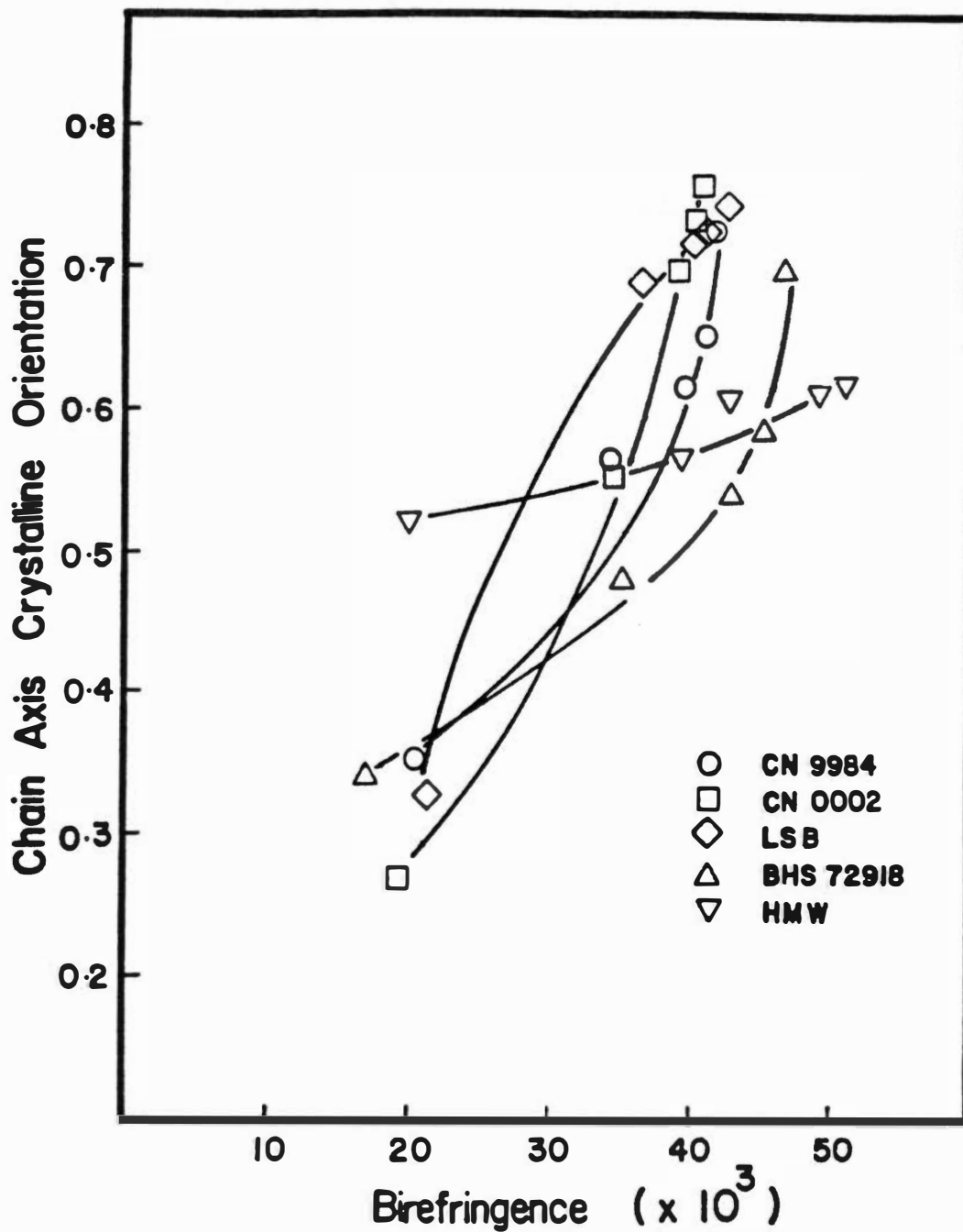
Figure IV-28. Crystalline orientation function of spun and con-
ditioned nylon-6 fibers as a function of
birefringence (mass throughput - 3.55 g/min).

Figure IV-29. Amorphous orientation function of spun and con-
ditioned nylon-6 fibers as a function of take-up
velocity (mass throughput - 3.55 g/min).

produced in the spinline due to higher take-up velocity result in higher crystalline orientation functions. One would therefore expect higher crystalline orientations for higher molecular weight samples, since they produce higher spinline stresses for a given take-up velocity. This is true for the present data only at low take-up velocities of 1000 m/min as seen in Figure IV-21 (p. 74). This does not seem to be the case for higher take-up velocity samples. The problem here apparently stems from the crystallization behavior and its changes with molecular weight as discussed earlier. As noted previously, the high molecular weight samples might not crystallize on the threadline as rapidly as the lower molecular weight samples do at higher take-up velocities and seem to be less sensitive to stress levels. These factors could have resulted in the lower crystalline orientations for the high molecular weight samples at high take-up velocities.

CHAPTER V

TENSILE PROPERTIES OF MELT SPUN FIBERS

A.   RESULTS FOR CONDITIONED FIBERS

The tensile properties of spun fibers conditioned in
65 percent relative humidity and 68°F for 24 hours were measured on
an Instron Tensile Tester. Typical engineering stress-elongation
data obtained are shown for the high and low molecular weight
samples at two different take-up velocities in Figure V-1. Variation
of tensile properties, such as tensile strength (based on the
initial cross-sectional area), tangent modulus (= initial slope of
the stress-elongation curve) and elongation at break with take-up
velocity are plotted in Figures V-2 through V-7. They also show the
changes in these properties with the variation of mass throughputs
for different molecular weight samples. The tensile properties are
cross plotted as a function of molecular weight in Figures V-8, V-9
and V-10 for the 5.55 g/min throughput. The tensile properties of
conditioned filaments are plotted against spinline stress in
Figures V-11, V-12 and V-13. The variation of these properties with
birefringence are shown in Figures V-14, V-15 and V-16.
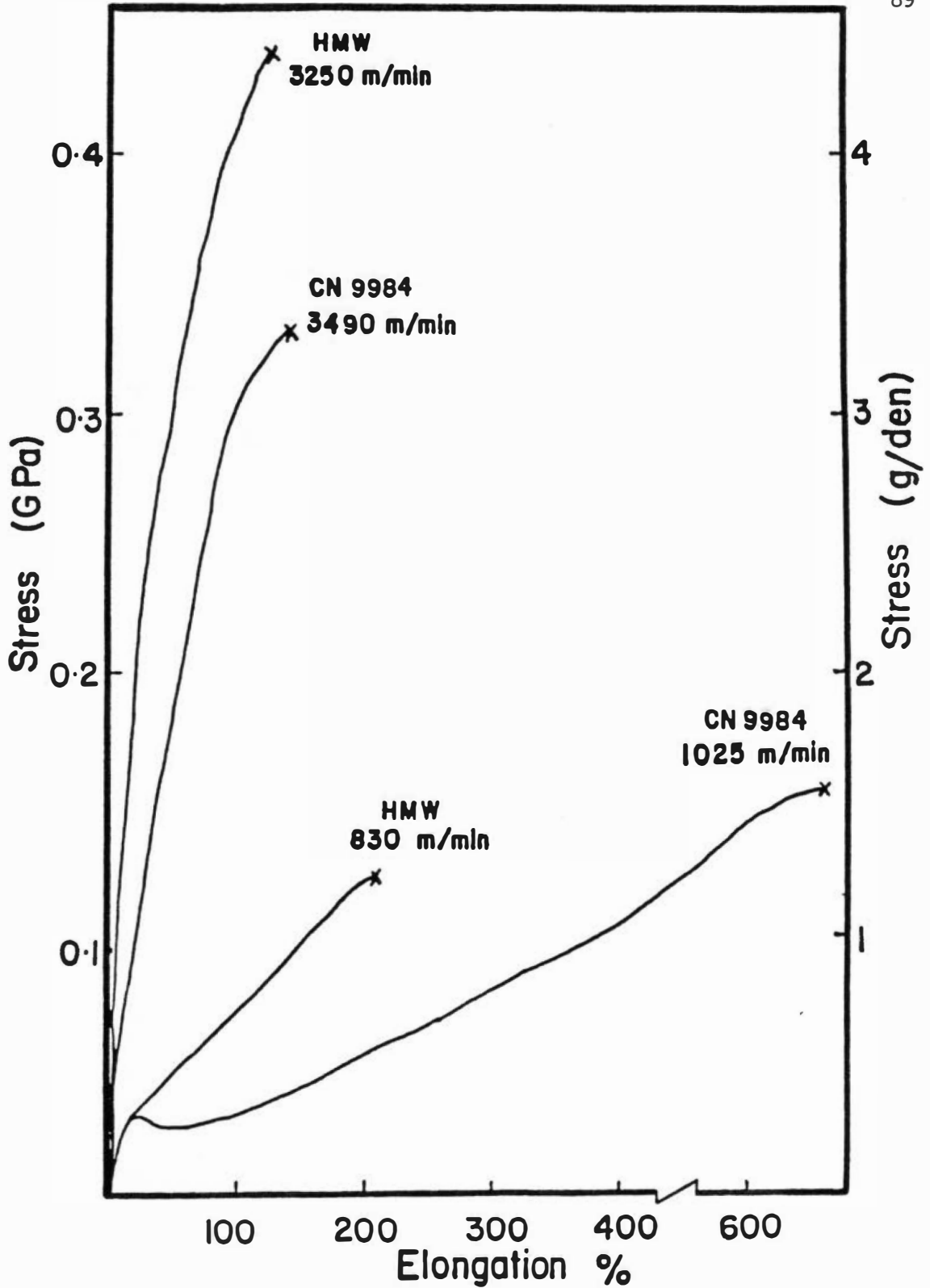
Figure V-1. Stress versus elongation of spun and conditioned
nylon-6 fibers (mass throughput - 5.55 g/min).

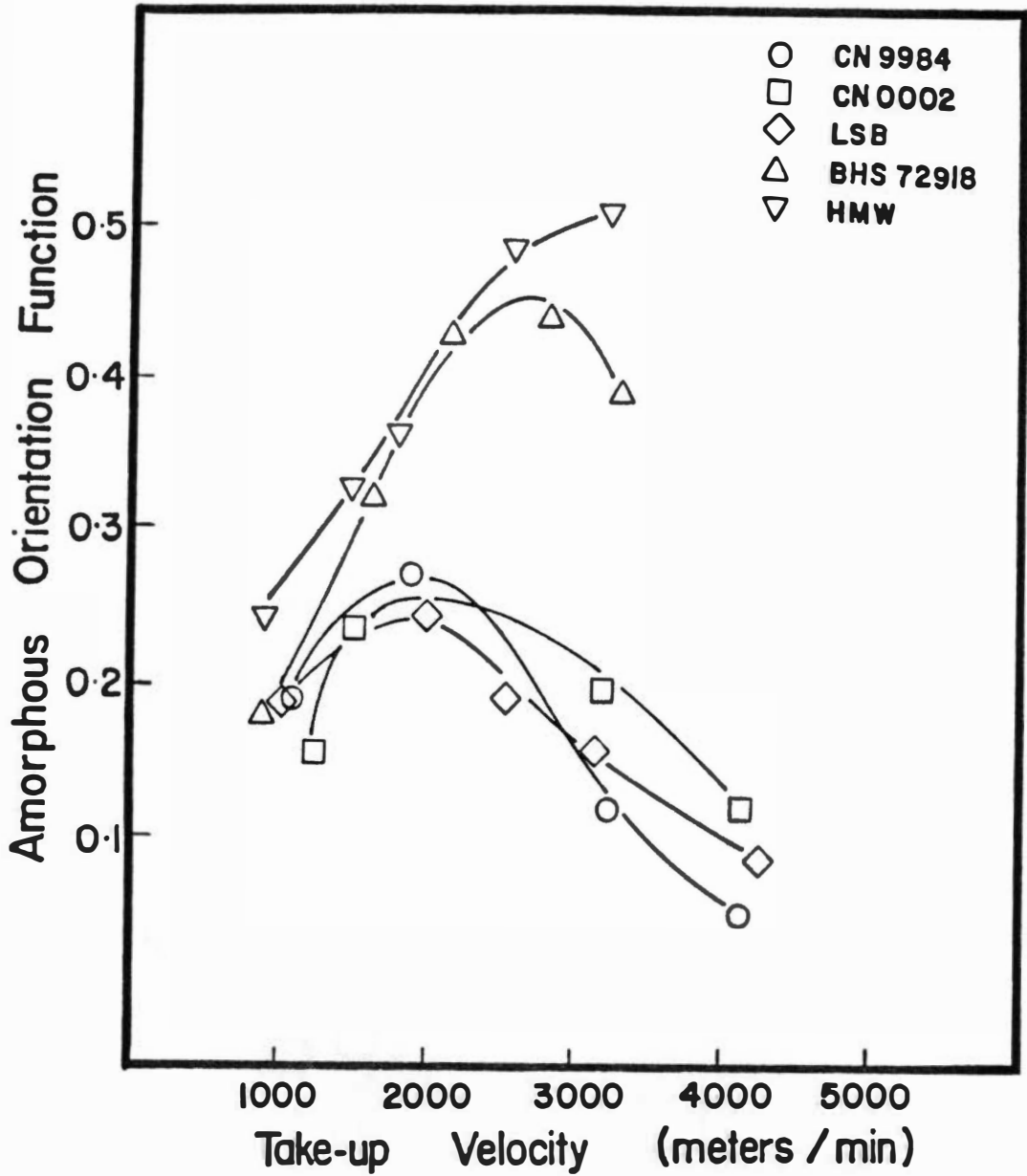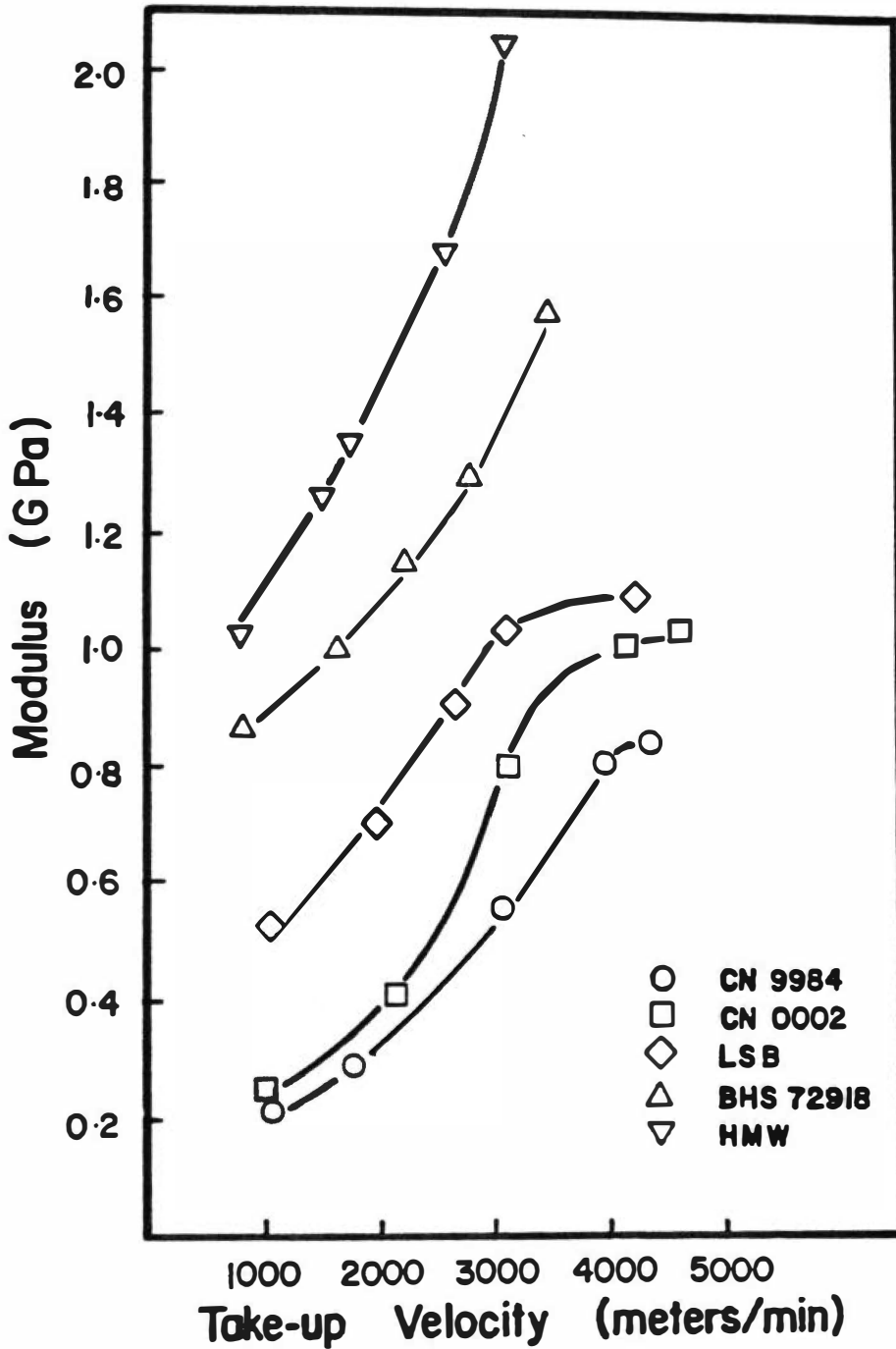Figure V-2. Modulus of spun and conditioned nylon-6 fibers as a function of take-up velocity (mass throughput - 3.55 g/min).
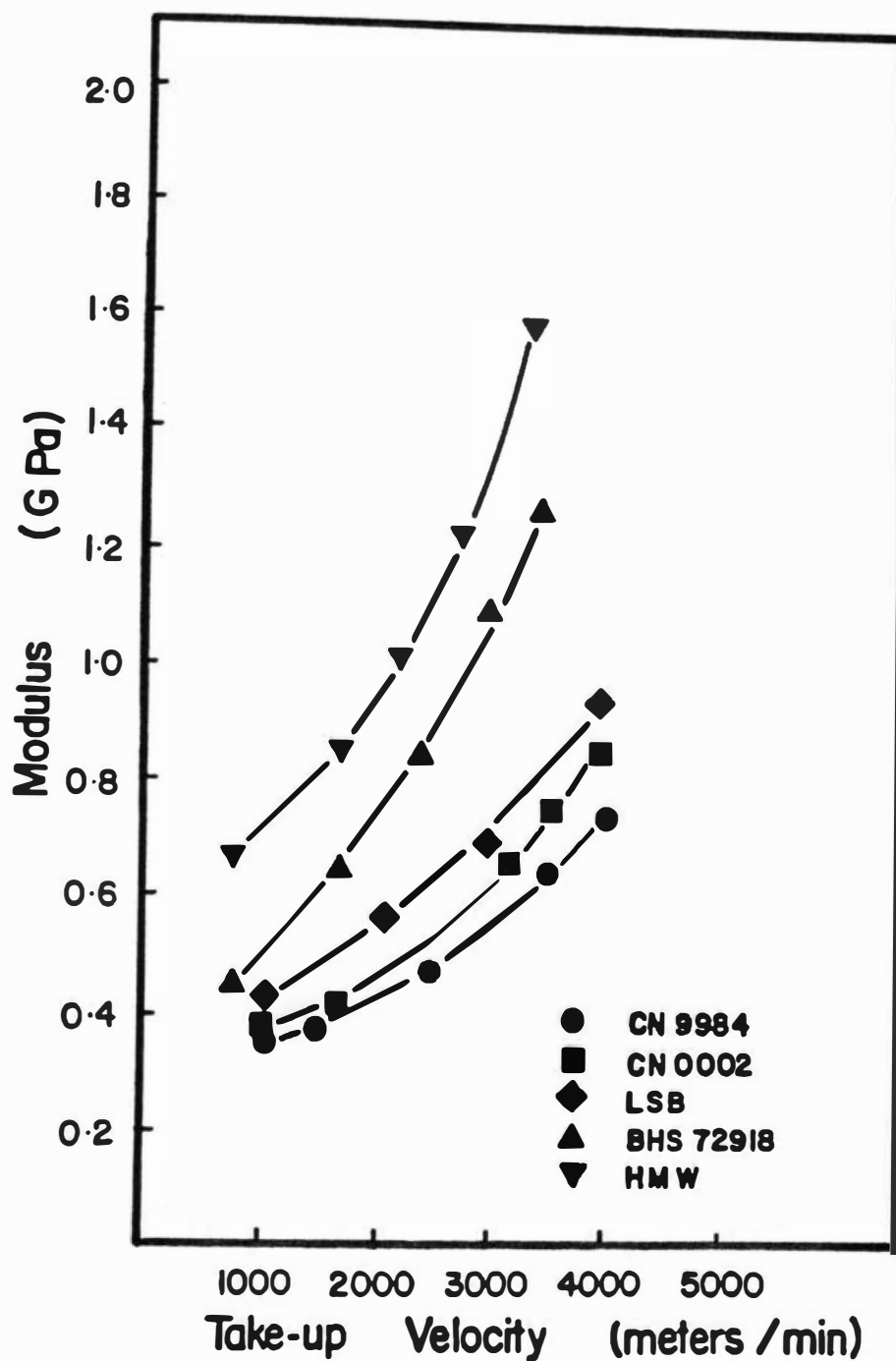
Figure V-3. Modulus of spun and conditioned nylon-6 fibers as a function of take-up velocity (mass throughput - 5.55 g/min).
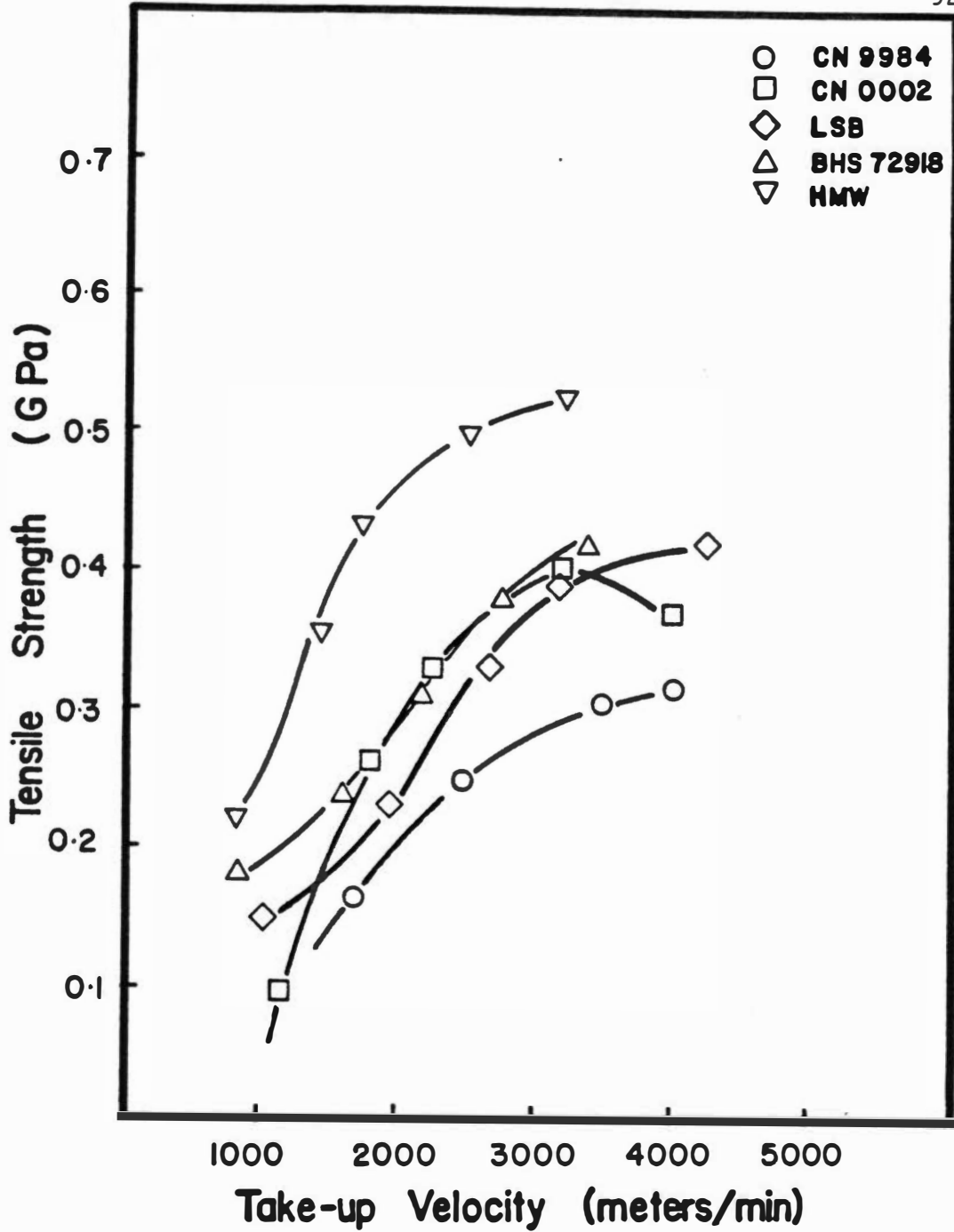
Figure V-4. Tensile strength of spun and conditioned nylon-6 fibers as a function of take-up velocity (mass throughput - 3.55 g/min).
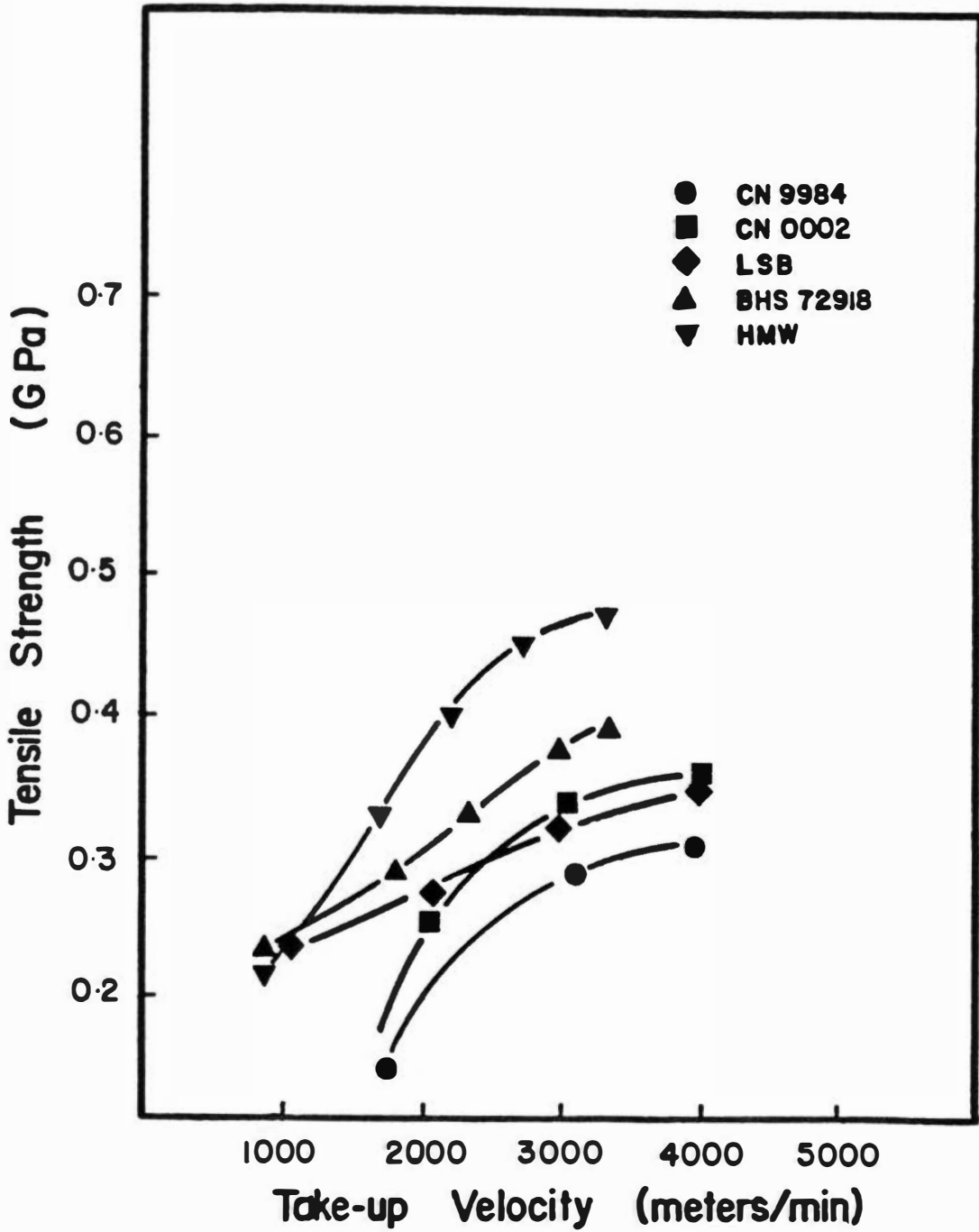
Figure V-5. Tensile strength of spun and conditioned nylon-6 fibers
as a function of take-up velocity (mass throughput -
5.55 g/min).
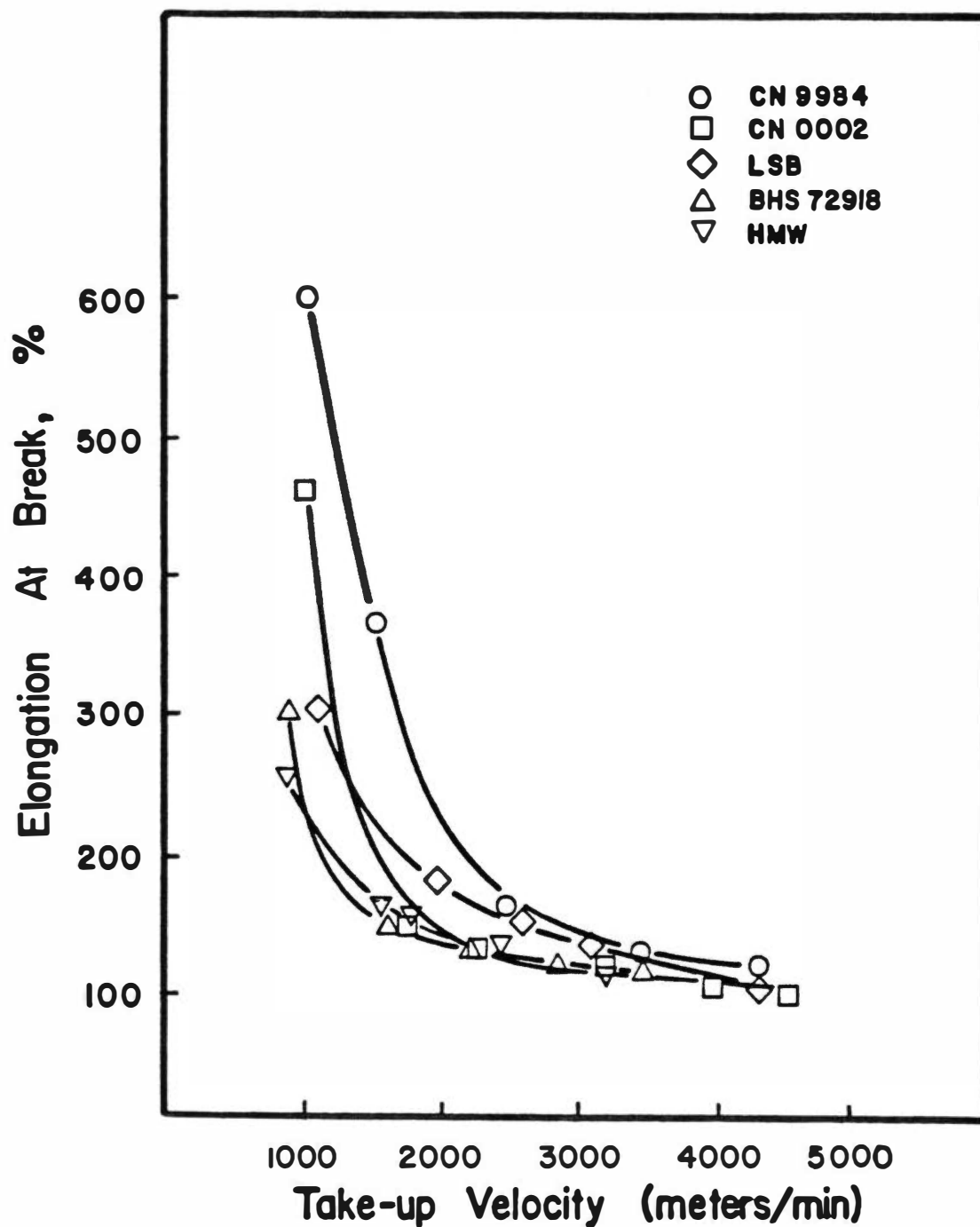
Figure V-6. Elongation at break of spun and conditioned nylon-6 fibers as a function of take-up velocity (mass throughput - 3.55 g/min).
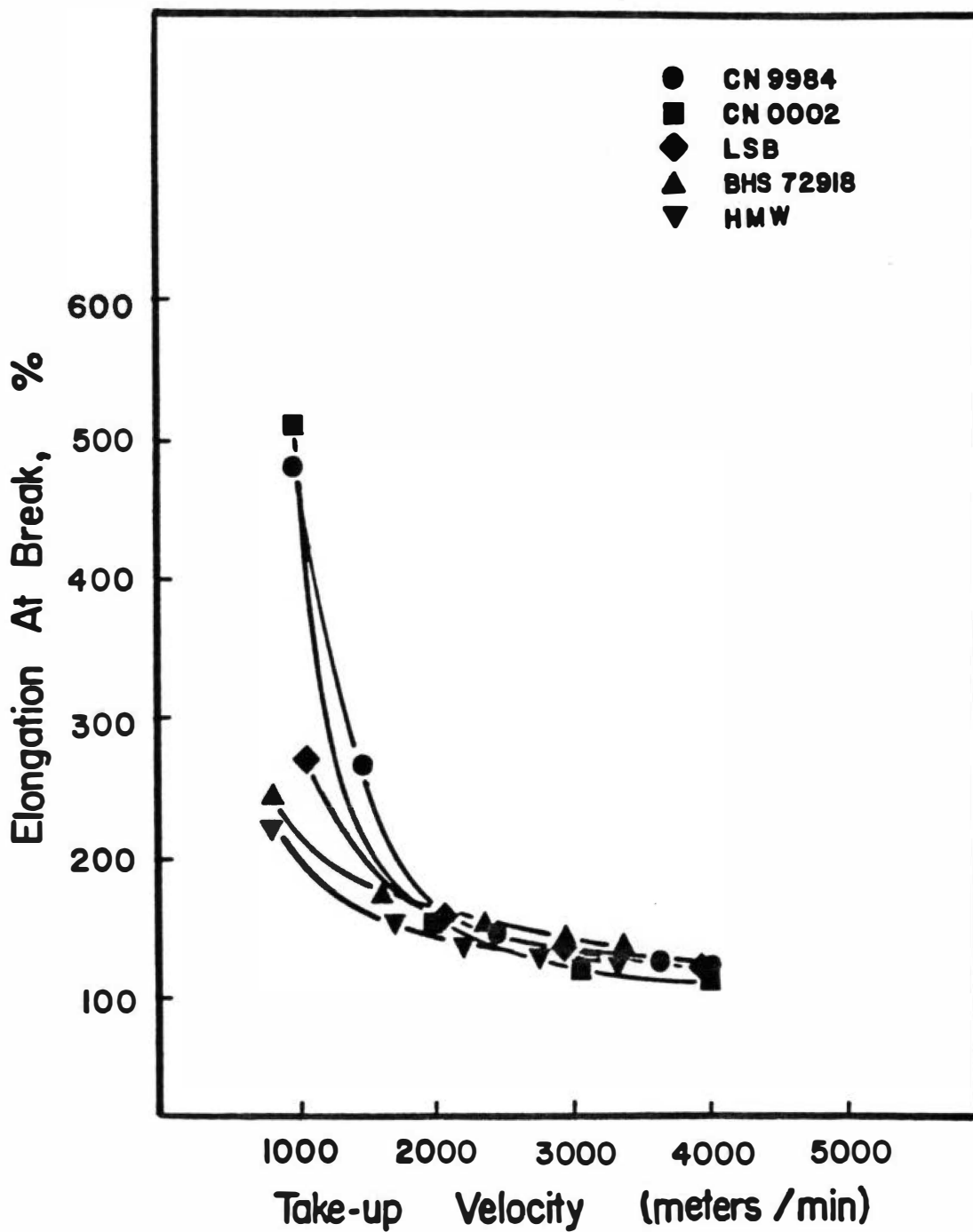
Figure V-7. Elongation at break of spun and conditioned nylon-6 fibers as a function of take-up velocity (mass throughput - 5.55 g/min).
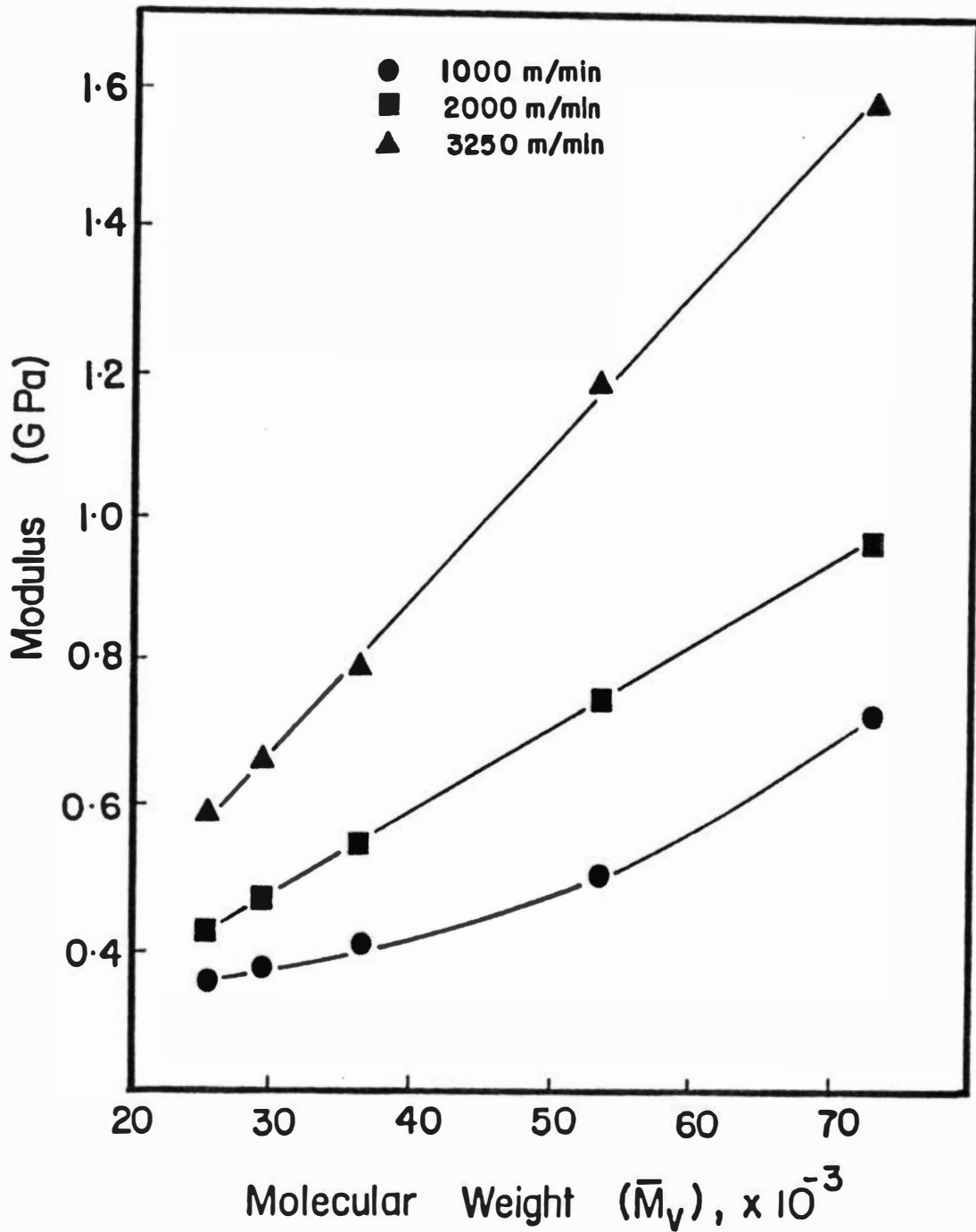
Figure V-8. Modulus of spun and conditioned nylon-6 fibers as a function of molecular weight (mass throughput - 5.55 g/min).
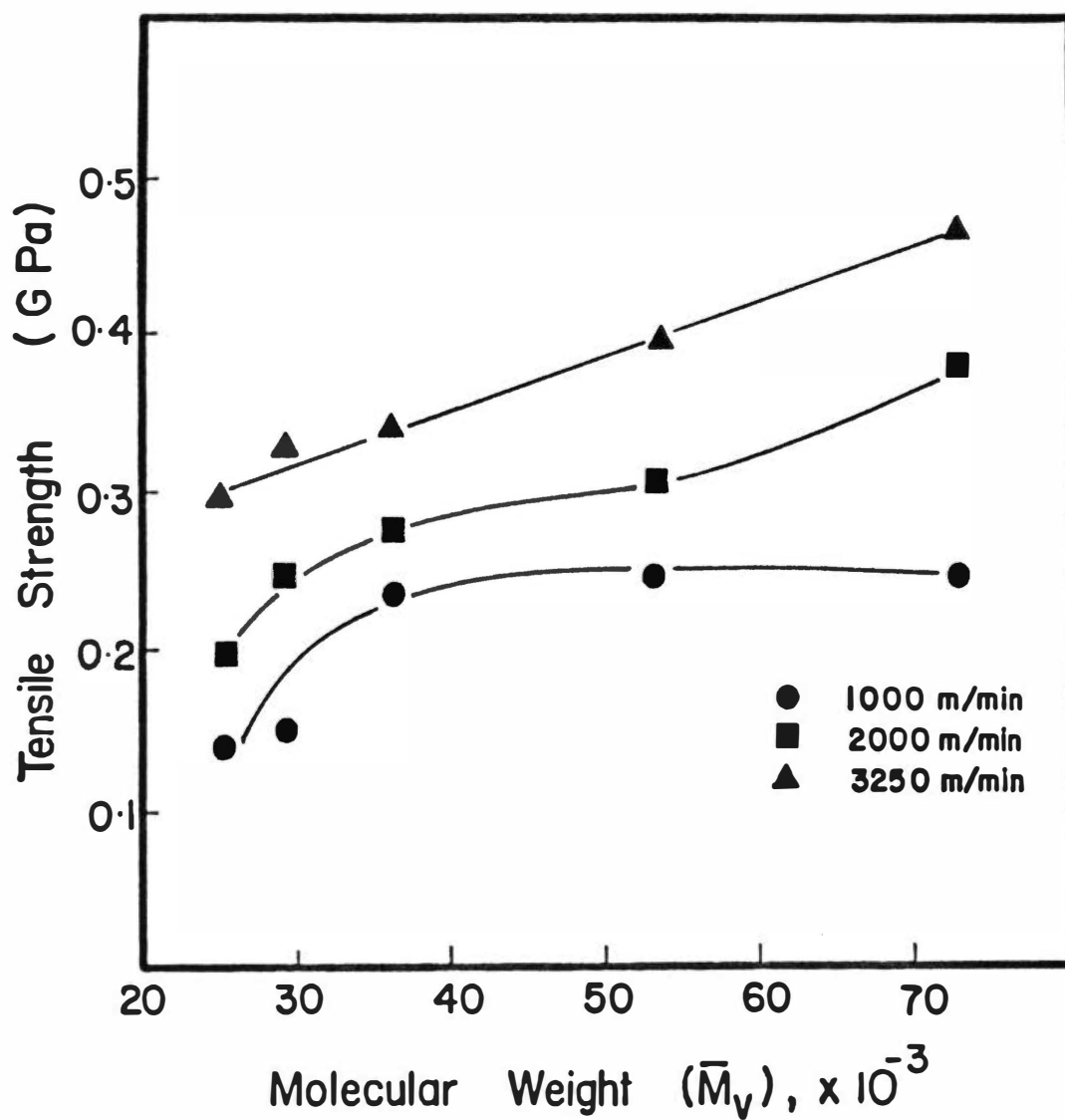
Figure V-9. Tensile strength of spun and conditioned nylon-6 fibers as a function of molecular weight (mass throughput - 5.55 g/min).
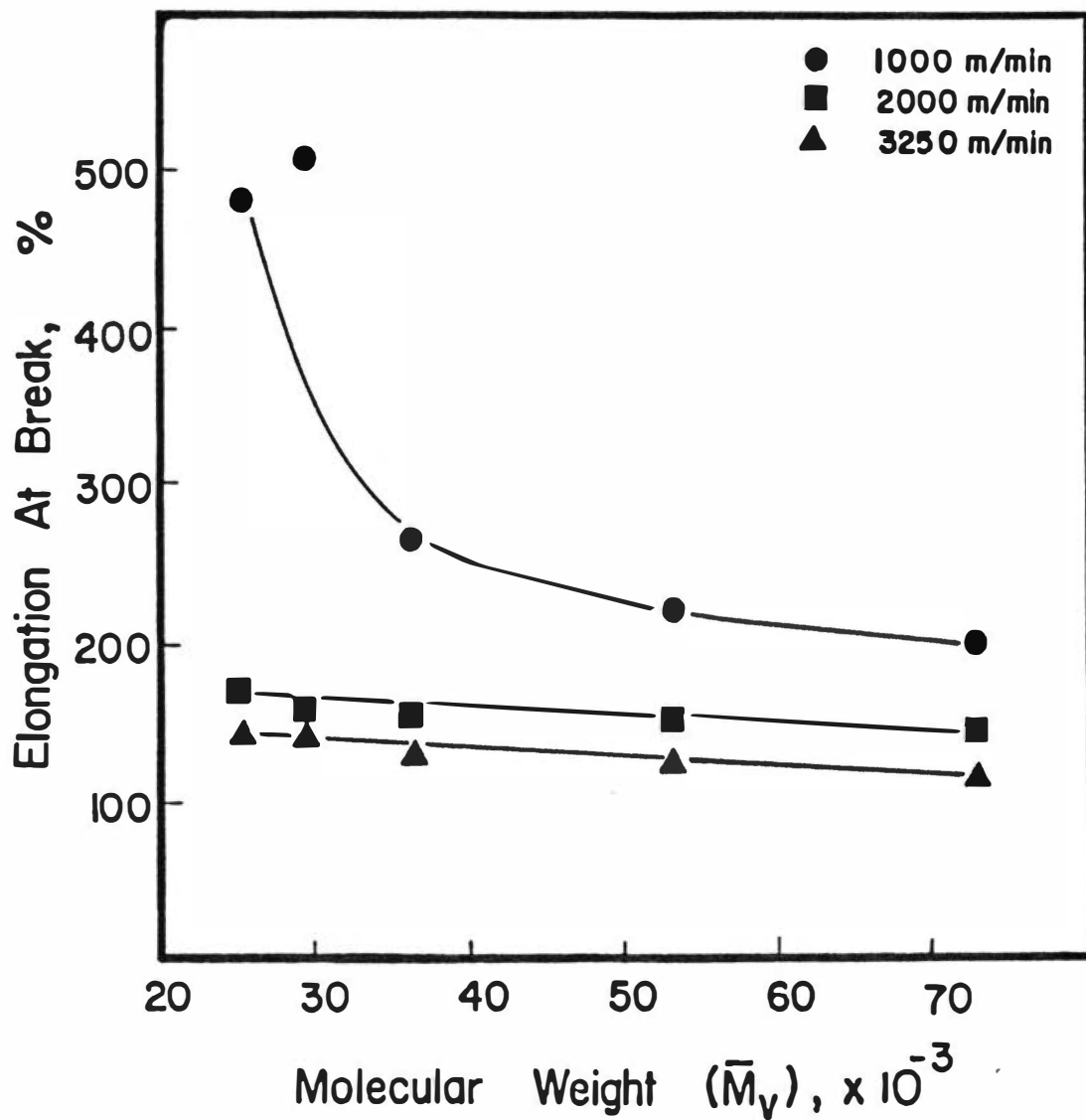
Figure V-10. Elongation at break of spun and conditioned nylon-6
fibers as a function of molecular weight (mass
throughput - 5.55 g/min).
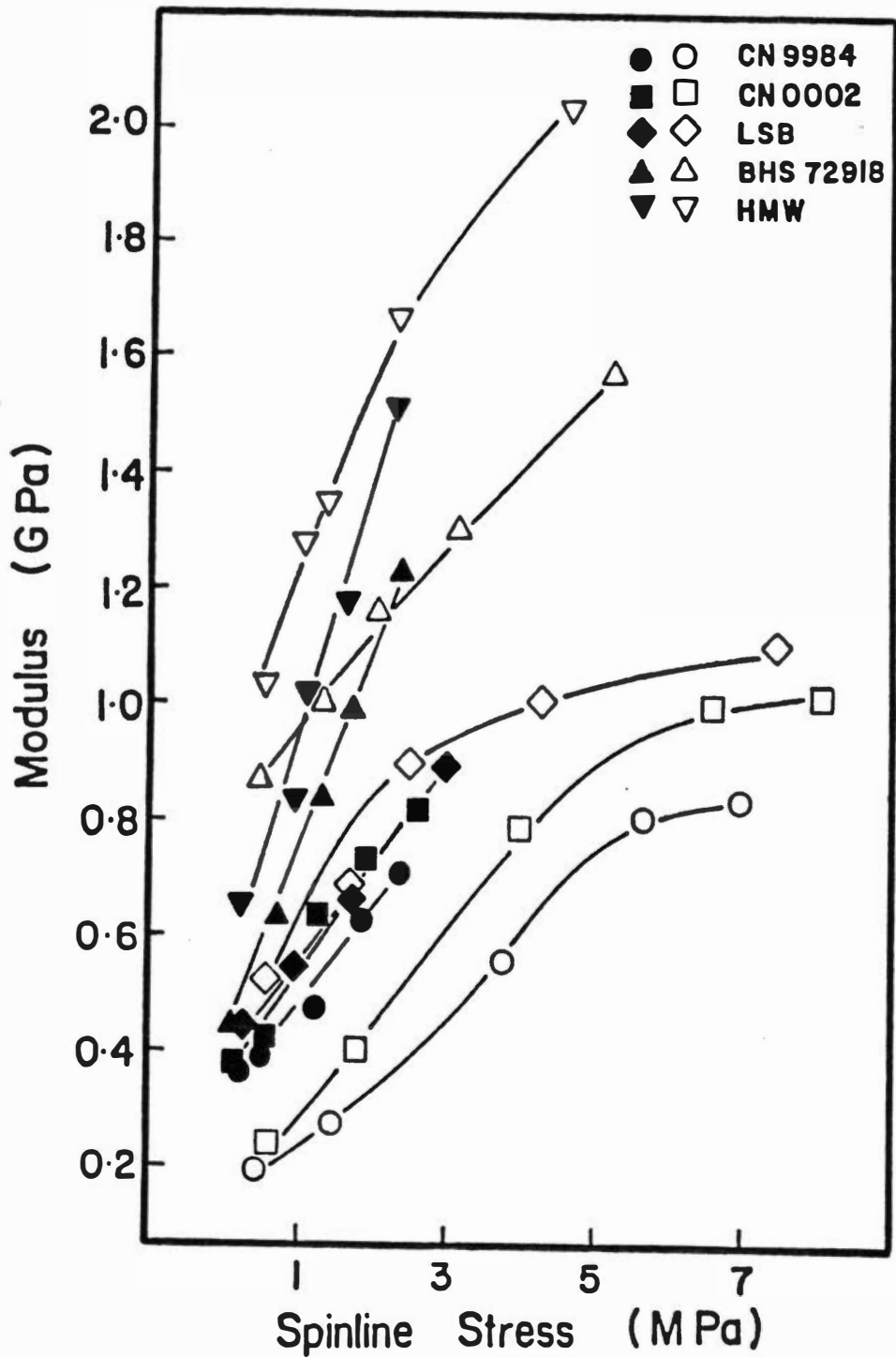
Figure V-11. Modulus of spun and conditioned nylon-6 fibers as a function of spinline stress (open data points - 3.55 g/min; closed data points - 5.55 g/min).
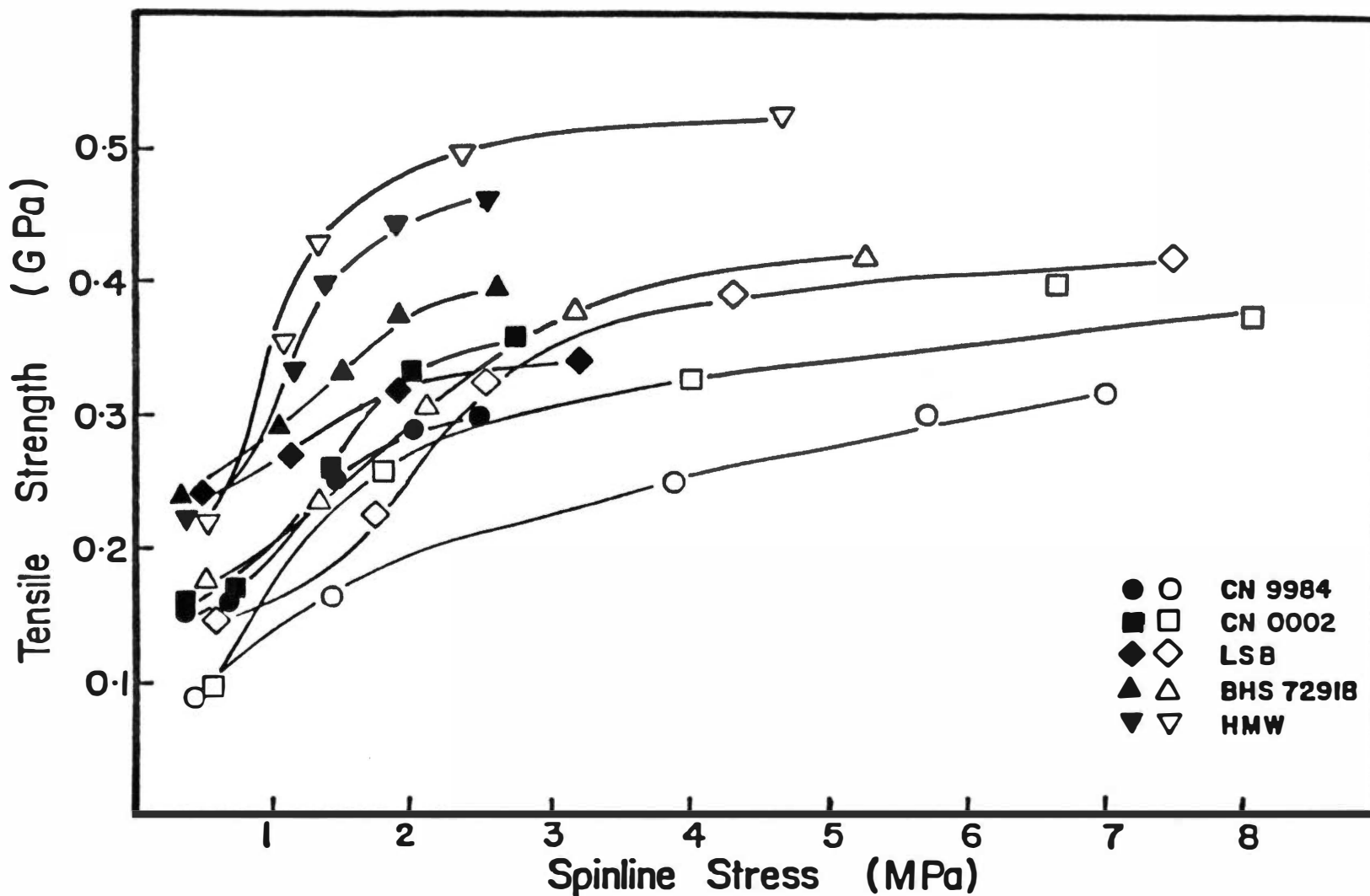
Figure V-12. Tensile strength of spun and conditioned nylon-6 fibers as a function of spinline stress (open data points - 3.55 g/min; closed data points - 5.55 g/min).
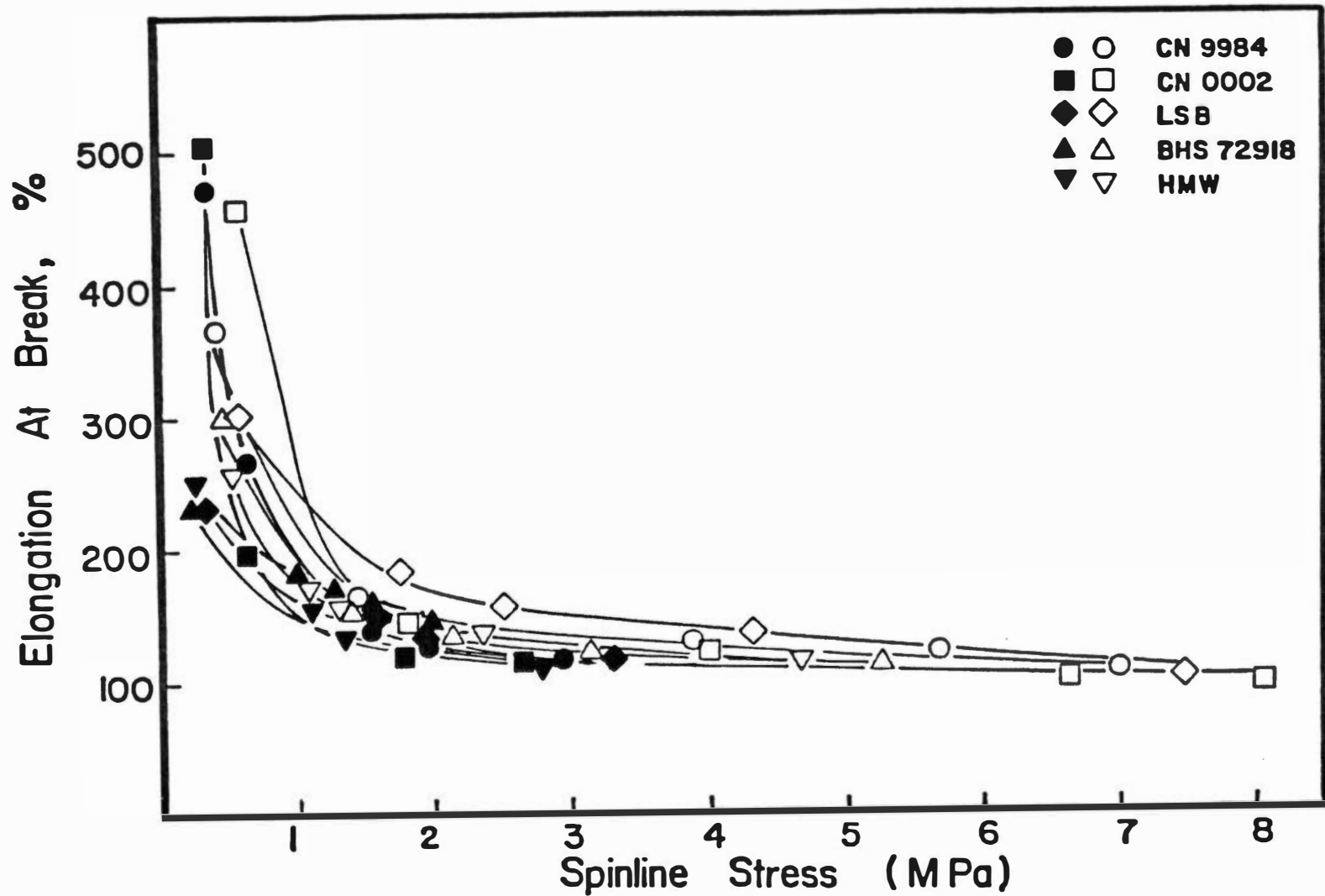
Figure V-13. Elongation at break of spun and conditioned nylon-6 fibers as a function of spinline stress (open data points - 3.55 g/min; closed data points - 5.55 g/min).
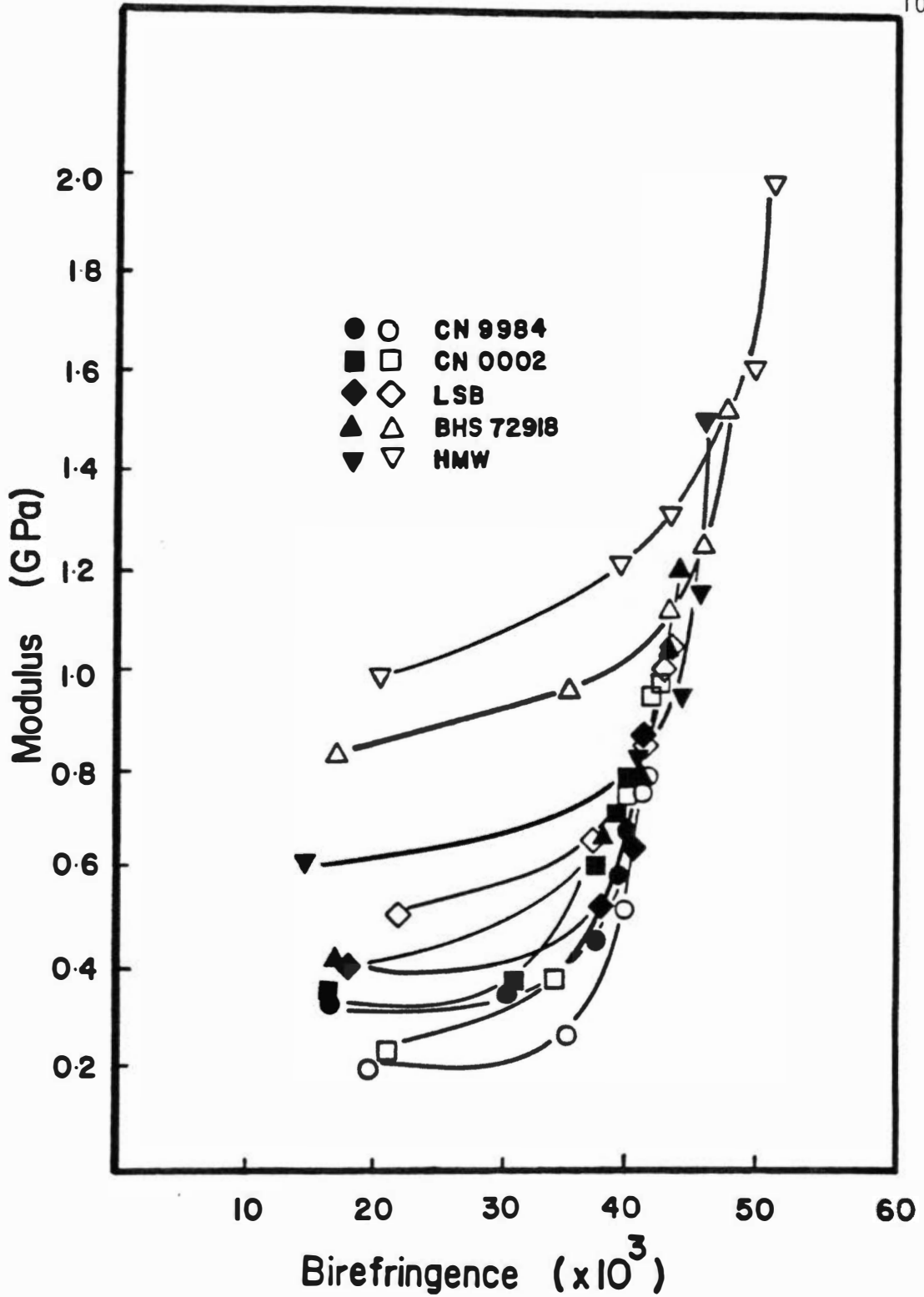
Figure V-14. Modulus of spun and conditioned nylon-6 fibers as a function of birefringence (open data points - 3.55 g/min; closed data points - 5.55 g/min).
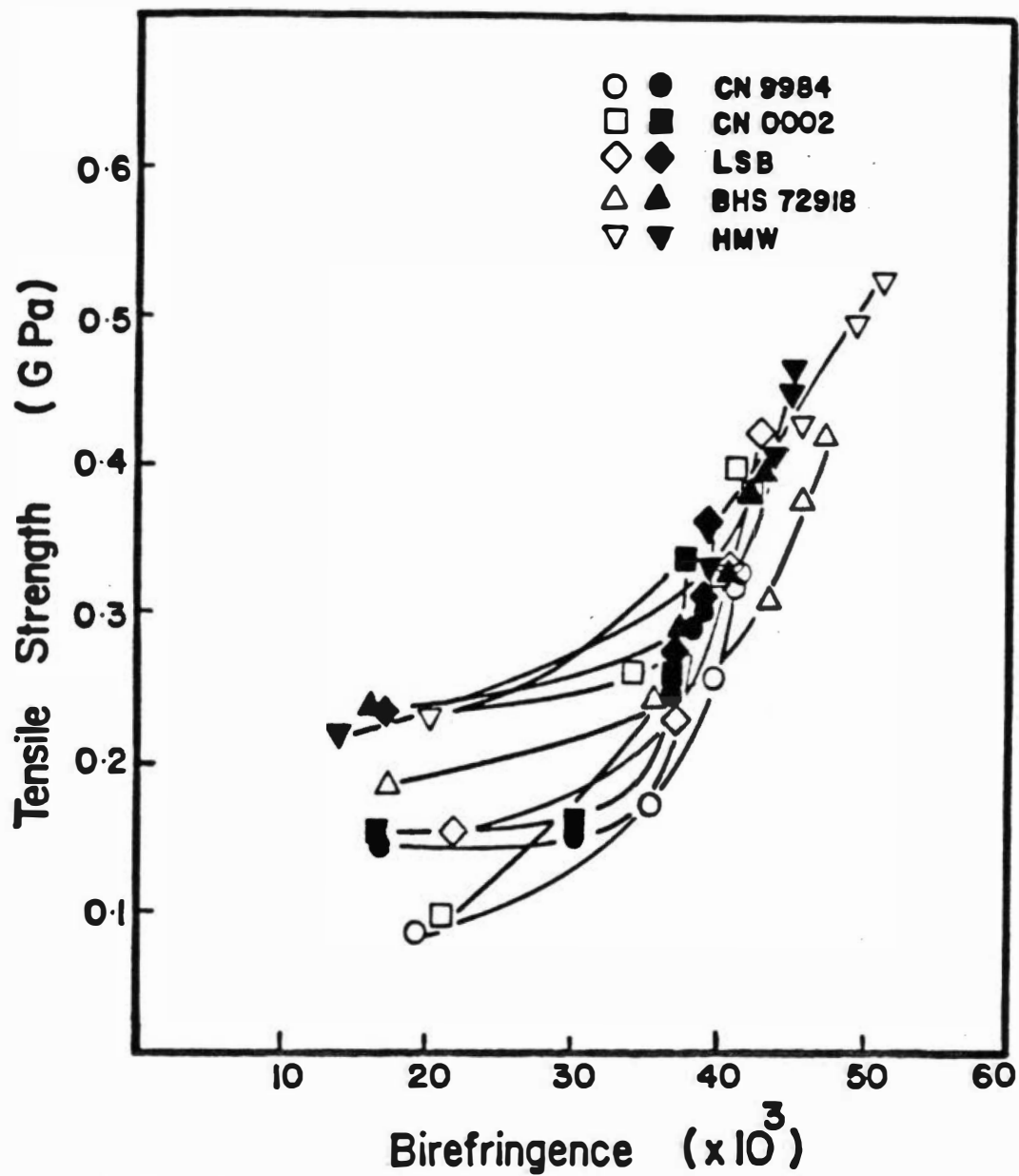
Figure V-15. Tensile strength of spun and conditioned nylon-6 fibers as a function of birefringence (open data points - 3.55 g/min; closed data points - 5.55 g/min).
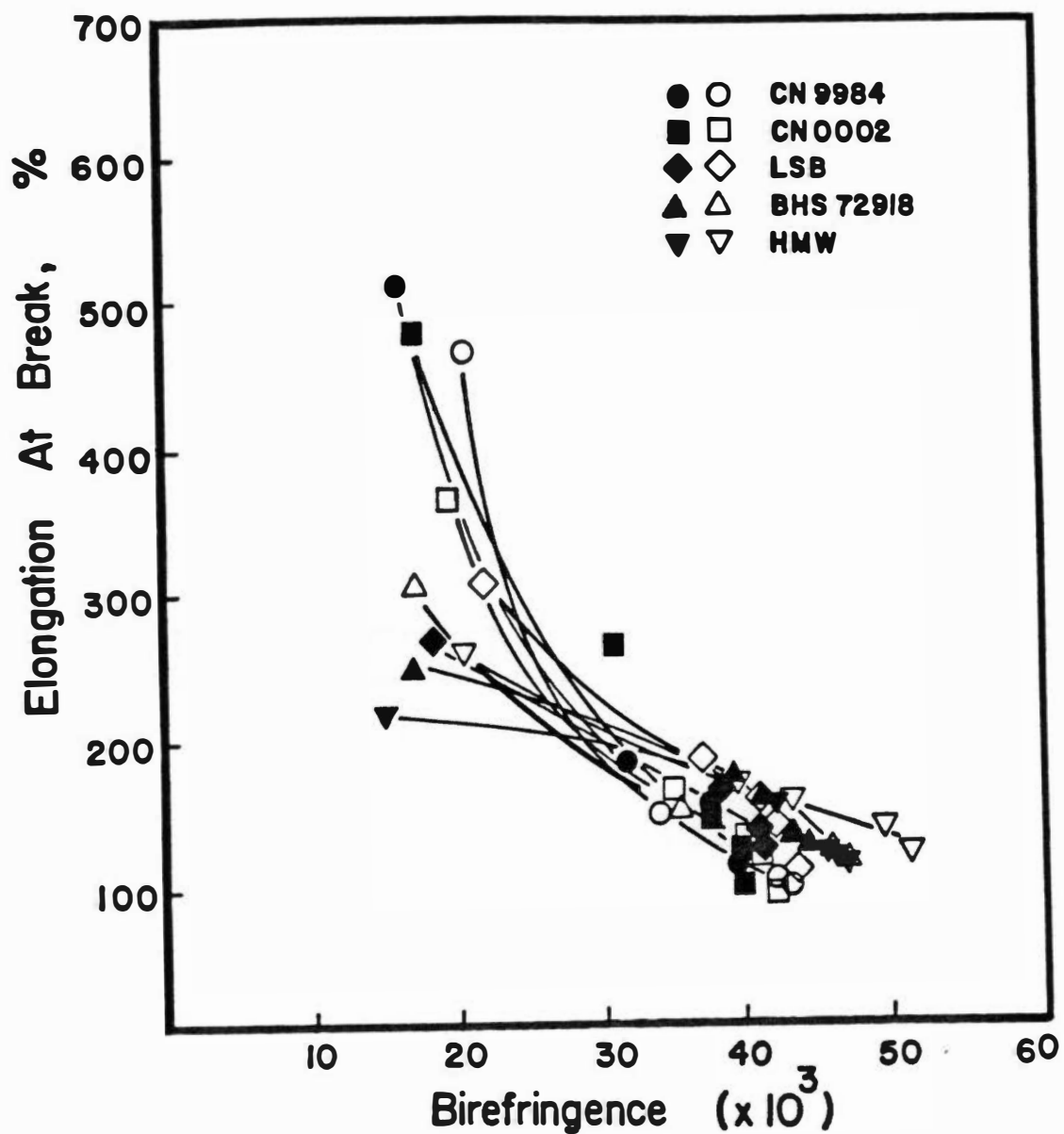
Figure V-16. Elongation at break of spun and conditioned nylon-6
fibers as a function of birefringence (open data points -
3.55 g/min; closed data points - 5.55 g/min).

B. DISCUSSION OF TENSILE PROPERTIES

Effect of Take-Up Velocity and Molecular Weight

Figure V-1 shows that the fibers spun at low take-up velocities show higher elongation to break but lower stress at break. Fibers spun at roughly the same take-up velocities but from a higher molecular weight material shows higher stress at break. At low take-up velocities (about 1000 m/min) the elongation at break is much larger for the low molecular weight samples than the high molecular weight, while at high take-up velocities there is very little difference between the high and low molecular weight samples. A distinctive yield point is observed only in the case of low molecular weight samples spun at low take-up velocity, while it is absent in the other fibers.

The variation of stress-strain behavior of nylon-6 filaments with take-up velocity was found to be similar to the results obtained by Gianchandani et al. (36) and Bankar (8). The modulus and tensile strength of the filaments increase while the elongation at break decreases with take-up velocity. The modulus is higher for lower mass throughputs. The effect of mass throughput is especially significant for the high molecular weight samples. The rate of increase of modulus increases at higher take-up velocities for high molecular weight samples. The tensile strength increases with increases in take-up velocity and molecular weight, while decreasing with increased throughputs. The tensile strength shows a sharp increase at initial take-up speeds and the increase becomes slower

at higher take-up speeds. The elongation at break shows only slight differences with changes in mass throughputs. A drastic reduction in the elongation at break is observed up to take-up velocities of about 2000 m/min, and beyond this point it is little affected by increase in take-up velocity or changes in molecular weight of the samples.

The rate of increase of modulus with molecular weight is greater at higher take-up velocities as shown in Figure V-8, and the combination of high molecular weights and high take-up velocities produce extremely high modulus spun fibers. The tensile strength also increases with increasing molecular weight. The increase is faster at higher take-up velocities. The elongation shows a trend which is decreasing at lower take-up velocities, but it is little affected by molecular weight at higher take-up velocities. There-fore the high tenacity filaments without much change in elongation at break can be obtained by increasing the molecular weight at high take-up velocities.

Correlation with Spinline Stress and Birefringence

The correlation of tensile properties with spinline stress were studied by Bankar et al. (8,10) for nylon-6 filaments and by Nadella et al. (82) and Henson and Spruiell (44) for polypropylene fibers. Their conclusions were that tensile properties showed excellent correlation with spinline stress. The spinline stress was shown to be the primary variable in determining the physical properties of nylon-6 and polypropylene fibers by these authors.

However, they did not examine the effect of molecular weight for the case of nylon-6.

In this study also the tensile properties exhibit good correlation with spinline stress for a given molecular weight polymer. It can be easily seen from Figures V-11, V-12 and V-13 that spinline stress does not reduce the results to a single master curve independent of molecular weight as in the case of polypropylene. Instead, the data for each molecular weight falls on a separate curve. A maximum value of 2.0 GPa was obtained for the modulus in the case of the high molecular weight sample. For the lower throughput case, modulus starts leveling off after stresses of about 5.0 MPa are reached for lower molecular weight samples. For the higher molecular weight samples, modulus seems to continue to increase even after the spinline stresses reach 5.0 MPa. The tensile strength shows a leveling-off trend after an initial rise. Beyond spinline stress values of 1.5 MPa and about 3.0 MPa for high and low molecular weight samples, respectively, there seems to be no change in the tensile strength. A plot of elongation at break versus spin-line stress shows a decrease in the elongation at break as the stress increases. The higher the molecular weight of the fiber, the lesser it can be elongated before it fractures. This is the case only for spinline stresses below 2.0 MPa above which the molecular weight of the sample does not make much difference in the elongations at break.

The correlations of tensile properties with birefringence are shown in Figures V-14, V-15 and V-16. Modulus and tensile strength

increase, while the elongation at break decreases with increase in birefringence. The increase in modulus and tensile strength is much sharper in the regions of high values of birefringence. This was observed in previous studies of nylon-6 (8,35) also. It is interesting to note that modulus and tensile strength increase sharply even though the birefringence attains a steady value.

Earlier studies by Nadella (80) on polypropylene fibers showed that the data on tensile properties collected over a range of different molecular weight fibers did not show any dependence on molecular weight. In the case of nylon-6, however, molecular weight seems to have a distinctive role in the development of tensile properties of the fibers. Danford et al. (25) showed that for nylon-66 fibers, the mass throughput does not affect the tensile properties independent of stress significantly. In the case of nylon-6, however, changes in throughput seem to have a slight effect on the tensile properties. This could probably be explained by the fact that changes in mass throughputs affect the cooling history sufficiently to produce differences in morphology that cause these differences.

By far, the best correlations of tensile properties seem to be with spinline stress. This could be due to the fact that spinline stresses present during the solidification process controls the morphology developed in the filaments for a given molecular weight. However, the crystallization kinetics and hence the morphology developed seems to be very sensitive to molecular weight in nylon-6.

CHAPTER VI

CONCLUSIONS AND RECOMMENDATIONS

This chapter summarizes the major conclusions resulting from this experimental study. These are followed by recommendations for future study.

A. CONCLUSIONS

The spinnability of the nylon-6's decreased with increased molecular weights. It was necessary to go to higher extrusion temperature for a high molecular weight polymer in order to obtain fibers even at low stresses. The percentage degradation in molecular weight increased with increasing molecular weight.

Spinline stresses increased with increase in take-up velocities and increase in molecular weights, and decreased with increased mass throughputs. The higher molecular weight samples are less sensitive to stress levels than the low molecular weight samples. Higher take-up velocity and higher molecular weight resulted in a high value of birefringence in the fibers. Birefringence increases monotonically with spinline stress. Density increased with take-up velocity and molecular weight. This is thought to be due to the high molecular weight samples having a greater amount of α-phase.

The total crystalline fraction and the γ-phase fraction increase while the amorphous fraction and α-phase fraction decrease,

109

with increase in take-up velocity. Higher molecular weight samples
have lower γ-phase content and lower crystallinity, probably due to
slower crystallization rates than the lower molecular weight samples.

Molecular chains tend to become more aligned with increase in
take-up velocity. The chain axis crystalline orientation function
decreases with increase in molecular weight at higher take-up speeds.
This is due to the lower crystallinity levels in the higher molecular
weight samples. Good correlations exist between crystalline
orientation functions and spinline stresses, but not independent of
molecular weight.

Spinline stresses determine the morphology developed, though
not independent of molecular weight and the mass throughput.

Low molecular weight fibers spun at low take-up velocities
show yield points on the stress-elongation curves, which are absent
at high take-up velocities and for high molecular weight samples.
Modulus and tensile strength increase with increase in molecular
weight and increased take-up velocity. They decrease with increase
in mass throughput. The modulus increases slowly at first and
rapidly as the take-up speeds increase. Tensile strength increases
rapidly at first and then levels off at higher take-up speeds. The
elongation at break decreases rapidly at first and is only slightly
affected at higher speeds. Higher molecular weight samples have
lower elongation at break at a particular take-up velocity. High
molecular weights together with high take-up speeds produce spun
fibers of very high modulus. When plotted against spinline stress

and birefringence, tensile properties show behavior similar to that when plotted against take-up velocity.

B. RECOMMENDATIONS FOR FUTURE RESEARCH

1. A wider range of mass flow rates and different extrusion temperatures should be studied to have a better understanding of their effect on the morphology developed.

2. SAXS studies should be conducted to provide information on any changes in the microfibrils of nylon-6 spun at high speeds.

3. Since the aerodynamic drag becomes important at high take-up velocities, it should be determined experimentally.

4. Online birefringence studies should be made and the birefringence measurement should be done on as spun fibers and followed up with time to understand the crystallization process in the different stages of high speed spun fibers.

5. Studies on high speed spinning and molecular weight variations should be made on other nylons to compare the results from the present study. This could be useful to generalize the results for all polyamides.

LIST OF REFERENCES

LIST OF REFERENCES

1. Abbot, L. E. and J. L. White, J. Appl. Poly. Sci., 20, 247 (1973).

2. Alexander, L. E., "X-Ray Diffraction Methods in Polymer Science," John Wiley & Sons, New York (1964).

3. Andrews, E. H., cited by A. B. Thompson in "Fiber Structure," J. W. S. Hearle and R. H. Peters, Eds., Butterworth and Text. Inst., Manchester, London (1962).

4. Aoki, H., Y. Suzuki and A. Ishimoto, cited by Bankar, V. G., Ref. 8.

5. Arimoto, H., Chemistry of High Polymers, Tokyo, 19, 204 (1962).

6. Arimoto, H., J. Poly. Sci., A-2, 2283 (1964).

7. Arimoto, H., M. Ishibashi, M. Hirai and V. Chatani, J. Poly. Sci., A-3, 317 (1965).

8. Bankar, V. G., Ph.D. Dissertation, University of Tennessee, Knoxville (1976).

9. Bankar, V. G., J. E. Spruiell and J. L. White, J. Appl. Poly. Sci., 21, 2135 (1977).

10. Bankar, V. G., J. E. Spruiell and J. L. White, J. Appl. Poly. Sci., 21, 2341 (1977).

11. Benaim, E., M.S. Thesis, University of Tennessee, Knoxville (1978).

12. Bennewitz, R., Faserforsch Textiltech, 5, 155 (1954).

13. Bradbury, E. M., L. Brown, A. Elliot and D. A. D. Perry, Polymer, 6, 465 (1965).

14. Bradbury, E. M. and A. Elliot, Polymer, 4, 47 (1963).

15. Bradley, T., (American Cyanamid), U.S. Patent 2,379,413.

16. Brill, R., Z. Physik. Chem., B53, 61 (1943).

17. Brody, H., J. Appl. Poly. Sci., 24, 301 (1979).

18. Campbell, G. A., J. Poly. Sci., 7B, 629 (1969).

19. Carothers, W. H. and G. J. Brechet, J. Am. Chem. Soc., 52, 5289 (1930).

20. Carothers, W. H. and J. W. Hill, J. Am. Chem. Soc., 54, 1566 (1932).

21. Carothers, W. H. and J. W. Hill, J. Am. Chem. Soc., 54, 1579 (1932).

22. Chappel, F. P., M. F. Culpin, R. G. Godsen and T. C. Tanter, J. Appl. Chem., 14, 12 (1964).

23. Chen, C. H., M.S. Thesis, University of Tennessee, Knoxville (1982).

24. Clark, E. S. and J. E. Spruiell, Poly. Eng. Sci., 16, 176 (1976).

25. Danford, M. D., J. E. Spruiell and J. L. White, J. Appl. Poly. Sci., 22, 3351 (1978).

26. Dees, J. R., Ph.D. Dissertation, University of Tennessee, Knoxville (1974).

27. Dees, J. R. and J. E. Spruiell, J. Appl. Poly. Sci., 18, 1053 (1974).

28. Density of Plastics by Density Gradient Technique, ASTM Designation, D 1505-68.

29. Dismore, P. F. and W. O. Statton, J. Poly. Sci., C-13, 133 (1966).

30. Dumbleton, J. H., Text. Res. J., 40, 1035 (1970).

31. Dumbleton, J. H., D. R. Buchanan and B. B. Bowles, J. Appl. Poly. Sci., 12, 2067 (1968).

32. Encyclopedia of Poly. Sci. and Techn., 10, 399.

33. Fung, P. Y. F. and S. H. Carr, J. Macromol. Sci.-Phys., B6, 621 (1972).

34. Geil, P. H., J. Poly. Sci., 44, 449 (1960).

35. Gianchandani, J., M.S. Thesis, University of Tennessee, Knoxville (1980).

36. Gianchandani, J., J. E. Spruiell and E. S. Clark, J. Appl. Poly. Sci., <u>27</u>, 3527 (1982).

37. Glauert, M. B. and M. J. Lighthill, Proc. Roy. Soc., <u>230A</u>, 188 (1955).

38. Gould, J. and F. M. Smith, J. Text. Inst., <u>No. 1</u>, 38 (1980).

39. Hamana, I., M. Matsui and S. Kato, Milliand Textilberichte, <u>50</u>, 382 (1969).

40. Hamana, I., M. Matsui and S. Kato, Milliand Textilberichte, <u>50</u>, 499 (1969).

41. Hamidi, A., A. S. Abhiraman and P. Asher, J. Appl. Poly. Sci., <u>28</u>, 567 (1983).

42. Hancock, T., J. E. Spruiell and J. L. White, "Wet Spinning of Aliphatic and Aromatic Polyamides," Poly. Sci. & Eng. Rep. No. 54, Jan. 1976.

43. Hasegawa, K., Seni-Gakkaishi, <u>38(11)</u>, 521 (1982).

44. Henson, H. M. and J. E. Spruiell, Paper presented at the Div. of Cellulose, Paper and Text. Chem., Philadelphia (1975).

45. Hermans, P. H., "Contributions to the Physics of Cellulose Fibers," Elsevier, New York (1946).

46. Hermans, P. H., J. J. Hermans, D. Vermoas and A. Weidinger, J. Poly. Sci., <u>3</u>, 1 (1947).

47. Heuvel, H. M. and R. Huisman, J. Appl. Poly. Sci., <u>22</u>, 2229 (1978).

48. Heuvel, H. M. and R. Huisman, J. Appl. Poly. Sci., <u>26</u>, 713 (1981).

49. Heuvel, H. M. and R. Huisman, J. Poly. Sci., Poly. Phys. Ed., <u>19</u>, 121 (1981).

50. Heuvel, H. M., R. Huisman and K.C.J.B. Lind, J. Poly. Sci., Phys. Ed., <u>14</u>, 921 (1976).

51. Hill, M. J. and A. Keller, J. Macromol. Sci.-Phys., <u>B3</u>, 153 (1967).

52. Hirami, M. and A. Tanimura, J. Macromol. Sci.-Phys., <u>B19</u>, 205 (1981).

53. Holmes, D. R., C. W. Bunn and D. J. Smith, J. Poly. Sci., <u>17</u>, 159 (1955).

54. Hoshino, S., J. Powers, D. G. Legrand, H. Kawai and R. S. Stein, J. Poly. Sci., <u>58</u>, 185 (1962).

55. Huisman, R. and M. M. Heuvel, J. Poly. Sci., Poly. Phys. Ed., <u>14</u>, 941 (1976).

56. Illers, H. K., H. Haberkon and P. Simak, Makromol. Chem., <u>158</u>, 285 (1972).

57. Indue, K. and S. Hoshino, J. Poly. Sci., Poly. Phys. Ed., <u>15</u>, 1363 (1977).

58. Inoue, M., J. Poly. Sci., <u>A-1</u>, 2013 (1963).

59. Ishibashi, T., K. Aoki and T. Ishii, J. Appl. Poly. Sci., <u>14</u>, 1597 (1970).

60. Ishibashi, T. and J. Furukawa, J. Appl. Poly. Sci., <u>20</u>, 1421 (1976).

61. Ishibashi, T. and T. Ishii, J. Appl. Poly. Sci., <u>20</u>, 335 (1976).

62. Joyce, R. M. (E. I. DuPont de Nemours & Co.), U.S. Patent 2,251,519.

63. Katayama, K., T. Amano and K. Nakamura, Kolloid Z. Z. Poly., <u>226</u>, 125 (1968).

64. Kawayguchi, Y., O. Yoshizaki and E. Nagai, Chem. of High Polymers, Tokyo, <u>20</u>, 337 (1963).

65. Keller, A., J. Poly. Sci., <u>15</u>, 31 (1955).

66. Keller, A., J. Poly. Sci., <u>21</u>, 363 (1956).

67. Keller, A. and M. J. Machin, J. Macromol. Sci.-Phys., <u>B1</u>, 41 (1967).

68. Konoshita, Y., Makromol. Chem., <u>1</u>, 33 (1959).

69. Kiyotosukuri, T., H. Hagesawa and R. Imamura, Sen-i Gakkaishi, <u>26</u>, 399 (1970).

70. Klare, H., "Technologie und Chemie der Synthetishen Fasern aus Polyamiden, Verlag Technik, Berlin, 1954, p. 13.

71. Kohan, M. I., in "Nylon Plastics," M. I. Kohan, Ed., Wiley-Interscience, New York, 1973, p. 9.

72. Kwon, Y. D. and D. C. Prevorsek, J. Appl. Poly. Sci., 23, 3105 (1979).

73. Kyotani, M. and S. Mitsuhashi, J. Poly. Sci., A-2, 1497 (1972).

74. Magill, J. H., Polymer, 3, 43 (1962).

75. Matsui, M., Trans. Soc. Rheol., 20, 465 (1976).

76. Matsui, M., Sen-i Gakkaishi, 38(11), T-508 (1982).

77. Matsumoto, K., cited by J. Gianchandani, Ref. 34, p. 29.

78. Migasaka, K. and K. Ishikawa, J. Poly. Sci., A-2, 1317 (1968).

79. Miyaki, A., J. Poly. Sci., 44, 223 (1960).

80. Nadella, H. P., M.S. Thesis, University of Tennessee, Knoxville (1976).

81. Nadella, H. P., J. E. Spruiell and J. L. White, J. Appl. Poly. Sci., 21, 3003 (1977).

82. Nadella, H. P., H. M. Henson, J. E. Spruiell and J. L. White, J. Appl. Poly. Sci., 22, 2131 (1978).

83. Nakamura, K., T. Watanabe, K. Katayama and T. Amano, J. Appl. Poly. Sci., 16, 1077 (1972).

84. Noether, H. and W. Whitney, Kolliid Z-Z. Poly., 251, 991 (1973).

85. Nylon Tech. Serv. Man., E.I. DuPont de Nemours & Co., Wilmington, DE, 1952.

86. Oda, K., J. L. White and E. S. Clark, Poly. Eng. Sci., 18, 53 (1978).

87. Ogawa, M., T. Ota, O. Yoshizaki and E. Nagai, Polym. Letters, 1, 57 (1963).

88. Ota, T., O. Yoshizaki and E. Nagai, J. Poly. Sci., A-2, 4865 (1964).

89. Parker, J. P. and P. H. Lindenmeyer, J. Appl. Poly. Sci., 21, 821 (1977).

90. Pasika, W. M., A. C. West III and E. L. Thurston, J. Poly. Sci., Poly. Phys. Ed., 10, 2313 (1972).

91. Prevorsek, D. C., P. J. Hargeet, R. K. Sharma and A. Reimschussel, J. Macromol. Sci.-Phys., B8, 127 (1973).

92. Roldan, L. G. and H. S. Kaufman, J. Poly. Sci., B-1, 603 (1963).

93. Roldan, L. G., R. Rahl and A. R. Paterson, J. Poly. Sci., C-8, 145 (1965).

94. Ruland, N., Polymer, 5, 89 (1964).

95. Sakiadis, B. C., AIChE J., 7(3), 467 (1967).

96. Sakoku, K., N. Morosoff and A. Peterlin, J. Poly. Sci., Poly. Phys. Ed., 11, 31 (1973).

97. Samuels, R. J., J. Poly. Sci., A-3, 1741 (1965).

98. Samuels, R. J., "Structured Poly. Properties," John Wiley, New York (1974).

99. Sano, Y. and K. Orii, Sen-i Gakkaishi, 24, 212 (1968).

100. Schlack, P., (I. G. Farben), German Patent 748,253 (1938); U.S. Patent 2,241,321 (1941).

101. Schrenk, H. A., (American Enka), U.S. Patent 2,735,839.

102. Schule, E. C., Encyclopedia of Chem. Tech., 16, 97 (1968).

103. Schultz, J. M., "Poly. Mat. Sci.," Prentice-Hall, New York (1974).

104. Shimizu, J., Sen-i Gakkaishi, 38(11), P-499 (1982).

105. Shimizu, J., N. Okui and Y. Imai, Sen-i Gakkaishi, 35(10), T-405 (1977).

106. Shimizu, J., N. Okui and Y. Imai, Sen-i Gakkaishi, 36(4), T-166 (1980).

107. Shimizu, J., N. Okui, A. Kaneko and K. Toriumi, Sen-i Gakkaishi, 37(2), T-64 (1978).

108. Shimizu, J., N. Okui and T. Kikutani, Sen-i Gakkaishi, 37(4), T-135 (1981).

109. Shimizu, J., N. Okui, T. Kikutani, A. Ono and A. Takaku, Sen-i Gakkaishi, 37(4), 143 (1981).

110. Shimizu, J., N. Okui, T. Kikutani and K. Toriumi, Sen-i Gakkaishi, 34(2), T-64 (1978).

111. Shimizu, J., N. Okui, T. Kikutani and K. Toriumi, Sen-i Gakkaishi, 34(3), T-91 (1978).

112. Shimizu, J., K. Toriumi and Y. Imai, Sen-i Gakkaishi, 33(6), T-255 (1977).

113. Shimizu, J., K. Toriumi and K. Tamai, Sen-i Gakkaishi, 33(5), T-208 (1977).

114. Shimizu, J., A. Watanabe and K. Toriumi, Sen-i Gakkaishi, 30(2), T-53 (1974).

115. Simpson, P. G., J. H. Southern and R. C. Ballman, Text. Res. Inst., 51(2), 97 (1981).

116. Slichter, W. P., J. Appl. Phys., 26, 1099 (1955).

117. Slichter, W. P., J. Appl. Phys. 35, 77 (1958).

118. Slichter, W. P., J. Poly. Sci., 36, 259 (1959).

119. Spruiell, J. E. and J. L. White, in "Fiber and Yarn Processing," J. L. White, Ed., Appl. Poly. Symp., 27, 121 (1975).

120. Starkweather, H., "Nylon Plastics," M. Kohan, Ed., SPE Wiley, New York (1973).

121. Starkweather, H., J. F. Whitney and D. R. Johnson, J. Poly. Sci., A-1, 715 (1963).

122. Stein, R. S., J. Poly. Sci., 31, 221 (1958).

123. Stein, R. S. and F. H. Norris, J. Poly. Sci., 16, 381 (1956).

124. Stepaniak, R. F., A. Garton, D. J. Carlsson and D. M. Wiles, J. Poly. Sci., 23, 1747 (1979).

125. Stepaniak, R. F., A. Garton, D. J. Carlsson and D. M. Wiles, J. Poly. Sci., Poly. Phys. Ed., 17, 987 (1979).

126. Sweeney, W. and J. Zimmerman, Encyl. Poly. Sci. & Tech., 10, 467 (1969).

127. Tsuruta, M., H. Arimoto and M. Ishibashi, Kobunshi Kagaku, 15, 619 (1958).

128. Ueda, S. and T. Kimura, Chem. High Poly., Tokyo, 15 (1958).

129. Vogelsong, D. C., J. Poly. Sci., A-1, 1055 (1963).

130. Wallner, L. G., Monatsh. Chem., 79, 279 (1948).

131. Wasiak, A. and A. Ziabicki, in "Fiber and Yarn Processing," J. L. White, Ed., Appl. Poly. Symp., 27, 111 (1975).

132. Wilchinsky, Z. W., J. Appl. Phys., 30, 792 (1959).

133. Wilchinsky, Z. W., J. Appl. Phys., 31, 1969 (1960).

134. Wilchinsky, Z. W., "Advances in X-Ray Analysis," 6, Plenum Press, New York, 1963, p. 231.

135. Yasuda, H., Sen-i Gakkaishi, 38(11), P-514 (1982).

136. Ziabicki, A., Kolloid Z.Z. Poly., 167, 132 (1959).

137. Ziabicki, A., J. Appl. Poly. Sci., 2, 24 (1959).

138. Ziabicki, A., Kolliid Z.Z. Poly., 175, 14 (1961).

139. Ziabicki, A., in "Man-Made Fibers," 1, John Wiley, New York, 1967.

140. Ziabicki, A., Sen-i Gakkaishi, 38(9), P-409 (1982).

141. Ziabicki, A. and K. Kedzierska, J. Appl. Poly. Sci., 2, 14 (1959).

142. Ziabicki, A. and K. Kedzierska, Kolloid Z.A. Poly., 171, 51 (1960).

143. Ziabicki, A. and K. Kedzierska, Kolloid Z.Z. Poly., 171, 111 (1960).

144. Ziabicki, A. and K. Kedzierska, J. Appl. Poly. Sci., 6, 111 (1962).

145. Ziabicki, A. and K. Kedzierska, J. Appl. Poly. Sci., 6, 361 (1962).

APPENDIXES

APPENDIX A

CALCULATIONS FOR THE AMOUNT OF SOLUTIONS
FOR A DENSITY GRADIENT COLUMN

The system used is Carbon Tetrachloride (CCl_4)-Toluene (C_7H_8). The range of the column was 1.10 g/cm^3 to 1.15 g/cm^3. The lower density (1.10 g/cm^3) was calculated at 20 cm and the high density (1.15 g/cm^3) at 80 cm of the column. This keeps the beads at the center of the column. The top and bottom of the column are least accurate.

(a) (high density - low density)/80 cm = density/cm of column

$$= (1.15 - 1.10)/80 = 6.25 \times 10^{-4} \ \frac{g/cm^3}{cm \ of \ coln.}$$

(b) density for 20 cm

$$6.25 \times 10^{-4} \times 20 = 1.25 \times 10^{-2} \ g/cm^3$$

(c) density at 0 cm

low density - density for 20 cm = density at 0 cm

$$1.10 - 1.25 \times 10^{-2} = 1.0875 \ g/cm^3$$

(d) density at 100 cm

high density + density for 20 cm = density at 100 cm

$$1.15 \times 1.25 \times 10^{-2} = 1.1625 \ g/cm^3$$

Let ρ_L be density at top of column.

$$\rho_L = 1.0875 \ g/cm^3$$

Let $_1$ be density at bottom of column.

$$_1 = 1.1625$$

The concentration of a CCl_4/C_7H_8 solution with a density of ρ_1

(1.1625 g/cm^3) is 56 percent CCl_4 by weight. This is solution X_A.
The solution density at the bottom of a 50 percent excess solution
(a 50 percent excess is needed to maintain a pressure head and for
safety measures).

$$\rho_L - \frac{\Delta\rho}{2} = \rho_2$$

$$1.0875 - \frac{(1.1625 - 1.0875)}{2} = 1.050 \text{ g/cm}^3 \ .$$

At this density (1.05 g/cm^3) the concentration of the light solution
(X_B) is 33 percent CCl_4 by weight. (The concentrations were
determined by placing a bead of known density in a beaker of C_7H_8.
Now CCl_4 is added slowly until the bead floats to the top. The
amounts of CCl_4 and C_7H_8 in the solution are known. The density of
this solution is equal to the density of the bead.) Now the average
concentration $(X_A + X_B)/2$

$(56 + 38)/2 = 47\%$ CCl_4 by weight.

The density at this concentration ρ_S is 1.105 g/cm^3, which is the
average density of the whole column. The volume of the column is
1100 cm^3 $\therefore$ the mass of the solution to fill this column is

1100 x 1.105 x 1.5 (50% excess)

= 1823.25 gm.

Mass of each (light and heavy) solution is

mass of column/2 = 911.625 gm.

The mass of C_7H_8 and CCl_4 for the heavy solution

$C_7H_8 = [911.625 + (30)(1.1625)][1 - 0.56]$

where 911.6125 - total mass (of CCl_4 and C_7H_8) required

(30)(1.625) - mass of solution required to fill the tube that runs

to the column to get the flow started (it requires

approximately 30 ml)

[1-0.56] - concentration of C_7H_8

$\therefore$ C_7H_8 = 416.46 gm = 481 cc. Similarly

CCl_4 = [911.625 + (30)(1.1625)][0.56]

CCl_4 = 530.04 gm = 333 cc.

Mass of CCl_4 and C_7H_8 required for light solution

C_7H_8 = 911.625 (1-0.38)(1.04)

where 911.625 - total mass (of CCl_4 and C_7H_8) required

(1-0.38) - concentration of C_7H_8

(1.04) - 4% excess required to initiate the flow from light

to heavy solution.

C_7H_8 = 587.82 gm = 679 ccm.

Similarly

CCl_4 = 911.625 (0.38)(1.04)

CCl_4 = 360.27 gm = 226 cc.

The final volumes of each liquid required are:

For heavy solution

C_7H_8 = 481 cc,

CCl_4 = 333 cc.

For light solution

C_7H_8 = 679 cc,

CCl_4 = 226 cc.

The densities used were

$$C_7H_8 = 0.866 \text{ g/cc,}$$

$$CCl_4 = 1.594 \text{ g/cc.}$$

Using these amounts of liquids in each solution, the density gradient column was built as described by ASTM D1505-68 (137).

APPENDIX B

Table 3. Diameter (in microns and denier) of spun and conditioned filaments at different take-up velocities and their densities

Mass Throughput - 3.55 g/min				Mass Throughput - 5.55 g/min			
Material and Take-up Velocity (m/min)	Diameter (microns)	Denier	Density (g/cm^3)	Material and Take-Up Velocity (m/min)	Diameter (microns)	Denier	Density (g/cm^3)
CN9984				CN9984			
1090	60.5	29.1	1.1248	1025	78.0	48.4	1.1256
1880	46.0	16.8	1.1255	1540	63.7	32.4	1.1282
3230	35.1	9.8	1.1276	2500	50.0	19.9	1.1286
4145	31.1	7.7	1.1287	3490	42.3	14.3	1.1296
4325	30.4	7.4	1.1300	4000	39.5	12.5	1.1304
CN0002				CN0002			
1240	56.3	25.3	1.1276	1020	78.3	48.9	1.1281
1500	51.6	21.2	1.1280	1680	61.0	29.7	1.1286
3170	35.5	10.1	1.1290	2260	52.5	22.0	1.1294
4140	31.0	7.1	1.1292	3160	44.4	15.7	1.1306
4600	29.5	6.9	1.1296	3980	39.6	12.5	1.1308
LSB				LSB			
1010	62.8	31.5	1.1287	1020	78.3	48.9	1.1287
1960	45.2	16.3	1.1295	2050	55.2	24.3	1.1295
2500	39.9	12.7	1.1301	3060	45.2	16.3	1.1302
3120	35.8	10.2	1.1302	3930	39.8	12.6	1.1318
4230	30.7	7.5	1.1302				
BHS72918				BHS72918			
870	67.7	36.6	1.1305	840	86.3	59.5	1.1302
1600	49.9	19.9	1.1307	1760	59.8	28.6	1.1303
2140	43.2	14.9	1.1316	2350	51.5	21.2	1.1303
2780	37.9	11.5	1.1319	2920	46.2	17.1	1.1312
3300	34.4	9.5	1.1322	3350	43.2	14.9	1.1317
HMW				HMW			
870	67.5	36.3	1.1284	830	86.3	59.4	1.1292
1480	51.9	21.5	1.1295	1760	59.5	28.3	1.1292
1750	47.8	18.2	1.1299	2140	54.0	23.3	1.1312
2520	39.8	12.7	1.1324	2700	48.1	18.5	1.1318
3180	35.4	10.0	1.1325	3250	43.8	15.4	1.1320

VITA

Jogendra Suryadevara was born on August 9, 1957, in Gudavalli of the Guntur district, in the state of Andhra Pradesh, India. He received his high school diploma from Timpany School, Visakhapatnam, in 1975. He then joined Andhra University in Visakhapatnam from where he received his Bachelor's degree in Chemical Engineering. In the Spring of 1981 he came to the United States and started graduate work in Chemical Engineering at The University of Kentucky, Lexington. In the Summer of the same year, he transferred to the Polymer Engineering program at The University of Tennessee, Knoxville, from where he received his Master's degree.

The author is a student member of the American Institute of Chemical Engineers, American Chemical Society and Society of Plastics Engineers. He was also the treasurer of the India Association of Knoxville.